Beiträge
zur Geologischen Karte der Schweiz
herausgegeben von der
Landeshydrologie und -geologie
und der
Schweizerischen Geologischen Kommission

Matériaux
pour la Carte Géologique de la Suisse
publiés par le
Service hydrologique et géologique national
et la
Commission Géologique Suisse

Lieferung 163
(Neue Folge)

Neil S. Mancktelow

Zürich

The Simplon Fault Zone

With 52 Figures, 3 Tables and 1 Plate

1990

Baumgartner AG Burgdorf

Foreword by the Editors

The Simplon area, with its major tectonic fault and its classic nappe pile, was one of the cradles of Alpine geology and has retained scientists' attention for more than a century. The evolving methods of investigation have underlined the complexity of geological structures present in this area and new observations have further enlivened the scientific debate.

Dr. Neil Mancktelow proposes a new approach to these problems in his habilitation work. He demonstrates, in an exemplary way, how the study of microstructures and lattice preferred orientations may be integrated into a tectonic synthesis, presenting this important fault zone in a new light. The work is admirably documented with numerous photographs of high quality, and the data presented are certainly of great interest as a reference for other similar studies.

This work was presented to the Swiss Geological Commission on the 24th. of February 1989 and, after recommendations from Prof. S. Schmid and Dr. M. Handy, who are thanked for their reviews, the Commission proposed its publication in the "Matériaux" series. The final manuscript was received by the Swiss National Hydrological and Geological Survey at the end of June 1989, which assumed the editorial preparation before printing, and transmitted it to the printer in May 1990.

The author is alone responsible for the content of the text and illustrations.

In May 1990

© 1990, Landeshydrologie und -geologie, 3003 Bern

Table of Contents

Page

Foreword by the Editors . . . 2

List of Figures, Tables, and Plate . . . 4

1. Introduction . . . 5
   - 1.1 Geographic Location . . . 5
   - 1.2 Previous Work . . . 5

2. Structural Elements . . . 7

3. Kinematic Indicators . . . 14
   - 3.1 Shear Bands . . . 14
   - 3.2 Obliquely Oriented Quartz New Grains . . . 14
   - 3.3 Asymmetric Mica Porphyroclasts and Broken Feldspars . . . 15
   - 3.4 Quartz Texture Asymmetry . . . 15
   - 3.5 Asymmetric Boudins . . . 15
   - 3.6 Asymmetric Fibre Growth . . . 15

4. Regional Geometry and Kinematics . . . 16
   - 4.1 Introduction . . . 16
   - 4.2 Structural Domains . . . 19
     - 4.2.1 Simplon Domain . . . 19
     - 4.2.2 Isorno Domain . . . 20
     - 4.2.3 Gebidum Domain . . . 21
     - 4.2.4 Berisal Domain . . . 21
     - 4.2.5 Toce Domain . . . 26
     - 4.2.6 Upper Pennine Domain . . . 26
   - 4.3 Summary . . . 27

Page

5. Rock Fabrics . . . 28
   - 5.1 Introduction . . . 28
   - 5.2 Microstructure . . . 28
   - 5.3 Metamorphic Conditions during Fabric Development . . . 29
   - 5.4 Quartz Textures . . . 30
     - 5.4.1 Introduction . . . 30
     - 5.4.2 Methods and Measurement Techniques . . . 30
     - 5.4.3 Observations . . . 31
     - 5.4.4 Discussion . . . 32
   - 5.5 Ribbon and Globular Grains . . . 34
   - 5.6 Effects of Recrystallization . . . 35

6. The Age of the Simplon Fault Zone . . . 38

7. Discussion and Conclusions . . . 40

Acknowledgments . . . 44

Summary . . . 45

Zusammenfassung . . . 46

References . . . 47

Appendices

A) Glossary *(Mylonite, Fabric, Texture, Recrystallization)* . . . 51
B) Orientation and Location of Specimens . . . 53
C) Quartz *C*-Axis Textures . . . 56
D) X-Ray Textures . . . 66

List of Figures, Tables, and Plate

Text Figures

		Page
Fig. 1	Location diagram	6
Fig. 2	Synoptic SW–NE profile through the SFZ	8
Fig. 3	View looking SSE towards Engiloch along the Simplon Line	8
Fig. 4	View of the SFZ looking ESE towards the Monscera Pass	8
Fig. 5	Typical outcrop exposure from the *hangingwall* above the Simplon Line	8
Fig. 6	Typical outcrop from the *footwall*	8
Fig. 7	Mylonitic S_m foliation from the footwall block	9
Fig. 8	Lineation L_m on an S_m foliation surface	9
Fig. 9	Well-developed shear bands in the Berisal unit	9
Fig. 10	Discrete shear bands in banded gneisses beside Lago di Dèvero	9
Fig. 11	Discrete shear bands in grey gneiss of the Lebendun unit below P. Diei	9
Fig. 12	Photomicrograph of a well developed shear band	9
Fig. 13	Difference in optical microstructure across the Simplon Line	11
Fig. 14	Difference in quartz *c*-axes textures across the Simplon Line	13
Fig. 15	Low angle between the two dimensional shape fabrics S_A and S_B	14
Fig. 16	High angle between S_A and S_B	14
Fig. 17	Asymmetric mica fish indicating a dextral sense of shear	15
Fig. 18	Asymmetric boudinage of a dolomite layer	16
Fig. 19	Stepped calcite fibres	16
Fig. 20	Simplified long-section with consistent asymmetric quartz textures	16
Fig. 21	Tectonic map with measured quartz textures	17
Fig. 22	Schematic transition from cataclastic fault to ductile shear zone	18
Fig. 23	Sketch map of the structural domains	18
Fig. 24	Orientation data for Simplon and Isorno Domains	20
Fig. 25	View to the northwest towards Crevola in the Ossola Valley	20
Fig. 26	Orientation data for the Gebidum Domain	21
Fig. 27	Calcite fibres developed on pyrite in the Rhone Valley	22
Fig. 28	Orientation data in the Berisal Domain	22
Fig. 29	Effect of folding on quartz textures in the Simplon Pass–Kaltwasser region	23
Fig. 30	Effect of the Berisal Synform on quartz textures	24
Fig. 31	Fold in the S_m foliation, of similar orientation to the Berisal Synform	25
Fig. 32	Orientation data for post-S_m folds	25
Fig. 33	Typical irregular kink-like fold style of the "late folds"	25
Fig. 34	Irregular folds in the S_m foliation of fractured mylonites	26
Fig. 35	Orientation data for the Staldener Lappen of the hangingwall	27
Fig. 36	Bulge nucleation at a quartz–quartz grain boundary	29
Fig. 37	Fractured quartz-rich mylonite from the "Furggwald Zone"	29
Fig. 38	Type I and Type II girdles, defined by the *c*-axis skeletons	31
Fig. 39	Most probable *m*, *r* and *z* pole orientations along the *c*-axis skeleton	32
Fig. 40	Idealized straight single girdle and Type I crossed girdle patterns	33
Fig. 41	Orientation of *c*-axes for ribbon grains and nearly equant "globular" grains	34
Fig. 42	Variation in grain boundary geometry with misorientation	35
Fig. 43	Misorientation angles across grain boundaries	36
Fig. 44	Stereograms of migration direction of lobate grain boundaries	37
Fig. 45	Interpreted cooling curves for the Simplon Alps	39
Fig. 46	Mineral zone boundaries in ultramafic schists in the Lepontine Alps	41
Fig. 47	Relation of the Periadriatic Line to the main subdivision of the Alps	42

Figures of Appendices

Fig. B_1	Key to the orientation of stereograms in Appendices C and D	53
Fig. B_2	Effect on shear sense of folding coaxial with the movement direction	53
Fig. B_3	Location of specimens	55
Fig. C_{1-57}	Quartz *c*-axis textures	57
Fig. D_{8-51}	Quartz X-ray textures	67

Tables

Table 1	Calculated Displacement versus Initial Dip of the Oligoclase Boundary	41
Table 2	Samples from the Footwall of the Simplon Fault Zone	54
Table 3	Samples from the Hangingwall of the Simplon Fault Zone	55

Plate

Plate	Interpretative Cross-Sections through the Simplon Alps	74

1. Introduction

The Simplon Alps was and is one of the classic areas for the development of theories of thrust and nappe tectonics. The complete section along the Simplon rail tunnel (finished in 1906), together with the excellent surface outcrop over ca. 2000 m of vertical relief, formed the basis from which a carefully constrained three-dimensional picture could be constructed. After considerable controversy around the turn of the present century, it was universally agreed that the folded gneiss bodies separated by thin metasedimentary zones could not be autochthonous, as was believed previously, but must represent major basement fold nappes overthrust on one another to form a tectonically thickened sequence (e.g. LUGEON 1903, LUGEON & ARGAND 1905, see MÜLLER 1982 for a review). It was not unreasonably assumed that the thrusting direction was approximately perpendicular to the major fold axes, from SSE towards NNW. More detailed studies showed that there were folds which overprinted the nappe boundaries and, in particular, a series of "backfolds" with a vergence towards the SSE (e.g. ARGAND 1911, 1916). However, the general assumption that movements within the Simplon Alps occurred exclusively in a NNW–SSE direction has been ingrained since this pioneering work at the turn of the century (ARGAND 1916). Profiles through the central Alpine chain have been drawn almost exclusively in this NNW–SSE plane, with the implicit assumption that this plane contains the tectonic transport direction throughout the long and complex deformation history. In the extreme, this has led to recent attempts to produce "balanced cross-sections" through the Alps along such profile sections (BOYER & ELLIOT 1982, BUTLER 1986).

It is, therefore, ironic that the present study, together with other recent work (MILNES 1974*b*, STECK 1984, MANCKTELOW 1985, MERLE et al. 1986, MERLE et al. 1989), has shown that this classic region for the development of the theory of nappe tectonics is strongly overprinted by post-nappe deformation, and that the geometry and kinematics of the nappe-forming phase is largely obscured. In particular, the rock fabrics (the dominant foliation, lineation and associated microstructure and crystallographic preferred orientation of the component minerals) are related not to a period of overthrusting towards the northwest, but to younger post-nappe deformation during which movements were directed towards the SSW. Just as the original theories of basement thrust and nappe tectonics developed in this region had wide applicability, so it is becoming increasingly obvious that important extensional structures within convergent orogenic belts, such as described here, are more common than has been previously realized (e.g. BURCHFIEL & ROYDEN 1985, BEHRMANN 1987, HERREN 1987, SELVERSTONE 1988).

It is emphasized in this study that the rock microfabrics in the Simplon Alps present an excellent opportunity to determine the kinematics and deformation mechanisms associated with this major post-nappe deformation. Practically mono-mineralic quartz veins, which are common throughout the region, provide a simple and constant lithology. The crystallographic preferred orientation of quartz (i.e. the quartz texture, WEISS & WENK 1985) can be partially measured optically (optic axis = *c*-axis) and more fully with an X-ray texture goniometer. The microstructure and measured textures from samples collected over a wide area provide constraints on the grain-scale deformation mechanisms operative during this period of late-Alpine deformation under retrograde metamorphic conditions. These results are of more than local interest and can be directly compared with results from other major displacement zones (e.g. the Moine Thrust, LAW et al. 1986). As these zones of strain concentration play a disproportionate role in accommodating the overall deformation in major orogens, the mechanisms involved are of great tectonic significance.

1.1 Geographic Location

The region considered in this study is roughly bordered by the Rhone Valley in the north, the Bognanco–Vigezzo–Centovalli Valleys in the south, the Saas Valley to the west and the Formazza Valley to the east. Locations mentioned in the text are shown on Figure 1 and coordinates, when given, refer to the Swiss national topographic map grid. The area is one of marked topographic relief, and elevation varies from over 4000 m in the Fletschhorn mountain group to around 200 m in the Ossola Valley near Domodossola. Access is generally good, aided by many well-kept paths in this area popular for mountain-walking and ski-touring. Unfortunately, many of the excellent fresh outcrops in road-cuttings along the Simplon Pass highway have recently been covered with concrete, continuing a trend already commented upon by BEARTH (1973).

1.2 Previous Work

The basic geological framework of the Simplon Alps was established by the work of GERLACH (1869, 1871, 1883), RENEVIER & GOLLIEZ (1894), SCHARDT (1894), SCHMIDT (1894, 1907, 1908), LUGEON (1903), LUGEON & ARGAND (1905), ARGAND (1911, 1916) and particularly by the outstanding regional geologic map of SCHMIDT & PREISWERK (1908), which is still the only detailed regional map available.

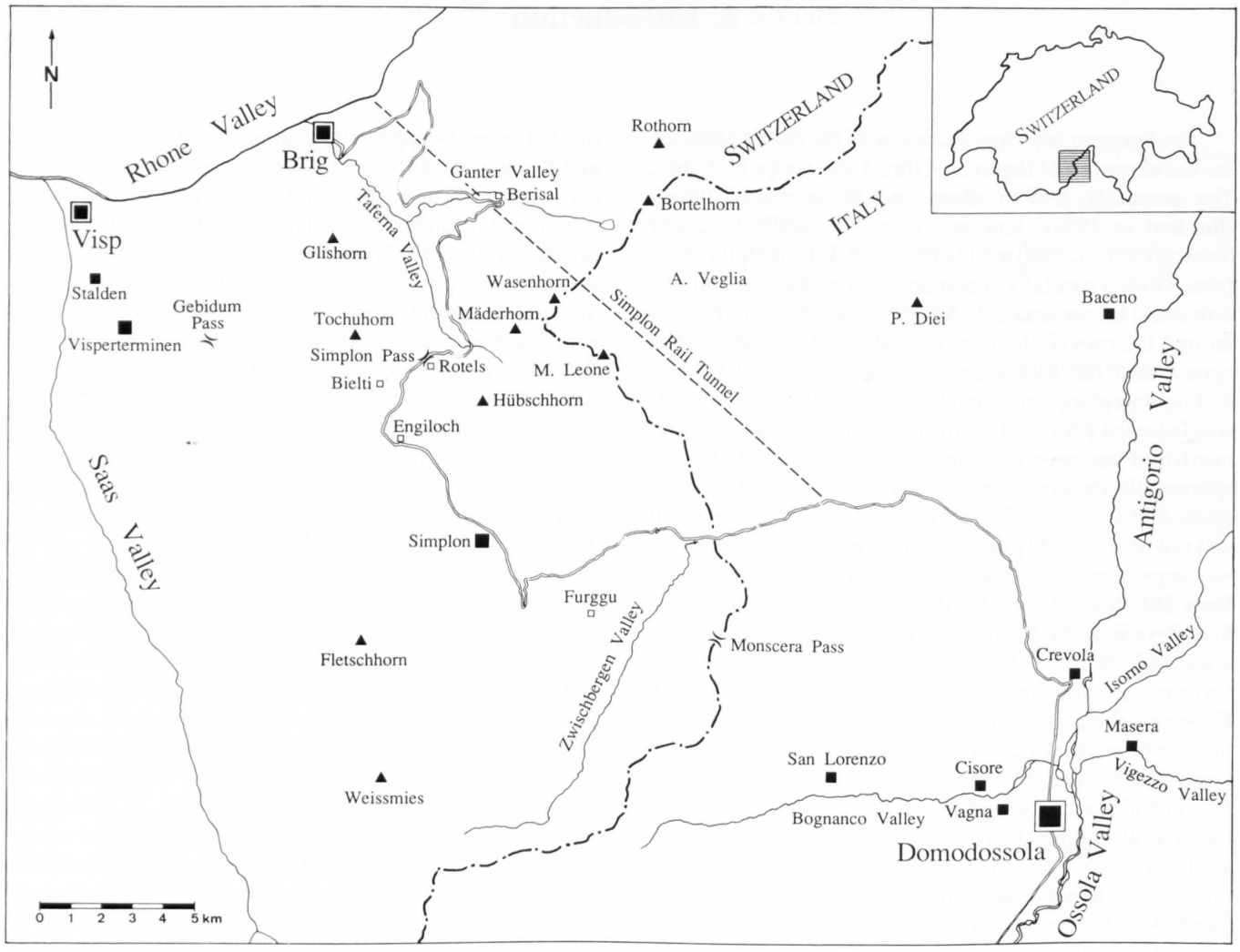

Fig. 1: Location diagram for the region of the Simplon Alps considered in this study.

AMSTUTZ (1954) was the first to recognize the existence of a major fault zone between Cisore and Simplon village (Fig. 1), marked by "mylonites" (meaning in the current sense "cataclasites", see Appendix A) and narrow lenses of Mesozoic metasediments. The accuracy of his mapping of this structural discontinuity has been confirmed in this study (cf. AMSTUTZ 1954, Planche 1). On his regional tectonic sketch map he proposed the continuation of this fault zone into the Vigezzo Valley and Centovalli to the east, and concluded that this fault zone represented the boundary thrust plane to the Monte Leone nappe. His section through the Bognanco Valley clearly shows the structural discontinuity, with concordant structures in the footwall and unrelated structures of different style in the hangingwall.

BEARTH (1956*a*) confirmed the existence of a major structural discontinuity but observed that the Monte Leone nappe boundary and the concordant foliation swing across the Ossola Valley into the Isorno Valley and not into the Vigezzo Valley (see also WENK 1955). He further noted that the Centovalli Fault Zone was independent of this nappe and lithologic boundary and clearly continued into the southern flank of the Bognanco Valley between Vagna and Domodossola (cf. Fig. 1 in BEARTH 1956*a*). From his mapping, BEARTH considered that at least part of the brittle faulting associated with the Centovalli Fault continued WSW along the upper Bognanco Valley, and that on the same line further westwards there were common young faults in the ophiolites of Antrona. He suggested, however, that part of this brittle zone may also continue northwest towards the Monscera Pass and that there might be a relationship between these young faults and the "mylonites" on the back of the Monte Leone gneiss, but considered that this required further detailed work. BEARTH (1956*a*) strongly rejected a relationship between the overthrusting associated with nappe development and the fault zone; the fault was considered to be a younger, post-nappe structure. He supported the view of AMSTUTZ that the internal structures of the crystalline masses south and north of the River Bogna were completely different, requiring the existence of a major structural discontinuity in the Bognanco Valley.

BEARTH (1956*b*) revised some of his earlier interpretations and came to agree (wrongly, as we will see) with AMSTUTZ (1954) that the "Simplon–Centovalli-Fault" continued to the east into Centovalli, but suggested that the younger fault diverged from the Monte Leone Nappe boundary in the Bognanco Valley. He followed the zone further north from Simplon village towards the Simplon Pass area to end in a question mark below the Tochuhorn

west of Simplon Kulm (cf. Fig. 2 in BEARTH 1956*b*). He noted a clear structural discontinuity between the hangingwall, with east striking fan-like structures, and the west to southwest dipping gneisses of the footwall. In all of these earlier studies, the use of the term "mylonite" differed from the current usage as employed here (cf. Appendix A), in that a brittle, cataclastic process was implied for the observed grain size reduction.

In summary, the existence of an important structural discontinuity had been established, marked by a rather narrow zone of "mylonite" of cataclastic origin which could be mapped between the Simplon Pass and Cisore, near Domodossola, on the west bank of the Ossola Valley. To the east, the fault was considered to continue as the Centovalli Fault Zone to eventually join the Insubric or Tonale Line near Losone. Towards the northwest the fault was either considered to be distributed as a series of splays into the Upper Pennine Zone (BEARTH 1972, 1973, SPICHER 1980) or continue as a simple, near planar surface to the northwest into the Rhone Valley (STECK 1984). Although the metamorphic grade and isotopic age jump indicated a considerable normal fault component (e.g. HUNZIKER & BEARTH 1969, HUNZIKER 1970), tectonic reconstructions prior to MANCKTELOW (1985) showed the Simplon Fault as a late, discrete fault plane with southeast directed movement of the upper block associated with the "back-folding" event (e.g. KLEIN 1978, MILNES et al. 1981, Fig 16 in MÜLLER 1983; STECK 1984, Planche I). In all cases the Simplon Fault was seen as a narrow, late fault which had little effect on the blocks to either side.

There has been a resurgence of interest in the Simplon Alps and the Pennine region in general over the past few years, with the realization that the importance of movements approximately parallel to the length of the Alpine chain has been underestimated (LAUBSCHER 1971, STECK 1980, 1984, 1987, MANCKTELOW 1985, MERLE et al. 1986, 1989, MERLE 1987, MERLE & LE GAL 1988). These advances have been due to a change in approach, with greater emphasis on the kinematics rather than the geometry alone, and a better appreciation and understanding of the use of rock fabrics to provide much, previously overlooked, information on the kinematics of deformation (e.g. SIMPSON & SCHMID 1983). The work of STECK (1980, 1984) was pioneering in this regard, as he was the first to appreciate the kinematic significance of the common WSW–ENE directed stretching lineations reported from the Pennine Alps (e.g. MILNES 1968).

In the late 1950's to 1970's, considerable, quite detailed work on quartz and calcite fabrics in rocks of the Central Alps was carried out (TROMMSDORFF & E. WENK 1963, TROMMSDORFF 1964, TROMMSDORFF & H.-R. WENK 1965, KVALE 1957, 1966, MILNES 1971, 1972), but contributed surprisingly little to the overall understanding of Alpine kinematics. A reasonable basis for the interpretation of such measurements has only been recently established through experimental (e.g. TULLIS et al. 1973, SCHMID 1982) and theoretical (e.g. LISTER et al. 1978, ETCHECOPAR 1977) studies of crystal deformation and fabric development and by measurement in stucturally simple areas with tightly controlled geometry (e.g. CARRERAS & GARCIA CELMA 1982, SCHMID & CASEY 1986, LAW 1986). The published textures from these earlier studies in the Central Alps do not always indicate their field orientation, and in some cases several thin sections (which were not uniquely oriented) were used for measurement of a single texture. This could explain the general lack of consistent asymmetry when compared to the results presented in this study.

2. Structural Elements

The general structural elements which can be recognized throughout the region are introduced here and briefly described. Local variation in these features will be discussed in the section on regional geometry and kinematics. The term *Simplon Fault Zone* (SFZ) is used in a broad sense to cover all structural elements which can be directly related to this major displacement zone. Deformation associated with these movements is attributed to a *Simplon Phase*, which may be extended to deformation of similar timing and kinematics in areas physically removed from the type Simplon locality. In the region considered for this study, the SFZ is generally moderately dipping and the definition of an upper *hangingwall* and a lower *footwall* is clear (Figs. 2, 3, 4). In general, these two blocks are separated by an abrupt structural discontinuity, termed the *Simplon Line* because of its linear map expression.[1]

The *hangingwall* corresponds to the Upper Pennine Zone of MILNES et al. (1981). Older, polyphase structures are unaffected by ductile deformation of the Simplon Phase, and are often clearly truncated by the structural discontinuity marking the hangingwall/footwall boundary (the Simplon Line, see Fig. 2 & Plate). Brecciation and chloritization is widespread in the hangingwall immediately adjacent to this discontinuity (Fig. 5). The relationships are particularly clear in the Zwischbergen Valley, where recent road construction has provided additional fresh outcrop. Open folding of the dominant tectonic foliation, with axial planes trending ca. NE–SW and with shallowly plunging fold axes, results in an irregular orientation to this foliation and a "blocky" outcrop pattern (Fig. 5). Quartz veins are generally poorly foliated and lineated, may be either concordant or discordant to the dominant foliation, and are often irregular or pod-shaped. They are medium- to coarse-grained, with a "sugary" field appearance.

[1] This terminology is directly analogous to the distinction between an *upper plate* and *lower plate*, separated by a discontinuity, in extensional terrains of the western USA.

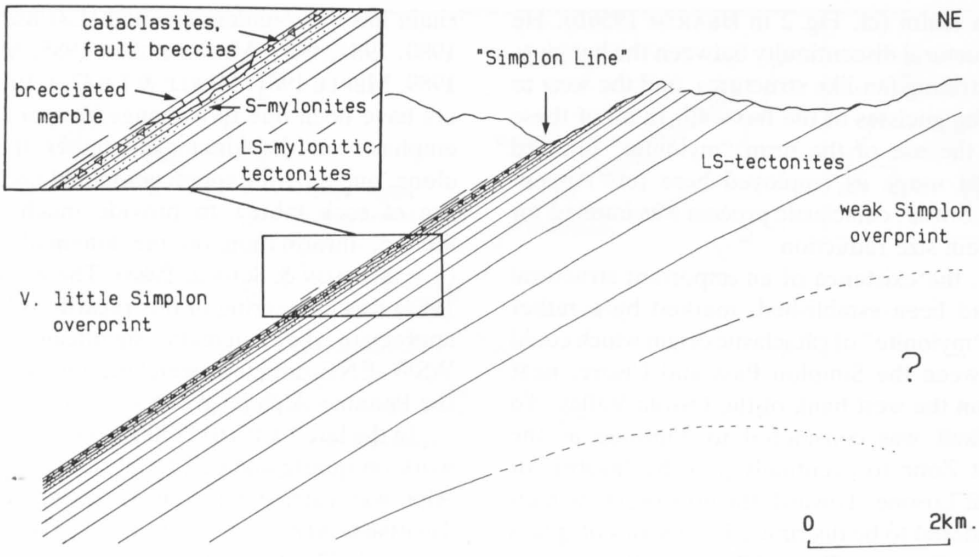

Fig. 2: Synoptic and simplified SW–NE profile through the SFZ, indicating the main structural elements as discussed in the text (from MANCKTELOW 1985).

Fig. 3: View from below Tochuhorn, looking SSE towards Engiloch along the Simplon Line. The distinction in outcrop style between the flaggy, planar-foliated footwall (to the left) and the more irregular, "blocky" style of the hangingwall (to the right) is obvious.

Fig. 4: View of the SFZ looking ESE towards the Monscera Pass from Furggu. Note the clear distinction between the strongly foliated footwall (to the left) and the more massive outcrop style of the hangingwall. Note also the sharp, planar contact (dipping ca. 30° SSW) separating these two blocks (the "Simplon Line") and the effective concordance between the footwall foliation S_m and the Simplon Line.

Fig. 5: Typical outcrop exposure from the *hangingwall* above the Simplon Line of Figure 4, showing the blocky outcrop style and the absence of a single, pervasive, planar foliation. Brecciation and fracture, which is typical of the hangingwall close to the Simplon Line, is extensive. Recent road-cutting on the east side of the Zwischbergen Valley below the Monscera Pass (Coords. 653.05/112.64).

Fig. 6: Typical outcrop from the *footwall* showing a single, mylonitic, planar foliation, to which the lithologic banding and quartz veins are effectively parallel. This outcrop is only 300 m from that of Figure 5, across the Simplon Line structural discontinuity and fabric boundary. Recent road-cutting on the east side of the Zwischbergen Valley below the Monscera Pass (Coords. 653.05/112.92).

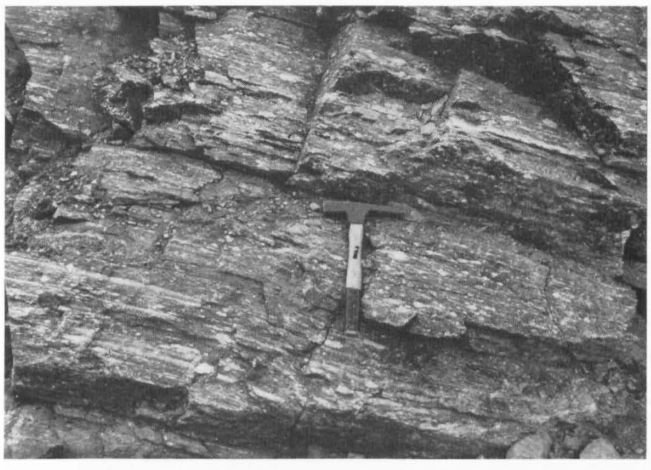

Fig. 7: Mylonitic S_m foliation from the footwall block. Berisal gneiss in road-cutting near Engiloch (Coords. 644.77/119.36).

Fig. 8: Lineation L_m on an S_m foliation surface. Berisal gneiss near Engiloch (Coords. 644.90/119.27).

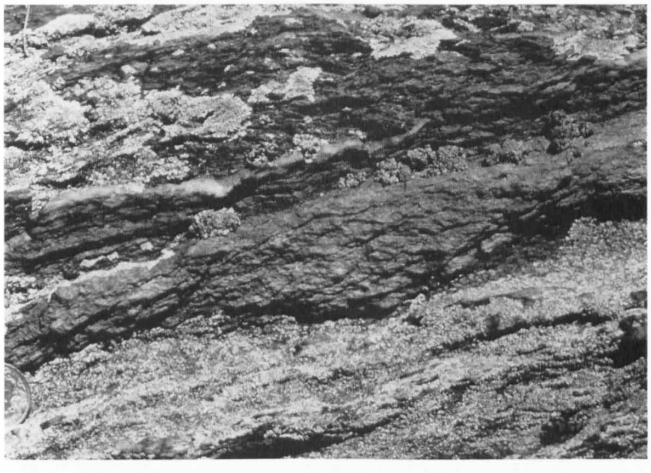

Fig. 9: Well-developed shear bands in micaceous schist of the Berisal unit northwest of the Simplon Pass (Coords. 645.35/123.03). Shear sense in this view towards the northwest is sinistral.

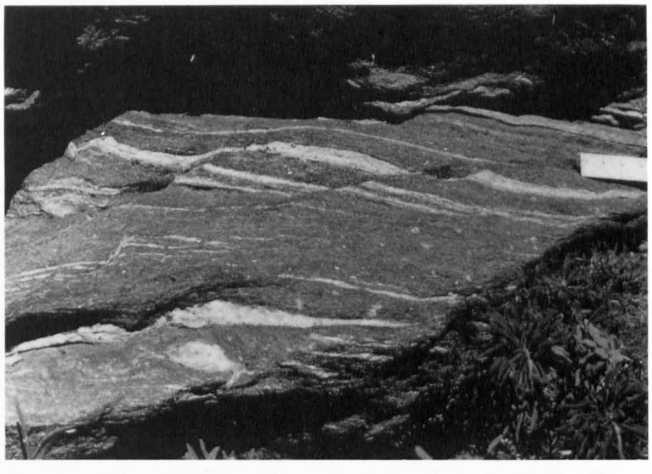

Fig. 10: Discrete shear bands in banded quartzo-feldspathic and biotite-rich gneisses from above the northwest shore of Lago di Dèvero (Coords. 665.77/133.36). Shear sense in this view towards the northwest is sinistral.

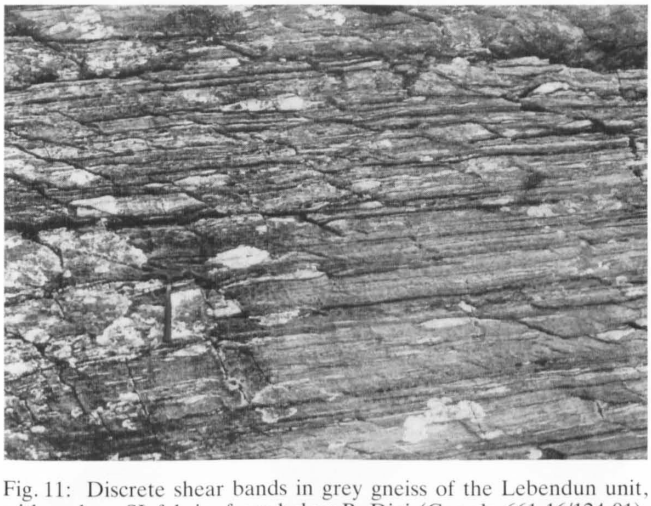

Fig. 11: Discrete shear bands in grey gneiss of the Lebendun unit, with a clear *SL* fabric, from below P. Diei (Coords. 661.16/124.01). For this view looking towards the SSE, the shear sense is dextral.

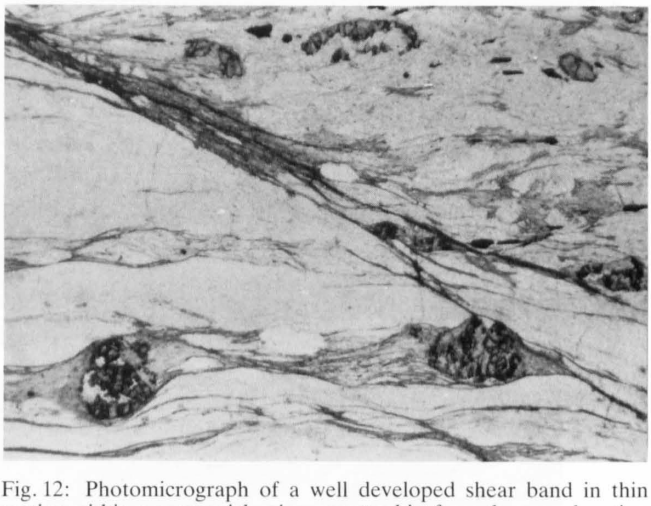

Fig. 12: Photomicrograph of a well developed shear band in thin section within a quartz-rich mica-garnet schist from the same location as Specimen 27 (see Appendices C, D). Retrograde chlorite is seen both within the shear band and as "pressure shadows" on garnet, which help define the L_m lineation within S_m. Width of field is 3.3 mm.

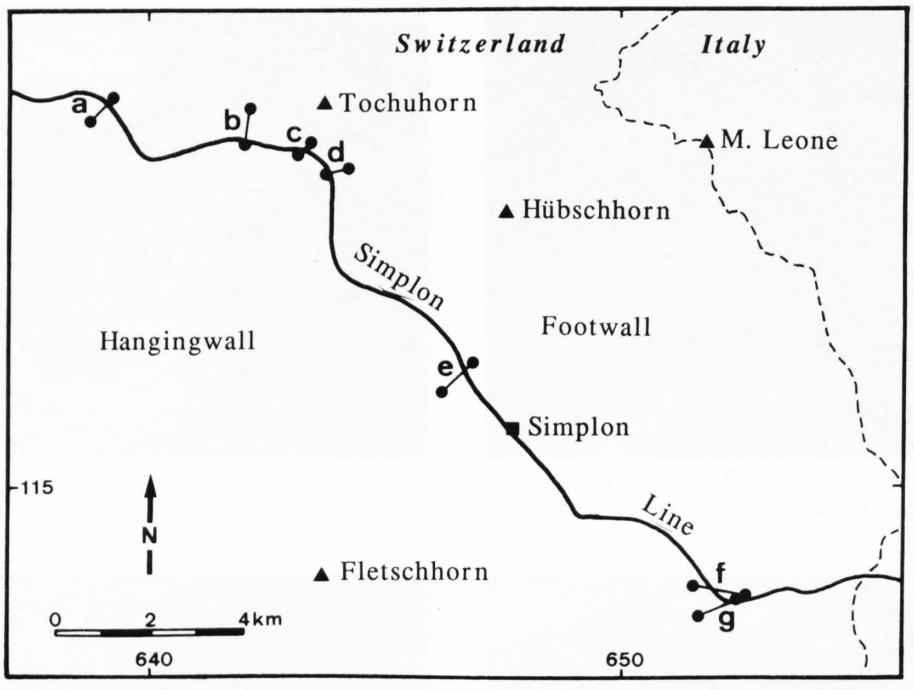

Footwall

Hangingwall

a

b

c

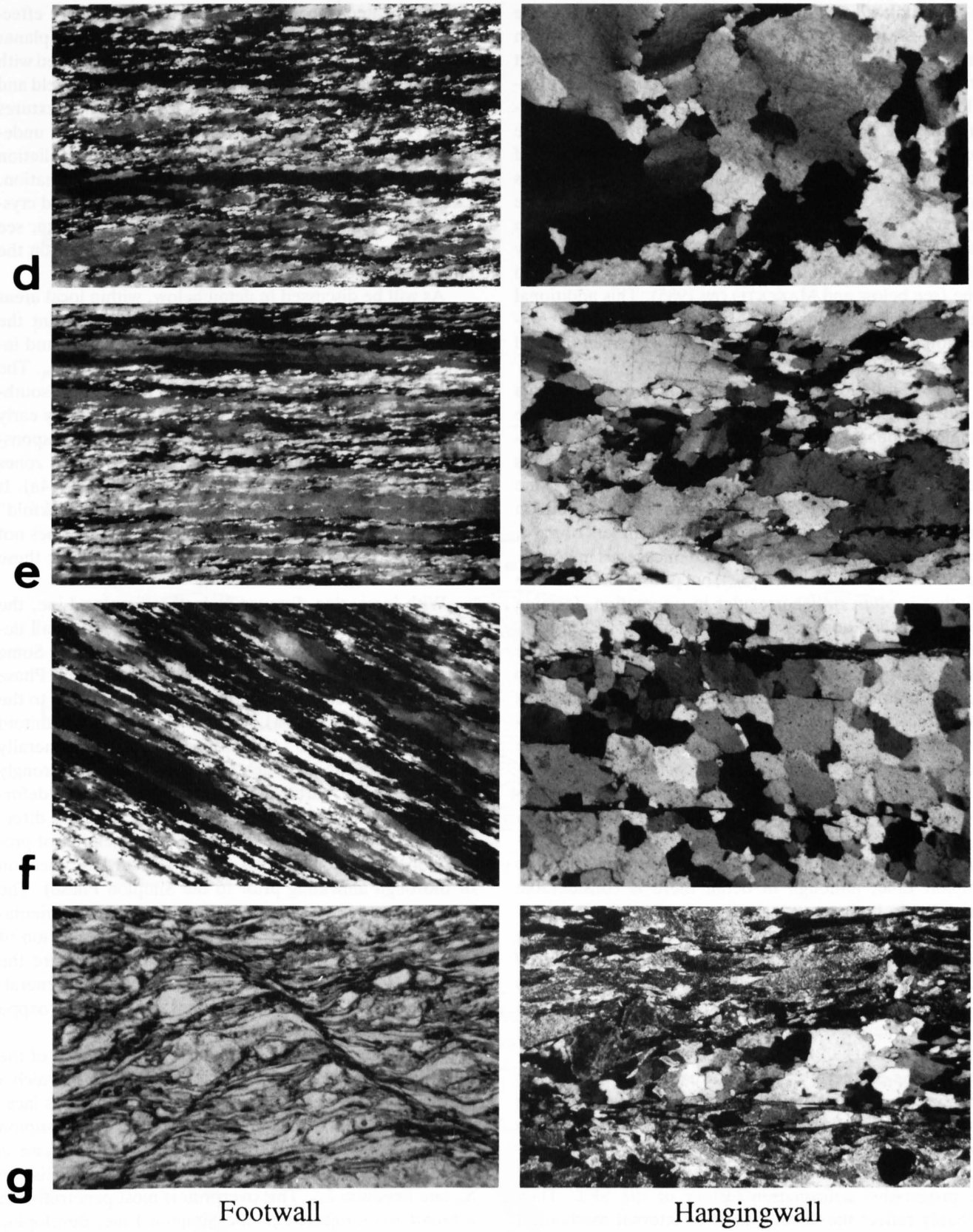

Fig. 13: Fabric difference across the Simplon Line as seen in the optical microstructure. (a)–(f) compare quartz-rich rocks (quartz veins and/or quartzites), (g) compares mica schists to either side of the Simplon Line. Width of field for all photomicrographs is 3.3 mm.

The *footwall* corresponds to the Lower Pennine Zone of MILNES et al. (1981). Within this block, the Simplon Phase of deformation is represented by two dominant structural elements: a foliation S_m and a variably developed lineation L_m (Figs. 6, 7, 8). The lineation is defined by the grain elongation (most clearly seen in the quartz veins and augen gneisses), by the alignment of elongate minerals (e.g. amphibole), by pressure shadows (commonly of chlorite on garnet, Fig. 12, but also of calcite on pyrite, Fig. 27) and as the fold axes and intersection lineation of tight to isoclinal folds, which are effectively parallel to the stretching lineation in the strongly foliated zone (see below and MANCKTELOW 1985). This additional intersection lineation is probably responsible for the compositional streaking which is commonly observed parallel to L_m.

The S_m foliation is particularly strongly developed in a broad, kilometre-wide zone immediately adjacent to the Simplon Line, resulting in a characteristic, flaggy topographic expression (Figs. 3, 4). In detail, where exposures are good (e.g. Monscera Pass and Bognanco Valley), the narrow (<10 m), brecciated zone marking the Simplon Line is often underlain by several tens of meters of dark, green-grey, fine- to very fine-grained micaceous mylonite. This unit is very well foliated (S_m), but poorly lineated. The foliation is often rather irregular in orientation, forming open basins and domes with a wavelength of 1–2 m (e.g. Monscera Pass). These rocks grade in turn into lighter coloured, strongly foliated (S_m) and lineated (L_m), fine- to medium-grained, quartzo-feldspathic mylonitic gneisses and micaceous schists. The darkening in colour with decreasing grainsize towards the Simplon Line is due to the breakdown of the originally rather coarse-grained, separated porphyroblasts of biotite and white mica into fine-grained cleavage platelets scattered throughout the rock. In general, the degree of foliation decreases and the grainsize increases in a gradual manner with distance from the Simplon Line, although in detail there is considerable variability in both parameters.

In strongly foliated zones, the S_m foliation is itself often overprinted by a *"shear band" foliation* or *extensional crenulation cleavage* (Figs. 9–12, cf. WHITE 1979, GAPAIS & WHITE 1982, PLATT & VISSERS 1980). The intersection trace of this new S_s foliation on the S_m plane makes a large angle with the lineation L_m, but is seldom strictly perpendicular. The geometry of the shear bands and their use as kinematic indicators is discussed further in the following section. Occasionally, the development of shear bands is so pervasive as to form the dominant foliation. The generation of the shear bands must have been a late-stage event in the progressive deformation history of the SFZ. They probably reflect the development of internal mechanical instabilities during the continued deformation of an already highly foliated, anisotropic rock (cf. COBBOLD et al. 1971, WHITE et al. 1980).

Along much of the strike-length of the SFZ considered here, the quartz veins of the footwall mylonites adjacent to the Simplon Line are very strongly foliated and generally clearly lineated, have a fine average grainsize, are effectively concordant with the foliation, and are very planar and elongate in shape. The difference when compared with quartz veins of the hangingwall is very clear in the field and is reflected in the optical microstructure and textures (Figs. 13, 14). Less common are late, irregular, undeformed quartz veins which crosscut the mylonite foliation and obviously postdate the Simplon Phase deformation. Late fissure veins, containing euhedral, undeformed crystals (predominantly quartz, adularia and muscovite, see STALDER et al. 1973) also occur, and place a limit on the minimum age of the Simplon Phase.

As will be discussed in detail below, within local areas there are major structures which variably overprint the SFZ, developing folds and associated crenulation and intersection lineations within the Simplon foliation S_m. The major folds have a vergence directed towards the southeast, which led to their being termed "backfolds" by early Alpine geologists. These backfolds are directly responsible for the steeply-dipping northern and southern zones within the Pennine Alps (e.g. Fig. 1 in MILNES 1974*a*). It should be emphasized, however, that the term "backfold" is based purely on the vergence of the folds, and does not necessarily imply an isochronous development for these structures.

With increasing distance from the Simplon Line, the intensity of S_m foliation development in the footwall decreases and the overprint is less pervasive. Some lithologies are still clearly affected by the Simplon Phase (e.g. the Lebendun Series in the region around and to the south of Alp Veglia), whereas massive granitoid lithologies (e.g. the Antigorio Gneiss) are generally weakly overprinted, though still with occasional strongly foliated zones. Quartz veins, where they contain a deformational fabric, usually still show the L_m lineation direction, presumably because they have little memory of pre-Simplon Phase deformation (either due to late injection or thorough annealing prior to the Simplon Phase). The host gneisses, however, display a more variable orientation of the mineral lineation due to the superposition of pre-Simplon and Simplon strain increments. Where the Simplon overprint is weak, the gneiss lineation is generally oriented NW–SE, related perhaps to the earlier nappe emplacement direction (MERLE et al. 1986).

In summary, the SFZ can be described in terms of the following structural elements: the hangingwall, in which a pervasive ductile overprint of the Simplon Phase is lacking, separated by a structural discontinuity (the Simplon Line) from the footwall, in which the Simplon Phase is clearly discernible and has produced a pervasive foliation S_m and lineation L_m. This overprint is most penetrative in a broad zone adjacent to the Simplon Line, developing mylonitic microstructures and strong textures, but can also be observed more variably developed throughout the studied extent of the footwall. The cataclasites of the Simplon Line brecciate ductile mylonites of the footwall and are clearly younger.

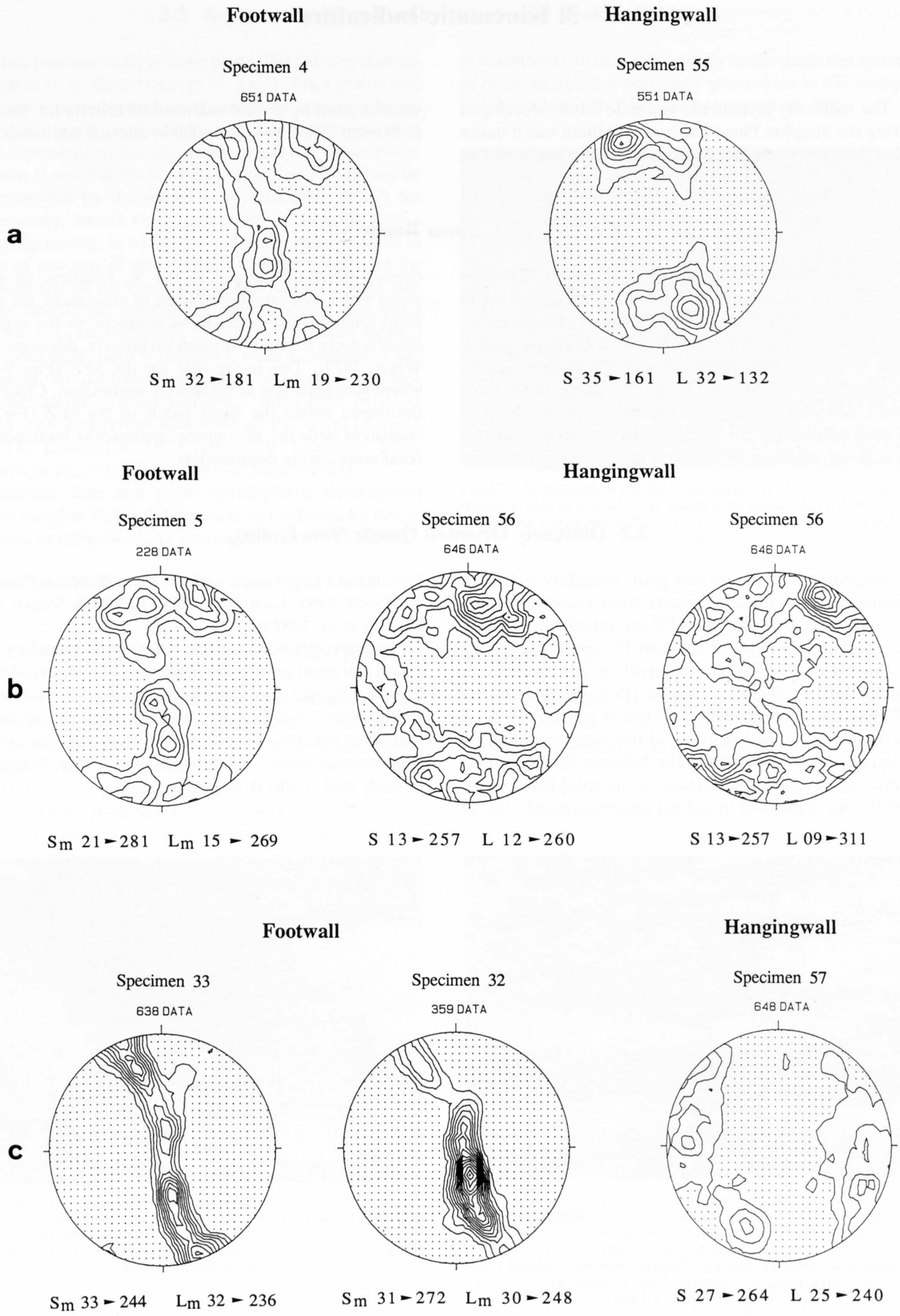

Fig. 14: Fabric difference across the Simplon Line as seen in the measured quartz *c*-axis textures. Textures from the footwall are related to the L_m lineation, plunging towards the WSW. Textures from the hangingwall are clearly not related to this direction; where clear patterns exist (as in the selected examples), they appear to be related to a SE–NW directed movement direction.

3. Kinematic Indicators

The markedly asymmetric tectonite fabrics developed during the Simplon Phase indicate that there was a major shear component to the deformation. The sense of this shear is given by several independent criteria (cf. SIMPSON & SCHMID 1983) with remarkable internal consistency.

3.1 Shear Bands

Strongly foliated mylonites often contain a conjugate set of two spaced, overprinting foliations making an angle of around 30–35° to the mylonitic foliation ("shear bands", WHITE 1979, GAPAIS & WHITE 1982; or "extensional crenulation cleavage", PLATT & VISSERS 1980). In thin section, the shear band foliation is defined by small, fairly short shear zones with further grain size reduction, which offset the earlier foliation. The sense of offset on each of the two shear band foliations is opposite and corresponds to an overall extension parallel to the S_m foliation. In shear zones with a well established sense of movement, the shear band foliation with shear sense synthetic to the regional shear is more strongly, or often exclusively, developed (cf. WHITE 1979). This is the case for the SFZ (Figs. 9–11), where conjugate sets are relatively uncommon. Chlorite is developed within the shear bands of the SFZ (Fig. 12), consistent with the retrograde, greenschist metamorphic conditions during deformation.

3.2 Obliquely Oriented Quartz New Grains

Subgrains, new grains and grain boundary bulges in dynamically recrystallizing quartz from mono-mineralic, fine-grained veins within the SFZ are invariably elongate and aligned at an angle of between 10° and 25° to the S_m foliation (Fig. 15). Within the field of recrystallization dominated by subgrain rotation (POIRIER & NICOLAS 1975), this oblique grain-shape fabric is considered to be the result of continual resetting of this dimensional fabric by dynamic recrystallization. The foliation S_B then represents a much smaller increment of the total finite strain than the S_A fabric, and in a shear deformation will, therefore, make a larger angle with the shear direction (SIMPSON & SCHMID 1983, LAW et al. 1984, LISTER & SNOKE 1984, SCHMID et al. 1987*a*).

In coarse-grained samples, where grain boundary migration and grain growth are important, the observed angle between S_A and S_B is much larger (Fig. 16, LAW et al. 1984), often exceeding 45°, and this explanation can no longer be tenable. Similar results were reported in the experimental shear experiments on Carrara Marble of SCHMID et al. (1987*a*).

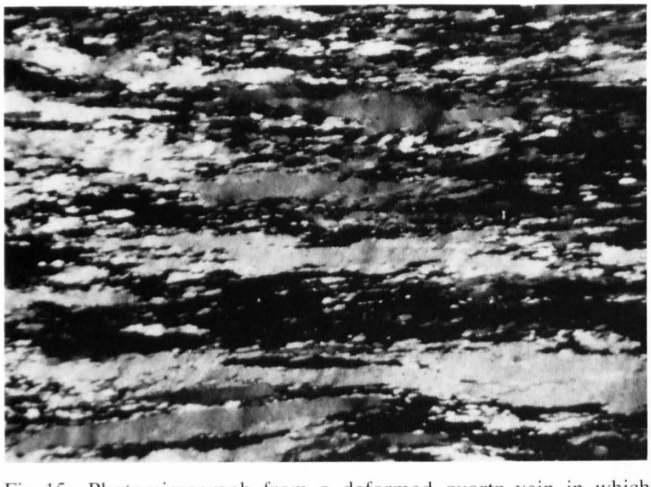

Fig. 15: Photomicrograph from a deformed quartz vein in which there is a low angle between the two dimensional shape fabrics S_A (parallel to the dominant foliation S_m) and S_B. Such microstructure is typical of the finer-grained quartz veins in which recrystallization is dominantly by subgrain rotation. Sample from the footwall above Bielti, ca. 40 m from the Simplon Line (Coords. 643.14/122.22). Width of field is 3.3 mm.

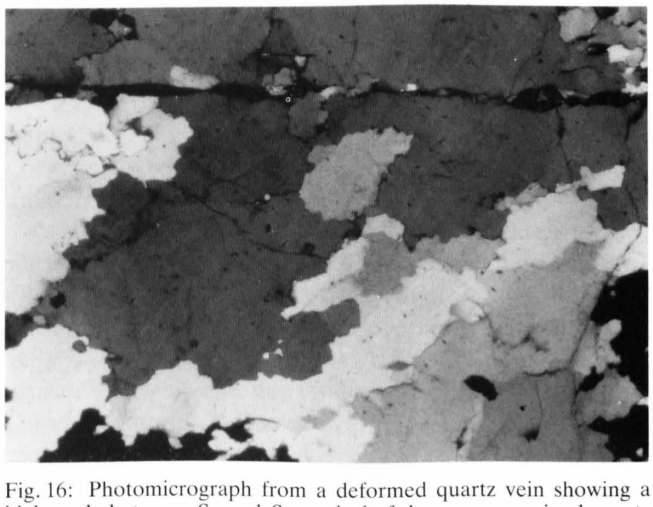

Fig. 16: Photomicrograph from a deformed quartz vein showing a high angle between S_A and S_B, typical of the coarser-grained quartz vein microstructures in which recrystallization is dominantly by grain boundary migration. Specimen 54 (Appendices B, C) from P. Diei. Width of field is 3.3 mm.

3.3 Asymmetric Mica Porphyroclasts and Broken Feldspars

Mica possesses only a single plane (001) of easy dislocation glide (e.g. ETHERIDGE et al. 1973). Mica grains are, therefore, incapable of homogeneous deformation by intracrystalline slip, and develop characteristic microstructures dependent on the original orientation of the individual grains (LISTER & SNOKE 1984). Their behaviour may be approximated by the model of ETCHECOPAR (1977) for plane strain, simple shear deformation of grains with a single slip system, in which the grains can be considered in terms of two sets of orientations. One set is oriented for synthetic slip on the single slip system and will rotate into an end orientation suitable for continued slip. The other set undergoes antithetic slip, deforming like books toppled on a bookshelf, until it reaches a locked orientation unfavourable for continued slip. These orientations produce the characteristic, porphyroclastic "mica fish" in shear zones, with geometries indicative of the sense of shear (Fig. 17, EISBACHER 1970, BURG & LAURENT 1978, SIMPSON & SCHMID 1983, LISTER & SNOKE 1984).

Feldspar does not show crystal-plastic deformation during Simplon Phase deformation but deforms by brittle fracture, commonly along cleavage surfaces. These fracture surfaces can then act similarly to the single slip systems in mica, to develop bookshelf geometries in the feldspar porphyroclasts (cf. Fig. 8*c* in MANCKTELOW 1985).

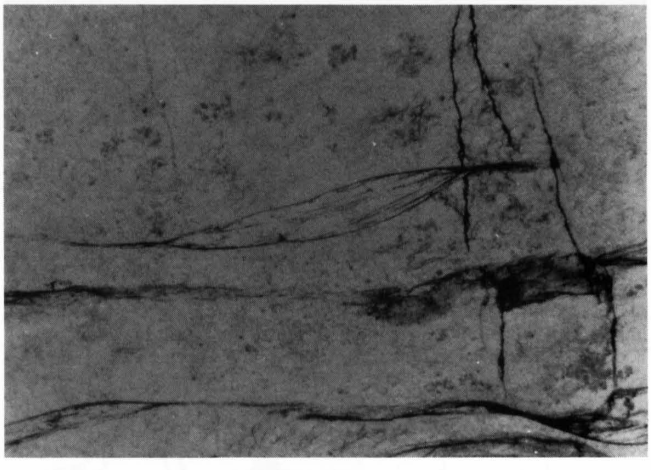

Fig. 17: Asymmetric mica fish indicating a dextral sense of shear. Border region of a quartz vein within mica schists of the Berisal unit. Specimen 8 (Appendices B, C) from above Bielti. Width of field is 3.3 mm.

3.4 Quartz Texture Asymmetry

Quartz textures measured from mono-mineralic veins within the mylonites and mylonitic gneisses of the foliated zone of the SFZ show a consistent pattern which departs markedly from orthorhombic symmetry (Appendices C, D). This is seen particularly clearly in the *c* (the pole to [0001] and <*a*> (pole to [1120]) fabrics. In general, there is a single strong <*a*> maximum developed between 20° and 30° to the lineation in the *XZ* plane. The *c*-axes define a variably kinked single girdle, occasionally with weakly developed vestiges of the missing crossed girdle segments. Such patterns are common in many low to moderate temperature deformation zones with a strong shear component. It is invariably observed that the sense of asymmetry of the quartz textures involves a rotation of the pattern *with* the sense of shear (e.g. BOUCHEZ 1978, SCHMID et al. 1981, BOUCHEZ et al. 1983, SIMPSON & SCHMID 1983).

3.5 Asymmetric Boudins

Boudinage of more competent layers, when observed in the SFZ, initiates by failure along a plane of synthetic shear, developing asymmetric trains of slightly offset boudins indicative of the sense of shear (Fig. 18). The necks of these boudins are approximately perpendicular to the stretching lineation L_m.

3.6 Asymmetric Fibre Growth

This is observed as a stepping of quartz or calcite fibres on the foliation surface (e.g. Fig. 19) and is restricted to areas of low temperature deformation. The surfaces always "step down" in the direction of shear, so that the surface appears smooth when the hand is rubbed in the direction of shear and rough for the opposite direction. The fibre elongation is parallel to the movement direction. The fibres develop during dilational shear along a discrete surface, the individual fibres growing parallel to the incremental elongation direction, probably by a mechanism of crack-seal (Fig. 13.33 in RAMSAY & HUBER 1983).

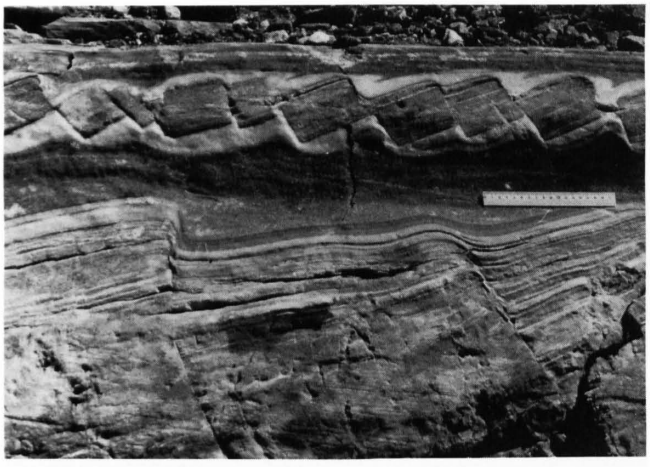

Fig. 18: Asymmetric boudinage of a dolomite layer within calcite marble from the presumably Mesozoic (Triassic?) cover of the Berisal unit. For this view towards the southeast, the shear sense is dextral. From the same outcrop location as Specimen 24 in the Kaltwasser area (Appendices B, C).

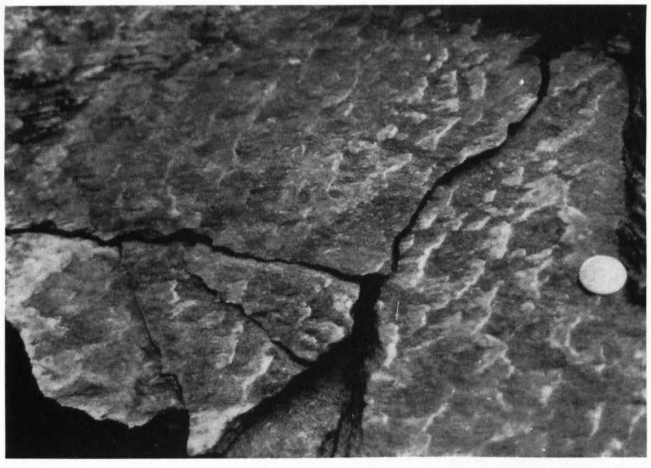

Fig. 19: Stepped calcite fibres plunging ca. 27° → 240°, from a road-cutting between Gampel and Hohten (Coords. 624.15/129.60). Viewed into the ground towards the southeast, the shear shear is dextral.

4. Regional Geometry and Kinematics

4.1 Introduction

The geometry and kinematics of the SFZ, as determined in the ductile mylonites of the footwall, is remarkably consistent and fairly simple: the hangingwall has moved down towards the WSW (→240–245°) relative to the footwall, with a major normal fault component (Figs. 20, 21, Plate). This is clearly demonstrated by the numerous kinematic indicators and the cooling history of the blocks themselves (MANCKTELOW 1985). Variations to this simple picture will be discussed below, when considering particular structural domains. Basically, the regional shape is complicated by the existence of two steep belts (the northern and southern steep belts of MILNES 1974*a*) related to south vergent "backfolds", and by a gradual change towards the northeast of the regional structural

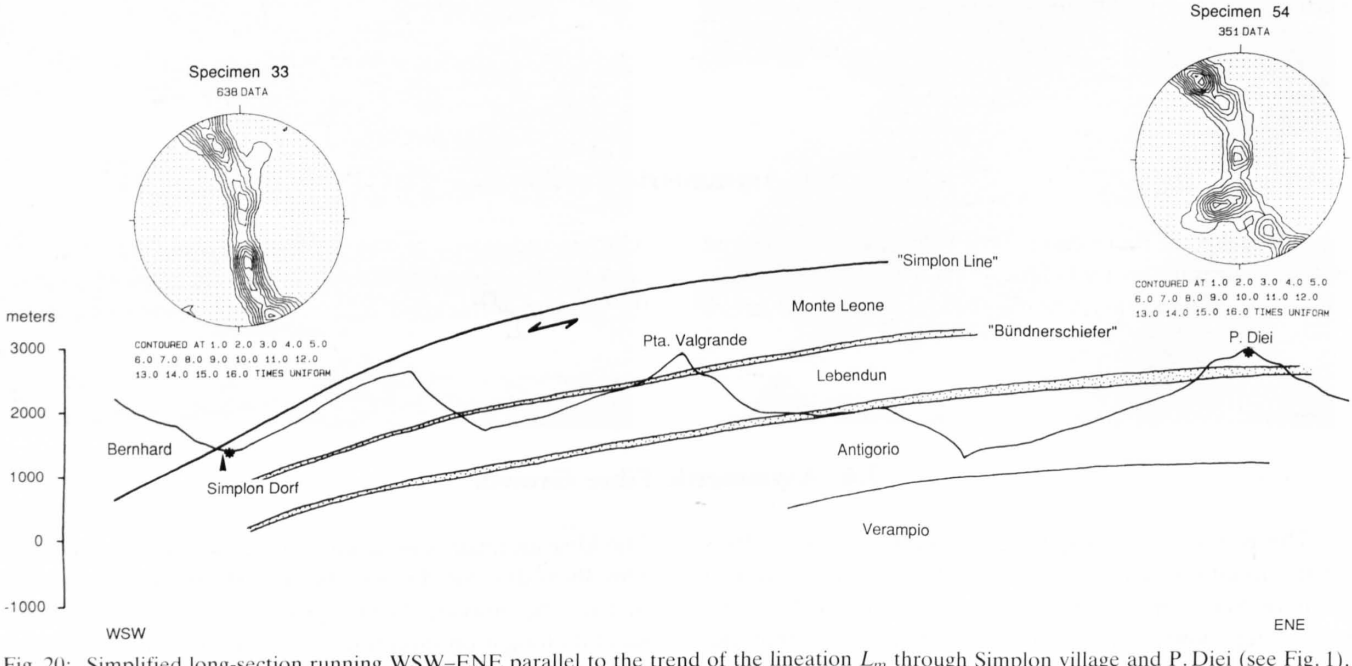

Fig. 20: Simplified long-section running WSW–ENE parallel to the trend of the lineation L_m through Simplon village and P. Diei (see Fig. 1). Note the consistent sense of shear, as demonstrated by the asymmetric quartz textures at these two localities, indicating a normal fault displacement of the upper block down towards WSW.

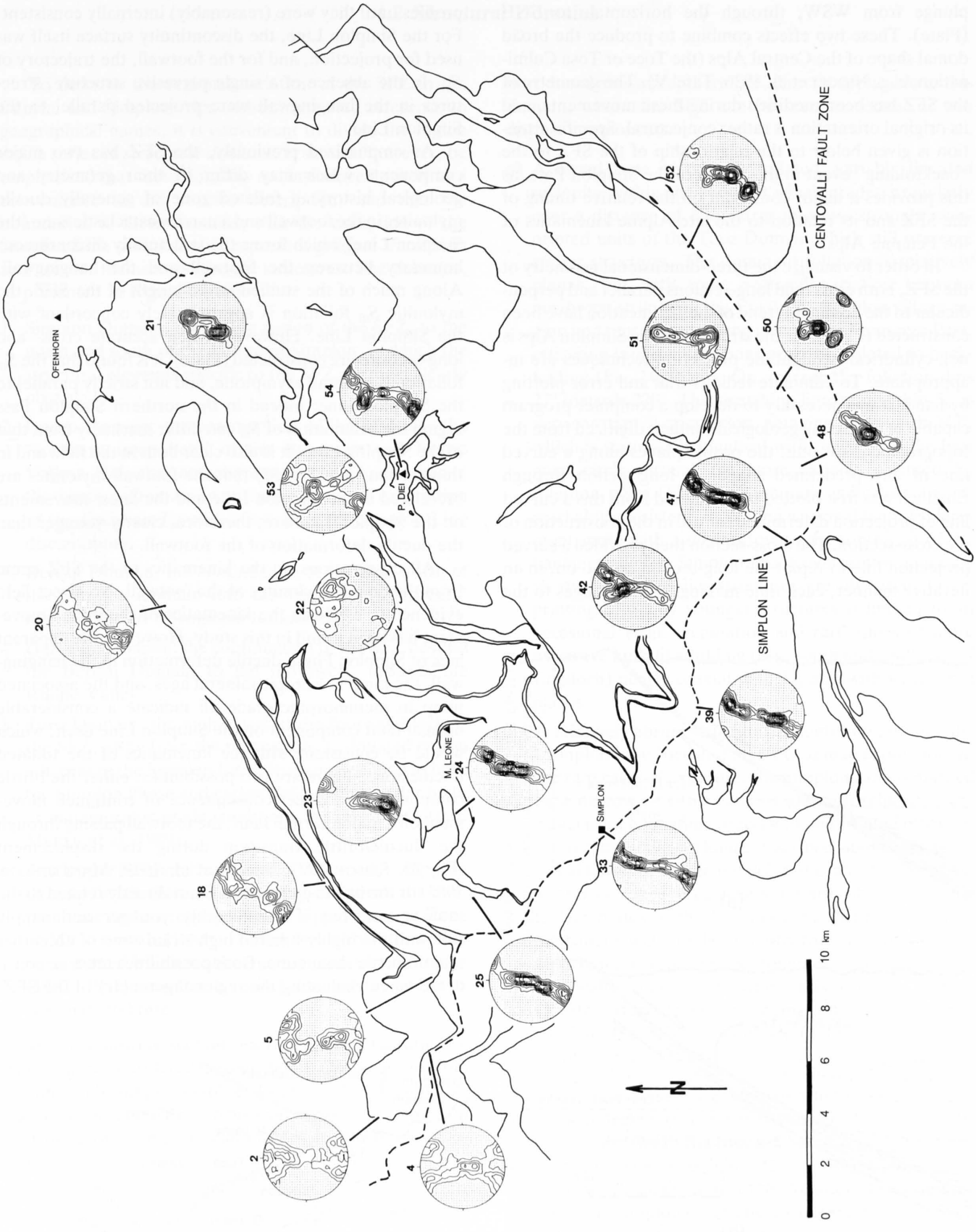

Fig. 21: Tectonic map of the Simplon Alps with some of the measured quartz textures indicated. The stereograms are oriented as in Figs. B_1 and B_2 (Appendix B), such that the effects of the later backfolding is eliminated and the very consistent shear sense related to the ductile component of the SFZ is obvious.

plunge from WSW, through the horizontal, to ENE (Plate). These two effects combine to produce the broad domal shape of the Central Alps (the Toce or Tosa Culmination, e.g. NIGGLI et al. 1936, Tafel V). The geometry of the SFZ has been modified during these movements, and its original orientation is rather conjectural. Specific attention is given below to the relationship of the SFZ to the "backfolding" event in the region of the Simplon Pass, as this provides a major constraint on the relative timing of the SFZ and its relation to the late-Alpine kinematics of the Pennine Alps.

In order to visualize the three-dimensional geometry of the SFZ, both cross- and long-sections parallel and perpendicular to the dominant trend of the L_m lineation have been constructed (Plate). As the structure of the Simplon Alps is non-cylindrical, straightline projection techniques are inappropriate. To eliminate tedious trial and error plotting by hand, it was necessary to develop a computer program capable of projecting geological contacts digitized from the topographic maps onto the profile planes along a curved line of any predefined shape. A long-section through Engiloch was first plotted by hand, and from this a curved line of projection determined for use in the construction of the cross-section. The cross-section then provided a curved projection line to replot the long-section and so on, in an iterative manner, each time making minor changes to the profiles until they were (reasonably) internally consistent. For the Simplon Line, the discontinuity surface itself was used for projection, and for the footwall, the trajectory of S_m. In the absence of a single pervasive structure, structures in the hangingwall were projected parallel to the Simplon Line.

As emphasized previously, the SFZ has two major components which may differ in their geometry and geological history: a foliated zone of generally ductile mylonites in the footwall and a narrow cataclastic zone (the Simplon Line) which forms the structurally discontinuous boundary between the footwall and the hangingwall. Along much of the studied strike-length of the SFZ, the mylonitic S_m foliation is approximately concordant with the Simplon Line. However, when accurate cross- and long-sections are constructed (Plate), it is found that the S_m foliation is in detail asymptotic, and not strictly parallel to the Simplon Line; indeed in the northern Simplon Pass region the orientation of S_m can differ markedly from that of the Simplon Line. It is also clear both in the field and in thin section (e.g. Fig. 37) that the footwall mylonites are brecciated at the Simplon Line and the latest movements on the Simplon Line are, therefore, clearly younger than the ductile deformation of the footwall.

All observations on the kinematics of the SFZ come from the ductile mylonites of the footwall. No direct field evidence to establish the kinematics of the brittle movement has been found in this study. However, the apparent lack of Simplon Phase ductile deformation in the hangingwall, the jump in isotopic mineral ages, and the associated jump in metamorphic grade all indicate a considerable normal fault component on the Simplon Line itself, which would be consistent with the kinematics of the foliated ductile zone. There are two possibilities: either the brittle component is a direct consequence of continued movement on a major normal fault, the footwall passing through the ductile/brittle transition during the displacement (Fig. 22, SIBSON 1977, SIBSON et al. 1979, MANCKTELOW 1985) or the brittle component is not directly related to the same event, but is considerably younger and simply followed the highly foliated high strain zone of an earlier major ductile shear zone. Both possibilities must be considered when evaluating the regional geometry of the SFZ.

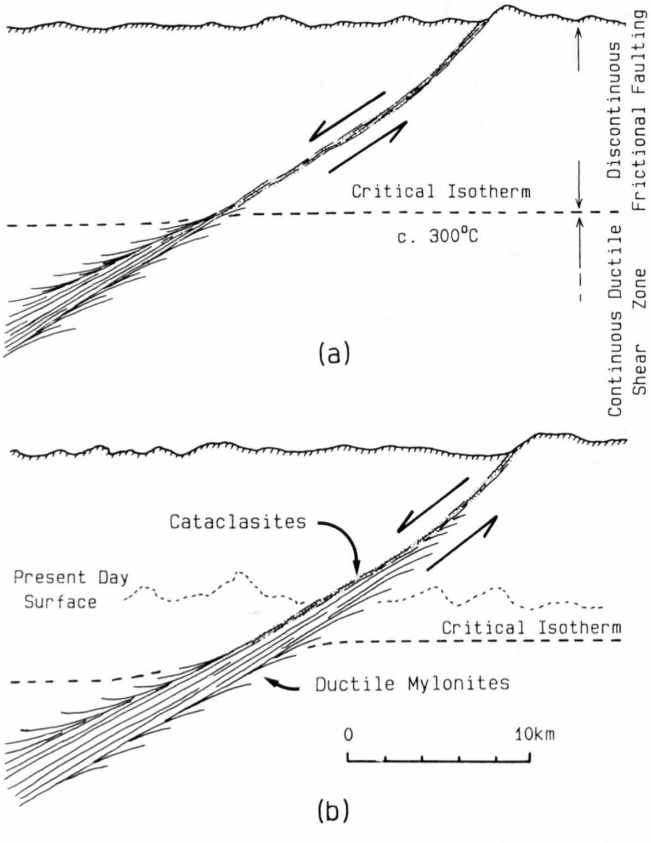

Fig. 22: Schematic section through a major normal fault zone, indicating the gradual transition from a narrow cataclastic fault to a broader ductile shear zone at depth, below a critical isotherm. With increasing displacement along this fault zone, the ductile mylonites of the footwall may be carried through the brittle-ductile transition, such that further displacement at this level is concentrated within a narrow cataclasite zone and the mylonites are passively transported within the footwall (from MANCKTELOW 1985, after SIBSON 1977 and SIBSON et al. 1979).

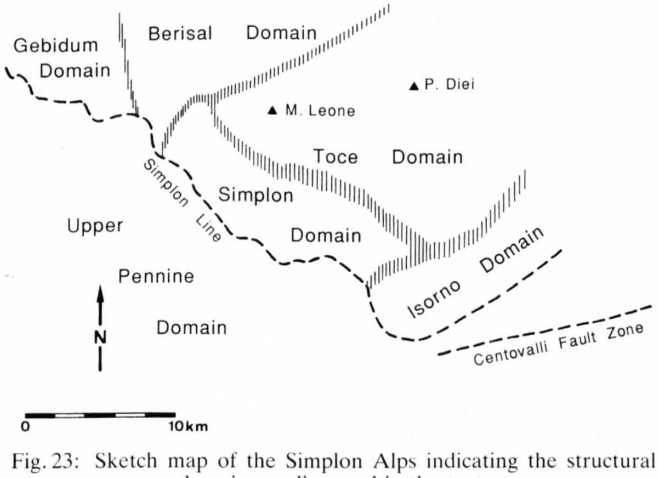

Fig. 23: Sketch map of the Simplon Alps indicating the structural domains as discussed in the text.

4.2 Structural Domains

To describe the regional variation of the SFZ in the Central and Simplon Alps without repeated reference to geographical names, it is convenient to divide the region into a series of *structural domains*. It should, however, be emphasized that these domains are introduced purely as a convenience to aid concise description, and that the boundaries to these domains, with the exception of the Simplon Line discontinuity, represent gradual transitions and are not themselves discrete structures. The domains, as presented in Figure 23, are:

1. Simplon Domain: the classic region of the SFZ, to the north and south of the village of Simplon, in which the structural elements specific to the SFZ are most clearly observed.
2. Isorno Domain: the continuation of the SFZ into the "southern steep belt" of the Bognanco and Isorno Valleys. Here the geometry is more complicated than in the Simplon Domain, with variation in the orientation of the lineation L_m and a less clear-cut Simplon Line discontinuity.
3. Berisal Domain: the continuation of the SFZ north of the Simplon Domain into the "northern steep belt" region affected by regional backfolding.
4. Gebidum Domain: the continuation of the SFZ beyond the Berisal Domain to the northwest, towards the Rhone Valley.
5. Toce Domain: the major part of the footwall block of the SFZ, away from the pervasively S_m-foliated region adjacent to the Simplon Line. Structures related to both the Simplon Phase and earlier deformation under higher metamorphic grade conditions are discernible (e.g. MERLE et al. 1989).
6. The Upper Pennine Domain: this is a broad, composite domain for all units of the hangingwall above the Simplon Line and corresponds to the Upper Pennine Zone of MILNES et al. (1981). During this work, it has only been studied where it abuts the Simplon Line. MÜLLER (1982, 1983) provides a recent detailed review of its regional structure.

In the following section, each of these structural domains will be considered in some detail. Observations from the relatively simple Simplon, Isorno and Gebidum Domains are presented first, to provide a basis for comparison with the more complex relationships in the Berisal Domain.

4.2.1 Simplon Domain

It is within this domain between Engiloch, south of the Simplon Pass and the Bognanco Valley, west of Domodossola (see Fig. 1), that the geometry and kinematics of the SFZ are most clearly observed (e.g. BEARTH 1956*b*, MANCKTELOW 1985). The general observations on the SFZ introduced above are, therefore, directly applicable to this domain, where the SFZ can be seen to consist of two distinct components:

a) A broad zone of strongly foliated, variably lineated mylonite within the footwall which grades irregularly over a distance of kilometres into less strongly overprinted units of the Toce Domain which still preserve earlier structures. The dominant foliation is relatively planar, but with some regional variation between northwest striking in the Engiloch–Simplon village region and more east striking around the Monscera Pass, reflecting broad undulations probably related to backfolding (Fig. 24, Plate). On average the foliation dips 27° towards 220°. The stretching lineation within S_m is very constant in orientation, plunging 25° towards 243°, which is statistically identical with the pole to the best great circle through the more variable oriented S_m foliation poles (Fig. 24). Kinematic indicators are remarkably consistent, indicating a normal fault displacement sense with a downthrow to the southwest of the hangingwall. The Simplon Phase overprint is generally so strong that earlier structures are obscured. Overprinting of S_m by younger structures is limited to an occasional weak crenulation and rare zones of more extensive kink-like folding (e.g. south and southeast of Engiloch) nearly coaxial with L_m and with steep axial planes.

b) A relatively abrupt structural discontinuity, termed the "Simplon Line" because of its linear map expression. In the rare cases of exposure, the Simplon Line is marked by a narrow (<10 m) zone of greenish (chlorite-rich) cataclasite, containing brecciated and rotated blocks of the more ductile mylonite described above and occasional lenses of brecciated dolomitic marble. Occasional narrow zones of cataclasis are also observed within the mylonites of the footwall zone. Structures within the hangingwall are discordantly truncated by the Simplon Line, whereas the S_m foliation of the footwall is practically concordant within this domain (Plate). Quartz textures from the hangingwall are clearly unrelated to the SFZ, in contrast to textures from the footwall (Figs. 13, 14).

The nature of the two components to the Simplon Fault Zone is reflected in the ease with which they can be mapped in the field. The broad foliated zone of the footwall is relatively easy to delineate; its position along strike is predictable from the trend of the foliation. This is not the case with the Simplon Line. The discontinuity surface itself is seldom exposed and accurate, direct measurement is practically impossible. Its position and orientation must be interpreted from mapping of the distinct blocks to either side. This problem becomes critical in regions more complex than the Simplon Domain (in particular the Berisal Domain, see below) and is also significant in determining the degree of concordance between the Simplon Line and the S_m foliation of the footwall.

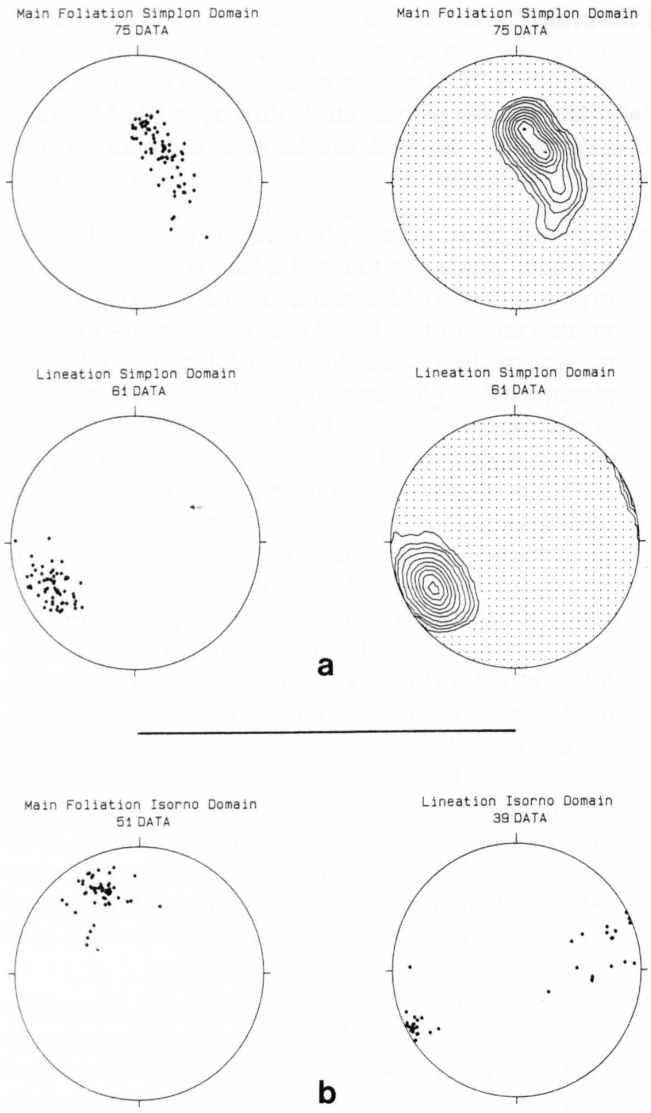

Fig. 24: Orientation data for Simplon and Isorno Domains.

(a) Orientation data for the SFZ foliation S_m and lineation L_m in the Simplon Domain. The diffuse maximum for the S_m foliation lies between 35°→190° and 27°→220°; the pole of the best great circle through the poles to S_m plunges 24°→243° (cf. MANCKTELOW 1981*b*). This can be compared to the maximum for L_m, oriented 25°→243°.

(b) Orientation data for the Isorno Domain. The S_m orientation averages ca. 62°→155°. L_m is generally shallowly plunging, but shows considerable variation within the S_m plane.

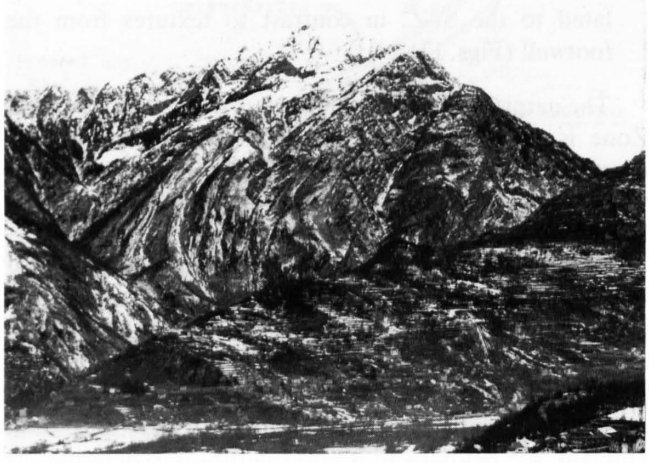

Fig. 25: View to the northwest towards Crevola in the Ossola Valley. The broad antiformal bend of the dominant foliation (S_m of the SFZ footwall) into the "southern steep belt" is clear.

4.2.2 Isorno Domain

The transition from the Simplon to the Isorno Domain is marked by a rapid but gradational swing in orientation of the S_m foliation in the area of San Lorenzo, at the head of the Bognanco Valley, as the SFZ enters the "southern steep belt" (Fig. 25). After this transition, the foliation in the Isorno Domain dips consistently steeply southeast (av. 62° towards 155°, Fig. 24). The lineation is usually shallowly plunging within this foliation, varying from generally southwest plunging in the southwestern section of the domain to shallowly to moderately northeast in the northeastern part of the domain. The projection of the Isorno Domain parallel to this lineation onto the profile of the Plate plots within a very small region and provides little information on the extent of this steep belt in the SFZ. In particular, the Simplon Line has only a short steep segment when projected parallel to this curved, but generally shallowly plunging, lineation. In the absence of seismic reflection profiles, subsurface information is completely lacking south of Domodossola, and hence the Simplon Line in the cross-section of the Plate ends to the southeast in a question mark. From the general form of the Simplon Line in this cross-section, however, it is possible that the discontinuity surface, south of this short steeper segment, may continue with a pitch angle of ca. 10–15° to the southeast. This minor fold structure may have its equivalent in the Masera Synform (MILNES 1979, MILNES et al. 1981) of the hangingwall. As can be seen from the cross-section of the Plate, the foliation S_m of the footwall in this domain appears to steepen more rapidly to the southeast than does the Simplon Line, such that a small angular discordance develops.

Compared to the Simplon Domain, the quartz veins and gneisses of the Isorno Domain are more strongly recrystallized and have a coarser grainsize due to advanced grain boundary migration. The measured textures are also more diffuse. Dynamic grain boundary migration (and an associated increase in grainsize) becomes more important towards the northeast. This strongly modifies the microstructure and texture such that the L_m lineation is often poorly defined and becomes difficult to establish as a true mineral stretching lineation. The kinematics, as established from asymmetric quartz textures, appears consistent at least as far as the Isorno Valley (Figs. 1, 21), indicating a dextral horizontal shear component for the present, generally shallowly plunging lineation orientation.

Simplon Phase retrograde metamorphism, with the development of chlorite at the expense of garnet and biotite, is much less pronounced in this domain than in the adjoining Simplon Domain. It is largely restricted to the immediate vicinity of the Simplon Line (e.g. near Cisore, Fig. 1). Together with the change in the deformational microfabric, this suggests a gradual increase in the temperature in the footwall block from northwest to southeast, probably indicating deeper structural levels during SFZ movement. Indeed, the distinction in structural style between footwall and hangingwall appears to decrease along the Isorno Valley towards the Swiss border in the east, and a distinct Simplon Line eventually becomes indiscernible. Rather, the SFZ appears to continue to the ENE as a broad

foliated zone parallel to the axial plane of the possibly coeval Wandfluhhorn Fold (MANCKTELOW 1985, KLAPER 1988). This could correspond to lower structural levels below the "critical isotherm" for ductile deformation of quartz-rich rocks in both the hangingwall and the footwall (Fig. 22).

4.2.3 Gebidum Domain

Northwest of the Tochuhorn area, away from the complications of the late backfolds (the Berisal Domain discussed below), the geometry is again relatively simple. This area is unfortunately one of rather poor outcrop and the precise location of the Simplon Line can seldom be mapped directly. However, due to the clear fabric boundary between footwall and hangingwall (Figs. 13, 14), its location can be quite well constrained and corresponds closely with the position postulated by BEARTH (1956*b*), SPICHER (1980) and STECK (1984, 1987).

The Gebidum Gneiss (STRECKEISEN et al. 1978) clearly lies within the footwall foliated zone, generally with a mylonitic S_m foliation dipping ca. 30° towards the west or southwest. The stretching lineation on average plunges 28° towards 231° (Fig. 26) and the quartz textures are directly related to this foliation and lineation. The grain shape fabric, and the asymmetry and degree of preferred orientation of the quartz textures is less marked than within the Simplon Domain (Appendix C). The microstructure and the increasing occurrence of brittle structures within the foliated zone suggest a steady decrease in temperature towards the northwest, i.e. towarts the Rhone Valley. Kinematic indicators, although less clear, are still consistent, indicating a downthrow to the southwest of the hangingwall block. A weak crenulation lineation on S_m plunging towards 260° is also visible in the more micaceous layers, and is most likely related to the similarly oriented late Berisal and Glishorn folds (see below).

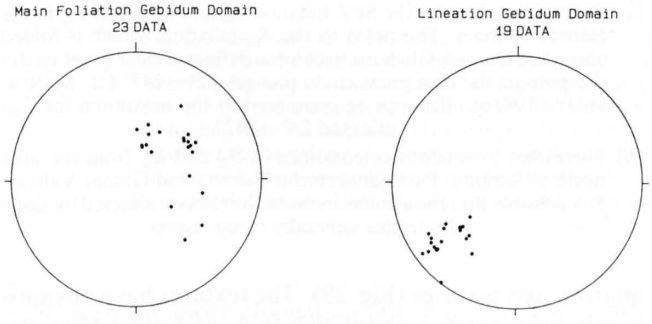

Fig. 26: Orientation data for the SFZ foliation S_m and lineation L_m in the Gebidum Domain.

The Staldener Lappen lithology clearly lies within the hangingwall. It consists dominantly of quartz-chlorite-muscovite schists, light coloured quartzites and impure sandstones. The thin quartz-rich layers are isoclinally folded with hinges plunging shallowly towards ca 260°, i.e. approximately coaxial with the L_m lineation in the footwall (cf. MANCEL & MERLE 1987). However, while the quartz vein textures from the northern footwall block are directly related to this lineation direction, textures from quartzites and quartz veins from the hangingwall block are clearly not Fig. 14). Instead they are related to a stretching lineation trending NW–SE, which is discernible in the field as a mineral stretching lineation at a high angle to the fold axes and the associated intersection and mica crenulation lineation. The fabric boundary is also very clear from the optical microstructure. Specimens from the footwall show evidence of extensive intracrystalline deformation (undulose extinction, deformation bands and lamellae), recrystallization by subgrain rotation and more limited grain boundary migration. Boundaries are irregular and lobate, with a correspondingly high surface energy (Fig. 13*a*, *b*). In marked contrast, the microstructure of hangingwall quartzite specimens shows evidence of extensive static recrystallization, with straight low energy boundaries and little preserved intracrystalline strain (Fig. 13*a*, *b*). This difference in structural history is also supported by the limited mineral ages from this area, which are consistently older in the hangingwall (e.g. HUNZIKER 1974).

Between the Staldener Lappen and the Gebidum Gneiss is a poorly outcropping zone which has been divided by BURRI (1979) and LEU (1986) into units belonging to the "Zone de Sion–Courmayeur" and the Mesozoic "Fäldbach Zone". The exact position of the Simplon Line within this zone is not unequivocally established. It is possible that the Simplon Line actually forms the contact between these two poorly outcropping zones. Further work may establish the true position, though considering the outcrop conditions, this is by no means certain.

A detailed investigation of the further continuation of the SFZ along the Rhone Valley is beyond the scope of the present study. However, DURNEY & RAMSAY (1973) and STECK (1980, 1984) have established the occurrence of a late stretching lineation of similar orientation to L_m throughout much of the western Helvetics and Aar Massif. The amount of extension in this WSW–ENE direction for rocks immediately adjacent to the Rhone Valley may be quite large (Fig. 27), consistent with that expected within the footwall of the SFZ. The kinematics are also similar, with a shear sense consistent with movement of the upper block down to the southwest (and a significant dextral transcurrent shear component in map view, cf. STECK 1984, Fig. 19). It appears likely, therefore, that the trace of the SFZ at the current erosion level continues further west within or adjacent to the Rhone Valley, and that the Helvetic domain to the north is within the footwall of this major shear zone. The Simplon Line discontinuity itself may form the northern contact to the Sion–Courmayeur Zone (cf. SPICHER 1980).

4.2.4 Berisal Domain

The Berisal Domain is geometrically complicated by the presence of at least three phases of post-nappe deformation, two of which produce major fold structures: tight to isoclinal recumbent folds and more upright "backfolds" with a southeasterly vergence. These structures are themselves overprinted by still younger, fairly upright, kink-like folds, which appear, however, to be of little regional significance.

Fig. 27: Calcite fibres developed on pyrite defining an elongation lineation plunging ca. 25°→235°, within grey Malm marbles on the north side of the Rhone Valley (Chalchofe quarry, west of Gampel, Coords. 622.30/129.27). Note the extreme extension consistent with the high strains within the footwall of the SFZ.

The orientation of the dominant foliation S_m is variable throughout the area, reflecting this large and small-scale folding. However, the fold-axes of these various folds are approximately coaxial with the elongation lineation L_m, and the orientation of this lineation is remarkably constant throughout the domain (Fig. 28*a*), plunging on average 23° towards 242°. The region between the Taferna river and the Simplon Pass road northwest of Ganter has slightly different orientations of S_m and L_m and the data are plotted as a separate subdomain in Figure 28*b*. These unusual orientations may be real, or they may simply reflect hill-slope creep in this steep region.

The major structures associated with the fold phases observed in the Berisal Domain will now be discussed in turn.

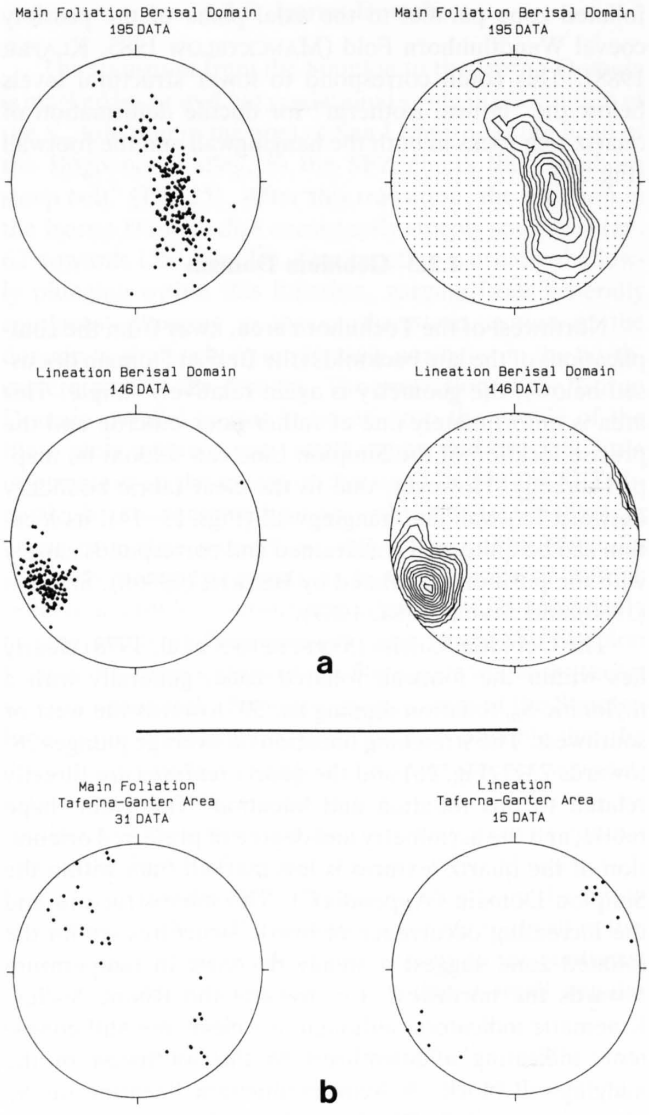

Fig. 28: Orientation data in the Berisal Domain.

(a) Orientation data for the SFZ foliation S_m and lineation L_m in the Berisal Domain. The poles to the S_m foliation, which is folded about the Berisal–Glishorn backfolds defines a clear great circle; the pole to the best great circle plunges 22°→247° (cf. MANCKTELOW 1981*b*). This can be compared to the maximum for L_m, oriented 23°→242°.

(b) Somewhat anomalous orientations of S_m and L_m from the area north of Simplon Pass between the Taferna and Ganter Valleys. It is possible that these measurements have been affected by slope slip in this generally steep region.

4.2.4.1 The Rotels–Monte Leone Recumbent Folds

These folds form a major, asymmetric *S* structure in the cross-sectional profile of the Plate. The upper, north-closing structure can be observed near Rotels on the Simplon Pass (the Rotels Fold) and the lower, south-closing fold forms a spectacular structure in the southeast cliff face of Monte Leone (the Monte Leone Fold, cf. Fig. 3 in MILNES 1973). In the hinge of the Rotels Fold, a very heterogeneously developed foliation, ranging from a weak crenulation to a mylonitic foliation, is discernible. The new cleavage is axial planar to folds in a pre-existing strong foliation and associated mineralogical banding in both the gneisses and the Mesozoic metasediments. On the limbs, a single strong foliation is generally observed, approximately parallel to the compositional banding. This is presumably a composite foliation. The axial plane foliation from the hinge region shows a stretching lineation statistically parallel to the fold axes and to the general Simplon Phase lineation in the footwall block, L_m, with an orientation ca. 25° → 245°.

Importantly, specimens from opposing limbs of the Rotels Fold show the same sense of movement relative to the stretching lineation. This is particularly clear from the quartz *c*-axis textures (Fig. 29). The textures have obviously not been rotated about this fold, and must have developed either by continued shearing of both limbs parallel to L_m during folding, or by overprinting and profound modification of a pre-existing structure.

4.2.4.2 The Mäderhorn–Wasenhorn–Rebbio Backfolds

In contrast, the more upright, south verging "backfolds" observable between Mäderhorn and Rebbio (cf. Plate I in MILNES 1974*b*) do not develop a clear axial plane foliation, but fold the earlier foliation and lineation. The fold axes and associated crenulation lineation have an orientation ca 15°→250–260°, making an acute angle of

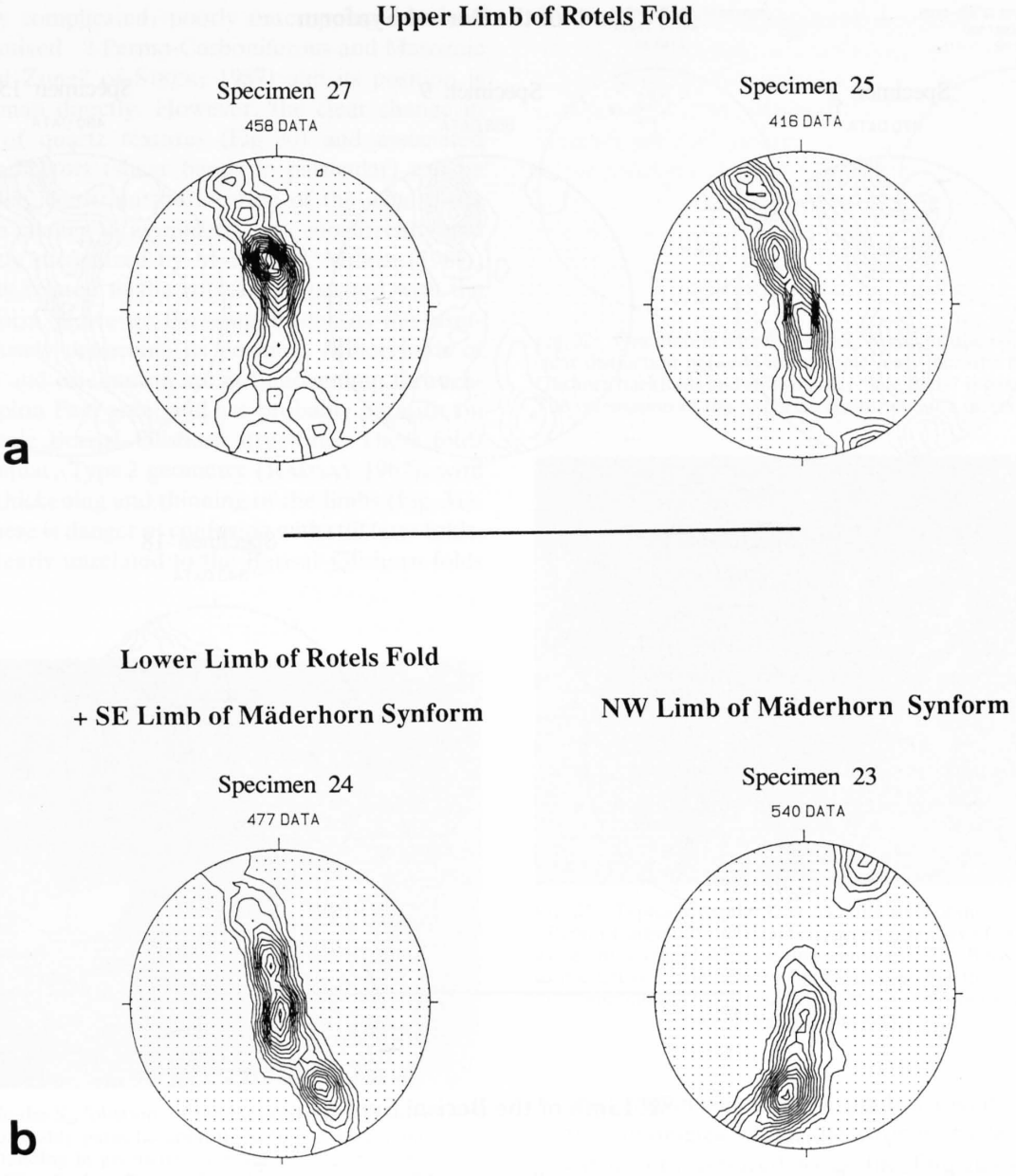

Fig. 29: Optically measured quartz *c*-axis textures showing the effect on shear sense of the major fold phases in the Simplon Pass to Kaltwasser region. Samples are oriented with the S_m foliation E–W and vertical and the L_m lineation horizontal, that is similar to Figure B_1, but with the important difference that in all cases we are looking into the ground towards the northwest (*N.B. this is not the same convention as in the Appendices*, where the effects of folding have been specifically eliminated to maintain a common kinematic orientation, cf. Fig. B_2). Refer to the Plate for the location of samples relative to the major structures; the interpreted sense of shear is also indicated on the cross-section of the Plate, with the arrowhead always pointing to the side which has moved out of the paper towards the viewer. Note that the shear sense is unchanged to either side of the Rotels Fold, but is reversed across the Mäderhorn Synform.

<20° with the older elongation lineation L_m. The quartz textures from similarly oriented specimens from opposing limbs of the Mäderhorn Synform are clearly rotated (Fig. 29*b*), reflecting a more or less passive rotation of the textures together with the fold limbs.

4.2.4.3 The Berisal–Glishorn Backfolds

The Berisal Synform–Glishorn Antiform backfold pair to the north of the Mäderhorn–Rebbio folds (Plate) show a similar geometry to that of the Mäderhorn–Rebbio Folds and may have developed during the same tectonic event. In the Simplon Pass area, the fold axes are approximately parallel to the Simplon Phase stretching lineation L_m (Fig. 28*a*, pole to best great circle through S_m foliation poles is oriented 22°→247°). In the few cases where small angular differences can be detected, the fold axes of the backfolds plunge towards ca. 250–260°, i.e. slightly north of the average L_m plunge direction (ca. 245°). Rotation of L_m on the limbs of Berisal–Glishorn folds does not result in any significant change in orientation of this lineation (Fig. 28*a*). The fold axial planes dip moderately towards the northwest, the dip increasing downward as the axial planes of the two major folds diverge from each other away from the Simplon Line (Plate). In the Simplon Pass region, the Berisal Synform is quite a tight structure and occurs in a

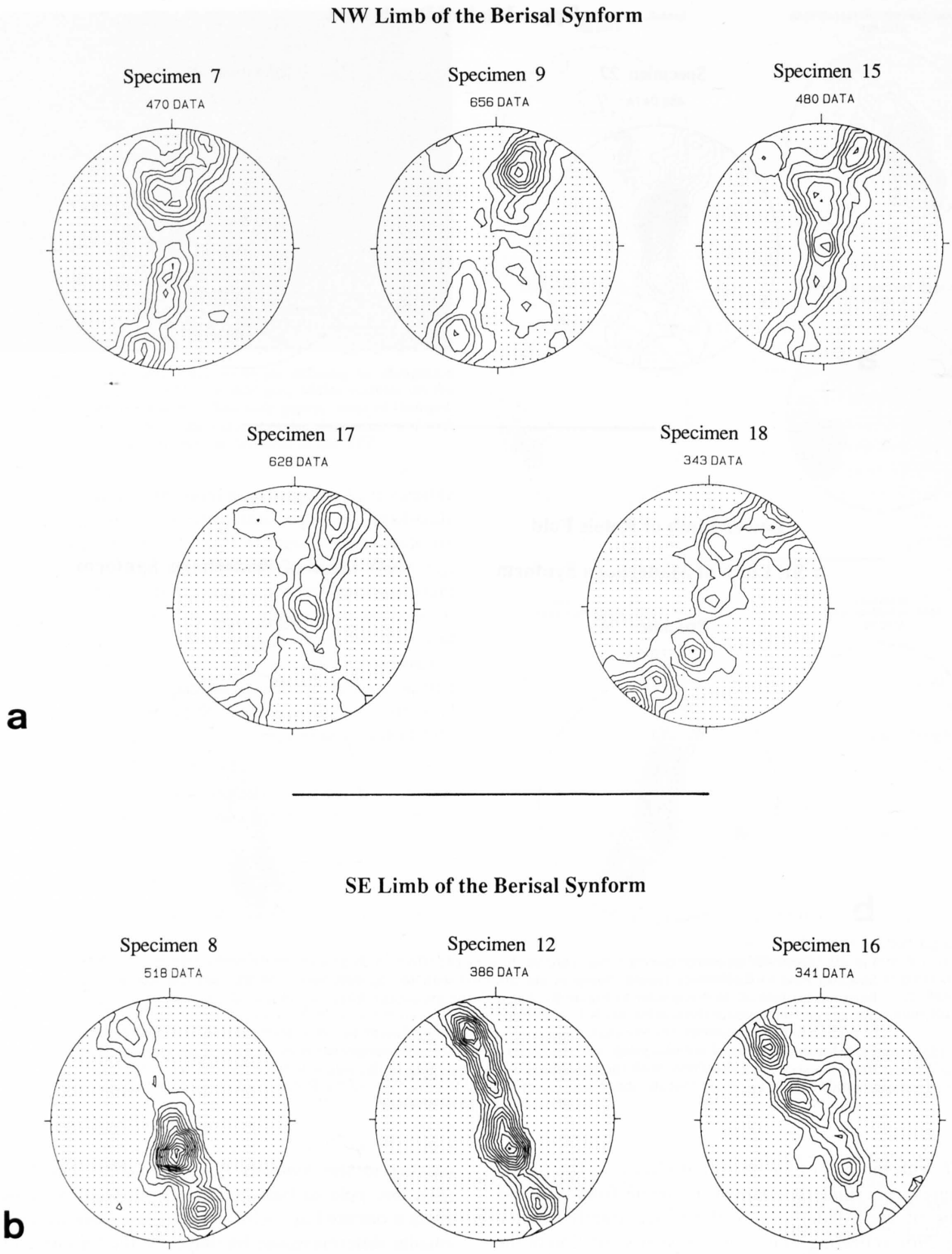

Fig. 30: Optically measured quartz *c*-axis textures showing the effect on shear sense of the Berisal Synform. The stereograms are oriented according to the convention established for Figure 29 and the locations relative to the Berisal Synform can be seen in the Plate. Note the clear reversal in shear sense across the Berisal Fold, as indicated by the opposite asymmetries of the quartz *c*-axis patterns in (a) and (b).

lithologically complicated, poorly outcropping area (involving the mixed ? Permo-Carboniferous and Mesozoic "Furgguwald Zone" of STECK, 1987) and its position is difficult to map directly. However, the clear change in asymmetry of quartz textures (Fig. 30) and associated kinematic indicators (shear bands in particular) can be used to closely constrain the location of the axial plane (Plate). This change in asymmetry was concurrently and independently recognized by MANCEL & MERLE (1987), and correctly related to the rotation associated with the Bersial Synform. However, the sampling density was insufficient to closely determine its position. Minor folds of similar style and orientation are not uncommon throughout the Simplon Pass area, and are probably parasitic on the larger-scale Berisal–Glishorn structures. These folds tend to a similar, Type 2 geometry (RAMSAY 1967), with clear hinge thickening and thinning of the limbs (Fig. 31). However, there is danger of confusion with still later folds, which are clearly unrelated to the Berisal–Glishorn folds (see below).

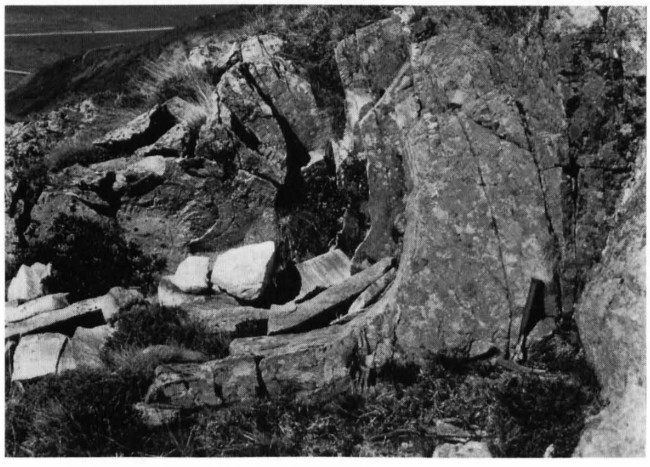

Fig. 31: Fold in the S_m foliation, of similar orientation to the Berisal Synform and probably parasitic upon it. Note the thickening in the hinge region, tending in geometry to a similar fold style. Between Bielti and the Simplon road (Coords. 644.60/121.17). Hammer for scale.

4.2.4.4 Late Folds

Late, open kink-like folds of the dominant S_m foliation are observed on the shared limb of the Glishorn–Berisal structures, which have the wrong vergence to be parasitic folds on these major backfolds (Figs. 32, 33). The presence of this additional phase of late folding, which is probably of little regional significance, further complicates the mesoscopic field relationships and makes the use of post-S_m fold vergence relationships rather unreliable.

4.2.4.5 The Relationship of the Backfolds to the Simplon Line

Study of the Simplon Line in the critical Bielti area of the Berisal Domain (Fig. 1) is impeded by poor outcrop conditions and the similarity of lithologies to either side. However, the location of the Simplon Line itself is clear from:

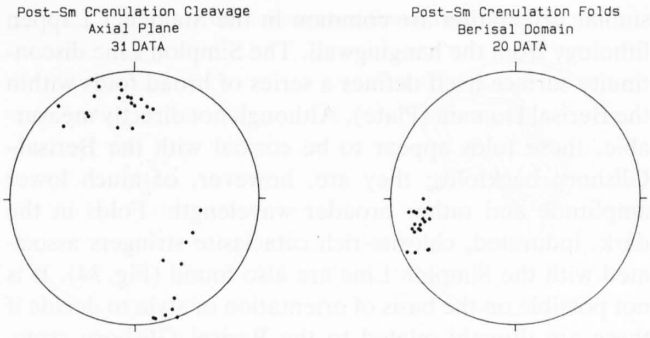

Fig. 32: Orientation data for post-S_m folds. As discussed in the text, a clear distinction between mesoscopic folds parasitic on the Berisal–Glishorn backfolds and still younger "late folds" is generally difficult. The orientation of the fold axes cluster about a direction 23°→255°.

Fig. 33: Typical irregular kink-like fold style of the "late folds" in the ? Permo-Carboniferous quartzitic schist lithology of the "Furgguwald Zone" of STECK (1987), looking southwest. The Berisal Synform lies to the left (i.e. southeast) of this outcrop, but the fold vergence of these unrelated, younger folds indicates a synform to the right. Below Tochuhorn (Coords. 643.75/122.73).

1. The jump in metamorphic grade across the discontinuity. Lithologies within the strongly folded and imbricated zone referred to as the Furgguwald Zone by STECK (1987) are basically identical to those of the Staldener Lappen in the hangingwall. However, in the hangingwall the quartz-rich pelites are dominated by chlorite and white mica; in the footwall there is also ubiquitous biotite and garnet (as also noted by STECK 1987). These footwall units of higher peak metamorphic grade have been retrogressed during the penetrative ductile deformation of the Simplon Phase (developing S_m and L_m) to produce new chlorite in the matrix, in pressure shadows on garnet and in shear bands.
2. The very clear quartz fabric boundary (Figs. 13*b*, *c*, *d*, 14*b*).
3. The abrupt truncation of the dominant foliation in the hangingwall (Plate; Fig. 4 in MANCEL & MERLE 1987).

The trend of the axial planes of the Berisal Synform and Glishorn Antiform within the footwall of the SFZ make a large angle with the trend of the Simplon Line. The axial planes also converge towards the Simplon Line (Plate). Tight folds of similar amplitude are not present in the hangingwall to the other side of this structural discontinuity, though crenulations and coaxial low-amplitude folds of

similar orientation are common in the Staldener Lappen lithology from the hangingwall. The Simplon Line discontinuity surface itself defines a series of broad folds within the Berisal Domain (Plate). Although not directly measurable, these folds appear to be coaxial with the Berisal–Glishorn backfolds; they are, however, of much lower amplitude and rather broader wavelength. Folds in the dark, indurated, chlorite-rich cataclasite stringers associated with the Simplon Line are also found (Fig. 34). It is not possible on the basis of orientation or style to decide if these are directly related to the Berisal–Glishorn structures or to the younger "late folds" described above.

Fig. 34: Irregular folds in the S_m foliation of fractured mylonites and in the dark stringers of indurated, very fine-grained chloritic cataclasite. The axial plane dips 68°→171°. Looking west, above Bielti, ca. 90 m from the Simplon Line (Coords. 643.24/122.24).

Although regionally there is a large angle between the orientation of the axial surface of the Berisal–Glishorn folds and the orientation of the Simplon Line (Plate), an abrupt truncation of the Berisal–Glishorn folds against the Simplon Line cannot be established in the field. The small area near Bielti, where truncation might be observed, is not well exposed. Within this region, however, the retrograde, mylonitic foliation within the footwall immediately adjacent to the Simplon Line appears practically concordant with the discontinuity surface. With distance from the Simplon Line (ca. 50 m), this foliation becomes less pervasive and there are localities where two mylonitic foliations are discernible (see inset, Plate); both have similar microstructures and kinematics (upper block down to the southwest) and intersect in a common L_m stretching lineation. The younger of these foliations is that which is approximately concordant with the Simplon Line. The older foliation is folded about the Berisal–Glishorn folds and is predominant away from the immediate vicinity of the Simplon Line.

It appears, therefore, that truncation of the Berisal–Glishorn folds began while the footwall was still within the ductile field and continued during transition into the brittle field (Fig. 22). The greenschist-facies retrograde S_m foliation folded about the Berisal–Glishorn structure was thus overprinted by a similar S_m foliation within a narrow zone adjacent to and concordant with the Simplon Line. The intersection between the folded foliation and the overprinting foliation would also parallel L_m; new folds which could characterize this overprint are, therefore, unlikely. Continued backfolding weakly folded the Simplon Line itself. This development history could be seen as a series of discrete events ("deformation phases") but it is more simply described as a continuous process.

4.2.5 Toce Domain

The Toce Domain includes those units of the footwall at some distance from the Simplon Line, which are not pervasively overprinted by the SFZ. Earlier structures unrelated to the Simplon Phase are still preserved within this domain and indeed, within the Antigorio Nappe in the Formazza and Bavona Valleys, original igneous relationships can be observed. The strain and associated structures within this zone are due to several strain increments of which the Simplon Phase is not necessarily predominant. The importance of the Simplon Phase strain increment can often be gauged from the preserved deformational fabrics within some of the quartz veins, which appear to have either formed or been completely annealed immediately prior to or in the early stages of the Simplon Phase. These show a mineral stretching lineation consistent with the regional orientation of L_m. In contrast, the host gneisses to these veins have a composite stretching lineation which varies in trend from northwest to WSW, depending upon the relative importance of pre-Simplon and Simplon Phase strain components. Certain (less competent?, pelitic and/or calcite-rich) lithologies appear to preferentially concentrate the Simplon Phase strain: in particular the Mesozoic metasediments ("Bündnerschiefer") and the schists ("Schisti bruni") and pelitic conglomerates of the Lebendun unit.

The foliation S_m makes a distinct dome within the Toce Domain and the lithological boundaries roughly parallel this foliation such that the foliation dome coincides with a structural culmination: the Toce Culmination (NIGGLI et al. 1936). The relief, although considerable (>2000 m), is insufficient to intersect the Simplon Line within this culmination. Textures from the highest peaks (e.g. P. Diei, Fig. 1), however, are generally strongly defined, related to the L_m lineation, and show an asymmetry that is consistent with the SFZ kinematics. This suggests that the Simplon Line is being approached with increased elevation (Fig. 20).

4.2.6 Upper Pennine Domain

The hangingwall Upper Pennine Domain is of very different structural style to the footwall and, at the current erosion level, lacks a pervasive ductile overprint related to the SFZ, such that structures older than the SFZ are still well preserved. MÜLLER (1983) and MILNES et al. (1981) have proposed that these structures can be grouped into four distinct phases:

D_1	: thrusting phase
D_2 (D_R; Ragno–Randa)	: isoclinal folding
D_3 (D_M; Mischabel)	: early backfolding
D_4 (D_V; Vanzone)	: late backfolding

According to MÜLLER (1983), the early backfolding (Mischabel Phase) was the result of southerly directed movement of competent blocks on incompetent shear zones, with a new axial plane foliation only developed in the strongly deformed units. When combined with the still younger Vanzone Phase backfolding, this produced a very heterogeneous structural style within this domain, with foliations of variable orientation and age. The result is the "blocky" outcrop style characteristic of the hangingwall and very different from the planar-foliated footwall (Figs. 3, 4). Movements within the Upper Pennine Domain have generally been considered to be in a NW–SE or N–S direction (e.g. MÜLLER 1983), and the preliminary results on quartz textures from the Staldener Lappen unit near the Gebidum Pass support this view (Fig. 14*a*). This may not be true of the Upper Pennine Domain as a whole (STECK 1984, 1987) and further work is warranted. In particular, in the upper Zwischbergen Valley (Coords. 650.85/108.95), a quartzo-feldspathic augen gneiss of very similar aspect to the Monte Rosa gneiss has a strong *LS* fabric, with the foliation near vertical, striking 080°, and the mineral elongation lineation pitching very shallowly westward. Asymmetric, partially recrystallized feldspar augen clearly indicate a dextral shear sense (under amphibolite facies conditions?) and the overall appearance of the augen gneiss is very similar to that of outcrops in the stream bed at Villadossola (cf. Fig. 1 in SIMPSON & SCHMID 1983). Quartz fibres on the foliation planes define a second somewhat steeper-pitching lineation (ca. 20° W) and are consistently stepped, again indicating dextral shear.

MILNES et al. (1981) suggested that the Vanzone Phase of late backfolding might be related to movements on the SFZ. Folds of the Vanzone Phase do not develop a new axial plane foliation and occurred after the final period of metamorphic mineral growth (KLEIN 1978); micas remain bent around microfolds and are not recrystallized (LADURON & MERLYN 1974). This folding phase is, therefore, clearly retrograde and late in the deformational history of the Upper Pennine Domain. Unfortunately, the absolute age of the most important structure (the Vanzone Antiform, Plate; BEARTH 1957), which is responsible for the transition to the "southern steep belt" in the Upper Pennine Domain, is not well constrained. Gold-bearing quartz veins occur within the hinge of this structure and apparently post-date its formation (BAUMANN 1979, CURTI 1987). Similar, late gold-quartz veins are found within the transition to the steep belt further southwest and these have been dated by DIAMOND & WIEDENBECK (1986) at ca. 30–32 Ma. The Vanzone Antiform may, therefore, be considerably older than the age proposed for the SFZ (see below). A more direct and reliable control on its age may come from dating of the gold veins that outcrop directly in the hinge region.

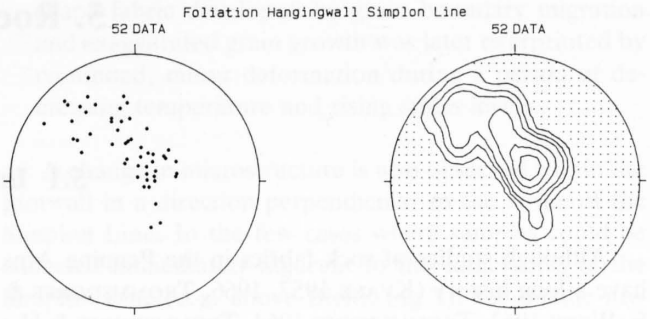

Fig. 35: Orientation data for the dominant foliation in the Staldener Lappen lithology of the hangingwall (Upper Pennine Domain).

4.3 Summary

In discussing the three-dimensional form of the SFZ, a distinction must be made between the geometry of the Simplon Line and the geometry of the foliation S_m within the footwall. As can be seen in the cross-section of the Plate, the S_m foliation defines three major structures in the footwall of the SFZ. These are, going from the northwest to the southeast, the Glishorn Antiform, the Berisal Synform, and the broad antiformal structure corresponding to the Toce Culmination, which is bounded in the south by the "southern steep belt" (MILNES 1974*a*). The structure of the footwall further to the southeast is entirely subsurface and currently unknown. As is also clear from the profile, the Simplon Line itself is also folded. In the northwestern region, broad folding of the Simplon Line occurs adjacent to the zone of Glishorn–Berisal backfolding in the footwall. The amplitude of the folds in the Simplon Line is, however, clearly much less than that of the folds of the S_m foliation in the footwall. The orientation of the folds in the Simplon Line are difficult to determine accurately, but are approximately coaxial with Berisal–Glishorn folds.

In the southeast, the Simplon Line also steepens into the "southern steep belt", but appears to do so less rapidly than the underlying S_m foliation. This results in an asymptotic relationship between the Simplon Line and the S_m foliation in cross-section (Plate). The overall impression in cross-section is that the fold structures in the footwall foliation and in the Simplon Line are directly related but that the amplitude of these structures is much greater in the footwall. This suggests a possible progressive development of these south-vergent backfolds during SFZ movement, as is also implied in the Berisal Domain by the complex relationship between retrograde, mylonitic foliations, backfolding and the Simplon Line discontinuity.

The geometry in long-section through Engiloch is relatively simple (Plate). Both the Simplon Line and the S_m foliation (and the approximately parallel lithologic boundaries) define an arc, with a pitch to the southwest of ca. 25° southwest of Hübschhorn and practically horizontal orientations further towards the northeast. Although not directly measurable in the field, this constructed profile suggests a low-angle asymptotic relationship between S_m and the Simplon Line consistent with the interpreted sense of shear (cf. the schematic long-section of Fig. 2).

5. Rock Fabrics

5.1 Introduction

Although studies of rock fabrics in the Pennine Alps have a long history (KVALE 1957, 1966, TROMMSDORFF & E. WENK 1963, TROMMSDORFF 1964, TROMMSDORFF & H.-R. WENK 1965), the results until recently were rather ambiguous (MILNES 1972, 1973). Following the practice of the time, stereograms of the measured textures were usually published with the lineation in the centre of the plot. This orientation looks approximately parallel to the movement direction (if the lineation represents the finite extension direction in a high-strain shear zone) and obscures any asymmetry in the pattern related to rotational deformation. Unfortunately, the full geographical orientation was also not always stated, making a later regional kinematic reinterpretation impossible.

This study, as well as concurrent studies along the Insubric Line (SCHMID et al. 1987*b*) and in the eastern Alps (BEHRMANN 1987, KLEINSCHRODT 1987, SCHMID & HAAS 1987, SELVERSTONE 1988) have established a remarkable consistency in rock fabrics associated with specific, high-strain deformation events in the Alps. The important difference, when compared to the earlier fabric work, is that all these studies have concentrated on individual structures, each with its own, relatively consistent kinematics (Simplon Fault Zone, Insubric Line, Schlinig thrust, Brenner Line, etc.). It is only with this approach that the inherent complexity of the polyphase deformation in the Alps can be circumvented to obtain consistent and interpretable results.

5.2 Microstructure

The microstructure varies both parallel and perpendicular to the strike of the Simplon Line. Within a broad band adjacent to the Simplon Line, three microstructural domains, corresponding approximately to the Gebidum, Simplon and Isorno Domains of Figure 23, can be recognized:

1. In the northwest, the quartz microstructure is dominated by heterogeneous intracrystalline strain with strongly developed undulose extinction, deformation bands and deformation lamellae (e.g. Spec. 3, Appendix C). Microfracturing is also observed. Limited recrystallization occurs by subgrain rotation and very subordinate grain boundary migration. Individual grains are moderately to strongly elongate, with the occasional development of bands and ribbons. However, the extreme foliation and grainsize reduction common in domain *2* described below is noticeably absent. Grainsize is very variable, reflecting the heterogeneity of deformation; grainsizes are commonly around 0.5–1 mm, but may range up to centimetres.
The microstructure is suggestive of low-temperature plasticity by dislocation glide (e.g. FROST & ASHBY 1982), in which diffusion-assisted climb has been insufficient to promote recovery and recrystallization. Lower initial temperatures during SFZ movement would mean that this domain cooled through the brittle/ductile transition for quartz-rich rocks earlier than the more southerly domains (cf. Fig. 22); more of the total displacement on the SFZ may have been accommodated in the cataclasite zone of the Simplon Line and less within the ductile mylonites of the footwall. This may explain the apparently lower-strain microstructure when compared to the mylonitic fabrics of domain *2*.
Both biotite and white mica are only weakly to moderately deformed in this area, with the development of bends and kinks and partial mechanical dismemberment into finer platelets. Retrograde chloritization is limited, but is occasionally observed both in the matrix and along shear bands. Feldspar remains as rigid porphyroclasts and occasionally separates along cleavage planes, with the gaps being filled by non-fibrous quartz.

2. Southeast of the Tochuhorn area, there is a transition to more advanced recrystallization of quartz with an accompanying transformation of the microstructure into a matrix of equant to moderately elongate, fine new grains (diameter < ca. 100 μm and ranging down to 4–5 μm) and very elongate ribbon grains, which often traverse whole thin sections (e.g. Specs. 32, 33, 37, Appendix C). This leads to a very strong development of the S_m foliation in quartz veins. Preliminary TEM studies indicate strong recovery and recrystallization by a process of progressive subgrain rotation (Fig. 3 in MANCKTELOW 1987*b*). Infilling of cracks in feldspar porphyroclasts by quartz demonstrates that diffusive mass transfer and neocrystallization also occurs. Most grain boundaries are strongly lobate, indicating considerable grain boundary mobility, and the ubiquitous occurrence of voids at grain triple points and along grain boundaries (Fig. 3 in MANCKTELOW 1987*b*) may be related to fluid-film assisted grain boundary migration as suggested for bischofite by URAI (1983).

3. Southeast and east of the Monscera Pass, there is a gradual transition to microstructures indicative of rapid grain boundary migration and exaggerated grain growth, to produce a much coarser average grainsize (ca. 0.5–3 mm). Individual grains are less elongate,

ribbon grains are absent, high angle grain boundaries are strongly lobate (e.g. Specs. 50, 51, 52, Appendix C), and the angle between the dimensional fabrics S_A and S_B is larger, often exceeding 45° (Fig. 15). In hand specimen, the quartz veins take on a sugary appearance in contrast to the flinty, strongly foliated samples typical of domain *2* above. The fabric in the gneiss units becomes more "homogeneous", with a more planar foliation in which shear bands are relatively rare. It should be emphasized that the transition from *2* to *3* is diffuse, and occasional samples from the region still show microstructures more akin to those of domain *2* (e.g. Spec. 48, Appendix B). Although the dimensional fabric indicates rapid grain boundary migration, the constituent quartz grains still show clear evidence of extensive intracrystalline deformation and recovery by polygonization and subgrain formation. Evidence for new grain formation through bulge nucleation is also seen (Fig. 36). However, the bimodal grainsize distribution typical of dynamic recrystallization by continued subgrain rotation is not preserved. One possibility is that the subgrain rotation mechanism of recrystallization is still largely responsible for the development of new grain orientations, but that new grains with orientations particularly favoured for easy slip have grown rapidly and consumed their less favoured neighbours, to establish a relatively coarse stable grainsize. An alternative possibility is that the shape fabric developed by grain boundary migration and exaggerated grain growth was later overprinted by continued, minor deformation during a period of decreasing temperature and rising stress levels.

A change in microstructure is also observed within the footwall in a direction perpendicular to the strike of the Simplon Line. In the few cases where samples could be collected immediately adjacent to the cataclasites of the Simplon Line (e.g. above Bielti, Fig. 1), the ductile mylonites show microstructures similar to those described for domain *1* above: ductile deformation of quartz was apparently within the field of low-temperature plasticity and was followed by strong microfracturing associated with the Simplon Line itself (Fig. 37). Within a few or tens of metres into the footwall, the microstructure changes to that of the domains described above. With further distance from the Simplon Line (in the order of kilometres), however, fabrics similar to domain *3* are practically ubiquitous. Quartz veins from this region still show textures consistent with the kinematics of the SFZ, but display a coarse grained, poorly-foliated microstructure strongly modified by grain growth (Specs. 18–22, 53, 54, Appendix C). This regional variation in microstructure with distance away from the Simplon Line probably reflects both higher strain rates and lower temperatures (due to cooling against the hangingwall) adjacent to the Simplon Line.

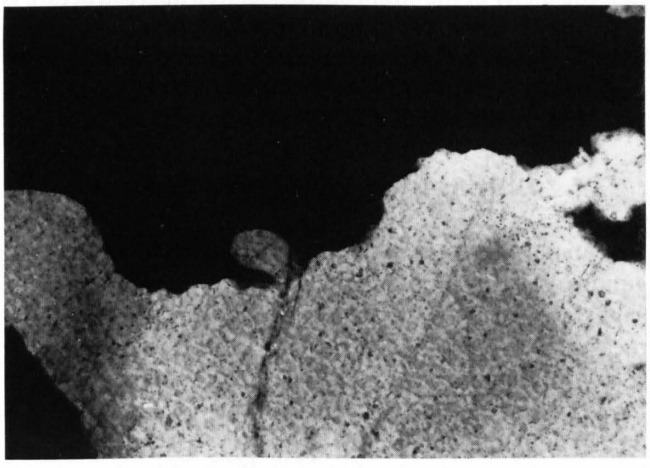

Fig. 36: Bulge nucleation at a quartz/quartz grain boundary. Specimen 51 (see Appendices B, D). Width of field is 0.8 mm.

Fig. 37: Photomicrograph of fractured quartz-rich mylonite from the "Furgguwald Zone" immediately adjacent to the Simplon Line. Above Bielti (Coords. 643.25/122.17). Width of field is 3.3 mm.

5.3 Metamorphic Conditions during Fabric Development

The Lepontine metamorphism of the Central Alps peaked prior to development of the SFZ and metamorphic mineral zone boundaries and isograds are clearly truncated by the SFZ (e.g. Fig. 46). This is particularly clear for the oligoclase (An >17) boundary (Bearth 1958, Wenk & Keller 1969, Trommsdorff & Evans 1974); the offset of this boundary across the SFZ can be used to make a rough estimate of possible displacement across the fault zone (see below). Frank (1979, 1983) investigated the metamorphic conditions within the Mesozoic metasediments along a traverse through the Simplon Alps and suggested that peak metamorphic conditions varied from 400–420 °C/2–3 kbar near Brig to 580–620 °C/6–8 kbar to the southeast around Crevola.

Simplon Phase deformation within the uppermost part of the footwall of the SFZ is clearly associated with retrograde metamorphism of lower greenschist facies from the Gebidum to Simplon Domains. North of Simplon village, chlorite develops at the expense of older garnet (often as pressure shadows and in extension fractures ca. perpen-

dicular to the lineation L_m) and biotite. South of here, new biotite growth is also observed (cf. MERLE et al. 1986, STECK 1987), suggesting an increase in temperature to the southeast compatible with the observed fabric transitions discussed above. Within the Isorno Domain (corresponding to fabric domain *3*), retrogression is limited to the immediate few metres of the footwall adjacent to the Simplon Line (e.g. the green chlorite-rich zones near Cisore). Elsewhere, clear retrogressive neocrystallization is limited to occasional chlorite grains in the matrix and within shear bands; the light-green and fox-red biotite observed in the gneisses of this region may also be products of a more pervasive retrograde metamorphism, but this requires additional petrographic work.

The retrogressive overprint consistently diminishes away from the Simplon Line into the footwall, again in harmony with the observed microstructure within the quartz veins. This may reflect the original perturbed isotherm distribution adjacent to a major fault, as well as additional later updoming of an originally more shallowly dipping fault zone.

5.4 Quartz Textures

5.4.1 Introduction

The texture[1] of a mineral measured from a rock sample is a function of several factors: the operative deformation mechanisms, the kinematic framework, the geometry of the strain (oblate, plane strain, prolate), the mechanism and degree of recrystallization, the initial texture (either from static crystallization or previous deformation), the homogeneity of the deformation and the degree of anisotropy of the material. It is the hope of the geologist that the measured texture, in association with other laboratory and field observations, will provide some constraint on these variables. The problem can be simplified if study is restricted to a single mono-mineralic rock type from a geometrically well-constrained area. This has been the approach adopted here.

Most samples for this study are taken from nearly mono-mineralic quartz veins or quartzites, so that the effect of lithological variation and the implicit heterogeneity associated with multi-component systems is minimized. Individual crystals are themselves markedly anisotropic, as intracrystalline deformation is accomplished by dislocation glide on specific crystallographic slip systems. Aggregates of such crystals, even when mono-mineralic, will still be markedly heterogeneous on the grain scale, the deformation of each individual grain being determined by its crystallographic orientation. Perfectly homogeneous deformation is only possible when five independent slip systems are available in every grain (MISES 1928), although this may be reduced if grain boundary coherence is aided by diffusional mechanisms (e.g. PATERSON 1969). Even in such situations, the available slip systems are liable to have differing critical resolved shear stresses for activation (e.g. LISTER et al. 1978), promoting heterogeneous deformation. This tendency towards heterogeneous strain on the grain scale will increase with decreasing crystal symmetry: homogeneity may be approached in aggregates of cubic minerals, but marked heterogeneity is expected in aggregates of triclinic minerals. The presence of an additional phase will further promote heterogeneous deformation. This is clearly seen in the current study, where the occurrence of a minor component of monoclinic mica or chlorite (with a single [001] slip plane) in a quartzite or quartz vein often introduces marked heterogeneity into the fabric (e.g. the development of shear bands). Rigid porphyroclasts (e.g. feldspar) cause strongly heterogeneous flow in their immediate vicinity, even leading to small regions of shear with opposite vergence to the bulk sense of shear (GARCIA CELMA 1983). This effect is clearly seen in thin section from the interference colours of quartz with crossed polars and the gypsum plate inserted. The increased heterogeneity of the strain and associated microstructure is reflected in a clear weakening of the overall quartz texture, which is completely out of proportion to the modal percentage of the additional phase.

5.4.2 Methods and Measurement Techniques

Samples were oriented in the field relative to the elongation lineation L_m and the foliation S_m. In the workshop, small blocks were cut and polished such that the face to be measured was perpendicular to S_m and parallel to L_m. For X-ray measurements, the blocks were mounted on the texture goniometer such that scanning occurred perpendicular to the foliation. The scan distance was ca. 14 mm. For complete analyses, nine crystallographic planes were measured in combined reflection and transmission mode following the method of SCHMID et al. (1981) and CASEY (1981), with a total measuring time of about one week per specimen. The ODF[2], plotted sections through the ODF, regenerated pole figures and inverse pole figures were calculated using the program package of CASEY (1981). On completion of the goniometer measurements, a thin section for optical study was then taken from the face of the reflection scan block. All optical *c*-axis measurements were made using standard universal stage techniques (e.g. TURNER & WEISS 1963) along spaced traverses and contoured and plotted using routines originally written by STARKEY (1970) and modified by M. Casey and the author.

[1] The crystallographic preferred orientation, see Appendix A.

[2] The Orientation Distribution Function, see page 32.

The orthogonal specimen reference system has the Z axis perpendicular to the foliation and the Y axis within the foliation and perpendicular to the lineation, X. Use of XYZ in the following discussion refers to this coordinate system and does not implicitly assume a parallelism with the finite strain axes.

All photomicrographs and stereograms of Appendices C and D are *kinematically* oriented and represent XZ sections, with the foliation XY vertical and aligned E–W, the lineation X horizontal, and the shear sense *dextral*. This minimizes confusion in comparing data but implies that when the fault zone is strongly non-planar the geographic orientation of samples varies greatly. To allow a ready realignment into geographic coordinates, the lineation "vector" and the approximate direction of the foliation normal "vector" are given for each stereogram in Appendix B. All stereograms are equal area, upper hemisphere projections.

5.4.3 Observations

There is a strong resemblance between all the measured quartz textures of this study. Basically, they are variably kinked ("dog-leg") single or partial crossed girdle patterns which pass through the intermediate axis Y at a high angle to the foliation XY. As such they can be considered in terms of three end-member geometries:

- a Type I kinked crossed girdle (Fig. 38, LISTER 1977),
- a Type II crossed girdle intersecting in the intermediate axis Y (Fig. 38, LISTER 1977),
- a contraction towards individual maxima along these skeletons.

One limb of the crossed girdle is usually much more strongly developed than the other, such that the overall pattern is asymmetric relative to XYZ and rotated towards the lineation X in the sense of the imposed shear (SIMPSON & SCHMID 1983). Often only a few grains define the vestiges of the crossed girdle limbs. These vestiges are more clearly seen on the scatter plots than on the contoured optic c-axis stereograms and the c-axis plots regenerated from the ODF (see below), where the statistics obscure these uncommon orientations. The asymmetry is also clear from the X-ray textures of Appendix D, in particular from the oblique $r+z$ patterns and the tendency to develop a single $<a>$ maximum oblique to the foliation (cf. BOUCHEZ 1978).

Not surprisingly, the patterns of Appendices C and D can be broadly divided into groups corresponding to the microstructural domains described above. The most coherent group (Specs. 24–42) are also from the domain with the simplest and clearest regional geometry (corresponding to microstructural domain *2*).

Consider first the optically measured c-axis textures (Appendix C). As discussed in MANCKTELOW (1987*a*), the angle $Z{:}c$ measured in the XZ plane between the Z specimen axis and the skeleton of the dominant kinked single c-axis girdle (Fig. 39, LISTER & WILLIAMS, 1979) shows a limited variation between 20° and 30°. The opening angle

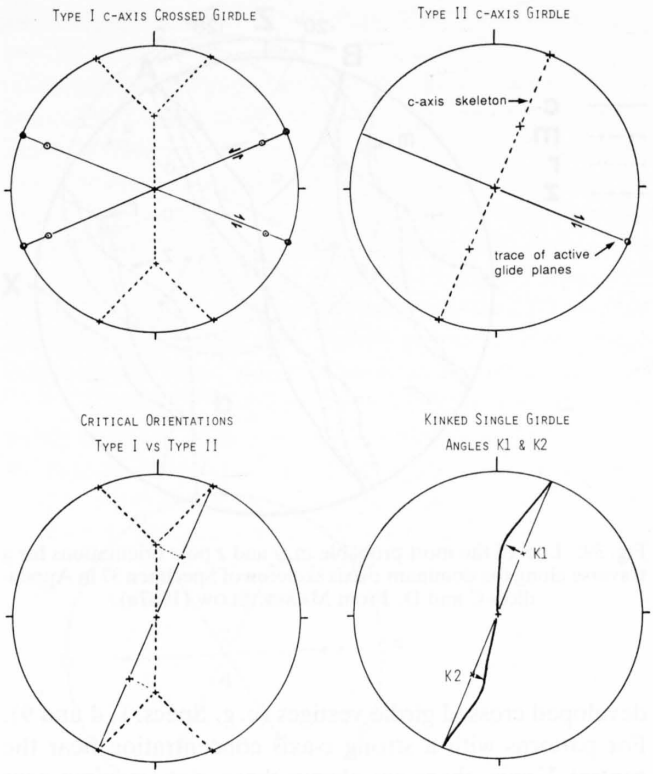

Fig. 38: Type I and Type II girdles, defined by the c-axis skeletons, after LISTER (1977). The trace of the active glide planes for specific c-axis orientations on these girdles (indicated by crosses) are shown. Angles K1 and K2 mentioned in the text, which provide a measure of the divergence from a Type II straight girdle pattern, are also defined.

between the two limbs of the crossed girdle within XZ (when determined) has a mean value of ca. 48° (Fig. 39). There is considerable variation in the degree of kinking, ranging from a practically straight girdle segment (e.g. Specs. 8, 17, 20, 30, 48, 53) to a maximum of around 20° divergence from a straight girdle (e.g. Specs. 15, 27, 28, 32, 33, 37, 42, 47, 51, 54, see Fig. 3 in MANCKTELOW 1987*a*), and this variation is not systematic along the strike of the SFZ. There is no consistent change in the obliquity of the single girdle (as measured on the primitive circle by the angle $Z{:}c$) as its shape becomes straighter and approaches that of a true great circle (Fig. 3*c* in MANCKTELOW 1987*a*). It follows that straight girdles are oblique to the foliation, whereas strongly kinked girdles are more nearly perpendicular to the foliation in the central section around Y. This is consistent with the observations of LAW et al. (1984) and CARRERAS & GARCIA CELMA (1982) that such pattern changes are observed without a change in orientation of the trace of the texture skeleton relative to the specimen coordinates.

Consider now the results of the texture goniometer analysis. Pole figures for the measured a, m, and the combined rhombs $r+z$, and the calculated r, z, and c textures are presented in Appendix D. In general, there is one dominant $<a>$ maximum in or near the XZ plane which makes an angle of between 20° and 30° with the lineation X in the sense of the imposed rotational deformation (this is the angle α of BURG & LAURENT 1978). This $<a>$ maximum is predominant for evenly distributed single girdles (e.g. Spec. 6); a subsidiary $<a>$ maximum to the other side of X is clearly developed for patterns with better

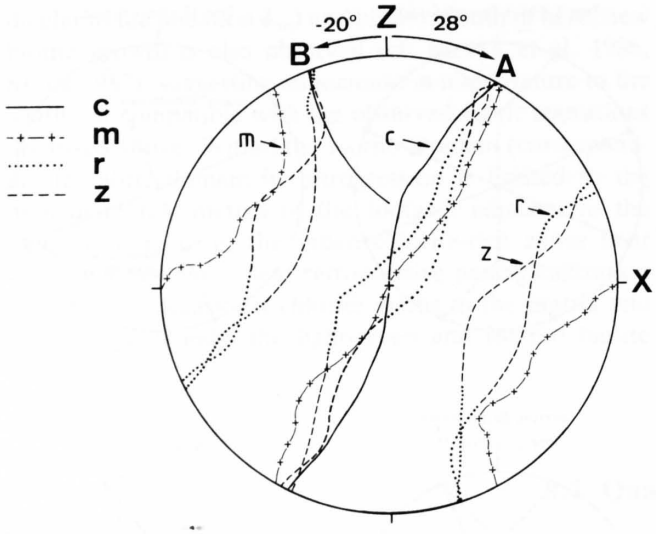

Fig. 39: Loci of the most probable *m*, *r* and *z* pole orientations for a traverse along the dominant *c*-axis skeleton of Specimen 37 in Appendices C and D. From MANCKTELOW (1987*a*).

developed crossed girdle vestiges (e.g. Specs. 1, 4 and 9). For patterns with a strong *c*-axis concentration near the central *Y* axis, there are always three <*a*> maxima near the primitive circle, simply due to the single crystal geometry (e.g. Spec. 7).

From the measured textures for nine different crystallographic planes, it is possible to calculate the full Orientation Distribution Function (the ODF, BUNGE 1969, BUNGE & WENK 1977, CASEY 1981), which fully describes the complete texture of the sample and from which the texture of any crystallographic direction can be regenerated. This has been done for 14 samples of Appendix D using the program package developed by CASEY (1981). The fully analysed samples are those for which *c*, *r* and *z* textures have been regenerated. The ODF allows the determination of the most probable full crystal orientation associated with any particular *c*-axis orientation. This allows a much more complete analysis of the *c*-axis patterns observed, as for every orientation along the *c*-axis girdle it is possible to determine the most favoured orientation for the other crystallographic directions (e.g. SCHMID et al. 1981). This has been done for Specimen 37 and the loci of the most favoured orientations of the *m*, *r*, and *z* poles associated with the favoured *c*-axis orientations are plotted in Figure 39. With the exception of the *c*-axes, these loci form approximate cones of revolution about the strong <*a*> axis maximum. Significantly, there are two orientations on the primitive circle (the *XZ* plane) where the loci tend to converge. These are indicated as A and B on Figure 39. If the most probable single crystal orientations corresponding to each of the seven loci intersections with points A and B of Figure 39 are plotted (Fig. 40), we find that two pairs of orientations corresponding to *z* at A and *r* at B very nearly coincide. This is possible because the angle between A and B is very near the 46° angle between *r* and *z* in quartz. It is suggested that these coincident orientations (3 and 5 in Fig. 40) may be important in defining a particular "ideal" Type I crossed girdle pattern, which would form one end-member for the observed *c*-axis patterns from the Simplon Fault Zone (Fig. 40*a*). The other end-member would be a straight *c*-axis girdle perpendicular to a single fixed <*a*> direction (Fig. 40*a*).

5.4.4 Discussion

Crystallographic preferred orientation of the component minerals (the texture) develops as a function of increasing strain, as has been clearly established by studies along measured strain gradients (BOUCHEZ 1977, BURG & LAURENT 1978, CARRERAS & GARCIA CELMA 1982, LAW et al. 1984, LAW 1986). Regionally heterogeneous deformation and the concentration of strain within band-like zones (shear zones of RAMSAY & GRAHAM 1970; the *S*- & *P*-bands of COBBOLD 1977*a*, *b*) is only possible if there is strain softening within these zones during progressive deformation, i.e. a decrease in the flow stress with increasing strain (RAMSAY & GRAHAM 1970, COBBOLD 1977*a*, *b*). Texture development provides a mechanism for geometric strain softening during crystal plastic deformation, through the preferential alignment of the component crystals for easy slip (e.g. WHITE et al. 1980). Dislocation slip systems with low critical resolved shear stresses can be preferentially utilized, lowering the bulk flow stress of the polycrystalline aggregate as the texture develops with increasing strain (and dynamic recrystallization). The observed textures can therefore be considered in terms of specific crystal orientations favourable for single or multiple slip on such easy slip systems (e.g. SCHMID et al. 1981, SCHMID & CASEY 1986, MANCKTELOW 1987*a*, *b*). Experiments on single crystals have established many dislocation slip systems in quartz (cf. CARTER 1976; see LINKER et al. 1984, Table 1, for a summary), of which (0001)<*a*>, *m*<*a*>, *r*<*a*>, *z*<*a*>, *a*[*c*] and *m*[*c*] have been most commonly cited as significant in the development of particular quartz textures (TULLIS et al. 1973, BOUCHEZ 1978, SCHMID & CASEY 1986). The preferred systems of easiest slip will be a function of extrinsic variables; mainly temperature, but also the activity of H_2O (GRIGGS & BLACIC 1965) and perhaps other impurities. For example, TULLIS et al. (1973), WILSON (1975) and BOUCHEZ (1977) have inferred from both natural and experimentally developed textures in quartzites that there is a transition from dominantly basal to increasingly prismatic slip with increasing temperature. MAINPRICE et al. (1986) suggest there may be a transition in the dominant slip direction from <*a*> to *c* above ca. 650°C.

The interplay of intracrystalline deformation by dislocation glide and dynamic recrystallization will determine the overall strength and pattern of the texture. In contrast, intercrystalline processes (diffusion, grain boundary sliding) tend to hinder its development (e.g. WHITE 1977, SCHMID 1982). Oriented neocrystallization due to the anisotropy of crystal growth in a non-hydrostatic stress field (e.g. KAMB 1959) may be important in foliation development in phyllosilicate-rich rocks (WHITE & KNIPE 1978, MANCKTELOW 1979) but is probably unimportant in the development of quartz textures (PATERSON 1969).

The development of quartz textures from the SFZ has been extensively discussed in MANCKTELOW (1987*a*, *b*) and

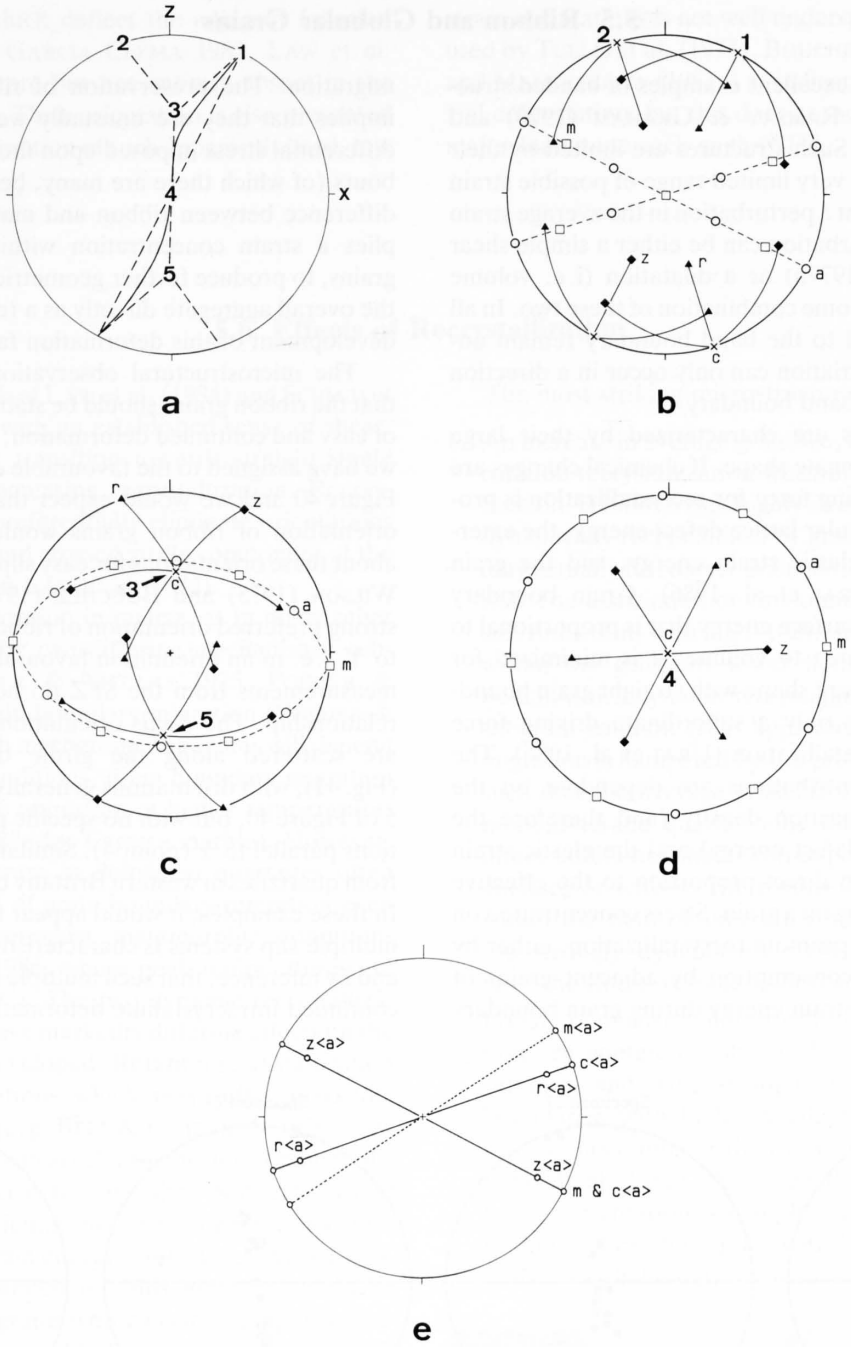

Fig. 40: Idealized straight single girdle and Type I crossed girdle patterns. From MANCKTELOW (1987*a*).

(a) Idealized straight single girdle and Type I crossed girdle patterns, with the *c*-axis skeleton of Specimen 37 for comparison. Positions *1* and *2* have orientations favourable for slip on (0001) <*a*>, *3* and *5* for slip on *r* <*a*> and *z*<*a*>, and *4* for slip on *m*<*a*>.

(b) Pole figure for the single crystal orientations corresponding to positions *1* and *2*.

(c) Pole figure for the single crystal orientations corresponding to positions *3* and *5*.

(d) Pole figure for the single crystal orientations corresponding to position *4*.

(e) Stereogram of the orientation of the favoured slip systems corresponding to positions *1* to *5*.

will not be repeated here. In summary, it can be noted that heterogeneity of deformation between individual grains and separate domains will promote the operation of duplex or multiple slip even if the bulk deformation is strict simple shear. To maintain this bulk geometry, however, slip systems straddling the shear flow plane must have the same shear sense as the overall deformation; otherwise the direction parallel to the flow plane must be extending and the bulk deformation cannot be simple shear (Fig. 10 in MANCKTELOW 1987*a*). This restriction is obviously no longer relevant when there is a component (perhaps only small) of background pure shear, and the fault zone represents a band of additional heterogeneous shear (i.e. an *S-P* band of COBBOLD 1977*a*, *b*). Then slip on a single system is geometrically insufficient to accommodate the bulk deformation, and duplex or multiple slip will be favoured, with the corresponding development of crossed-girdle patterns.

5.5 Ribbon and Globular Grains

Ribbon grains are excellent examples of banded structures as defined by RAMSAY & GRAHAM (1970) and COBBOLD (1977*a*, *b*). Such structures are limited by their specific geometry to a very limited range of possible strain states. If they represent a perturbation in the average strain of the rock, this perturbation can be either a simple shear (*S*-bands, COBBOLD 1977*a*) or a dilatation (i.e. volume change, *P*-bands), or some combination of these two. In all cases, lengths parallel to the band boundary remain unchanged and strain variation can only occur in a direction perpendicular to the band boundary.

The ribbon grains are characterized by their large grainsize and very elongate shape. If chemical changes are not involved, the driving force for recrystallization is provided by the intragranular lattice defect energy, the external load-supporting elastic strain energy, and the grain boundary energy (URAI et al. 1986). Grain boundary energy ist primarily a surface energy that is proportional to the ratio of surface area to volume: it is minimized for larger grainsize of equant shape with straight grain boundaries and is probably only a subordinate driving force during dynamic recrystallization (URAI et al. 1986). The other two energy contributions are dependent on the stress. Both the dislocation density (and therefore the intragranular lattice defect energy) and the elastic strain energy will increase in direct proportion to the effective differential stress acting on a grain. Stress concentration on a particular grain will promote recrystallization, either by subgrain rotation or consumption by adjacent grains of lower intracrystalline strain energy during grain boundary migration. The preservation of ribbon grains therefore implies that they are unusually weak grains, with lower differential stress imposed upon them than on their neighbours (of which there are many, because of the grain size difference between ribbon and matrix). This in turn implies a strain concentration within these weak ribbon grains, to produce further geometrical strain weakening of the overall aggregate directly as a result of the progressive development of this deformation fabric.

The microstructural observations, therefore, suggest that the ribbon grains should be stable orientations capable of easy and continued deformation. This is a characteristic we have assigned to the favourable end orientations 1–5 in Figure 40 and we would expect that the crystallographic orientation of ribbon grains would be tightly clustered about these orientations for easy slip. The earlier studies of WILSON (1975) and BOUCHEZ (1977) did indeed find a strong preferred orientation of ribbon grain *c*-axes parallel to *Y*, i.e. in an orientation favourable for prism slip. The measurements from the SFZ do not show such a simple relationship. The *c*-axis orientations of the ribbon grains are scattered along the girdle defined by all grains (Fig. 41), with orientations generally between points 3 and 5 of Figure 40, but with no specific preference for orientations parallel to *Y* (point 4). Similar results were reported from quartzites in western Brittany by LAW (1986, Fig. 10). In these examples, it would appear that concurrent slip on multiple slip systems is characteristic of the ribbon grains, and by inference, that such multiple slip promotes easy and continued intracrystalline deformation.

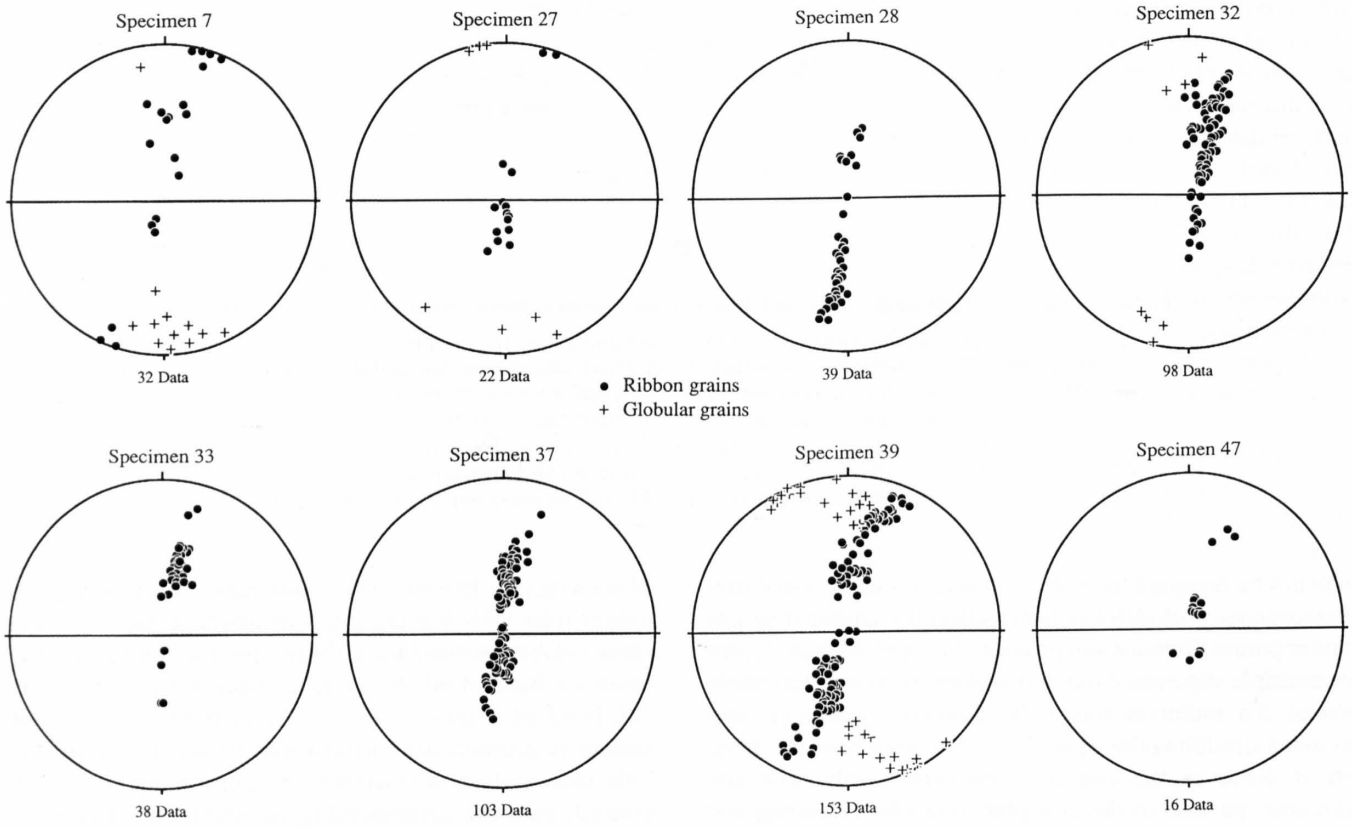

Fig. 41: Orientation of *c*-axes for very elongate ribbon grains (•) and nearly equant "globular" grains (+).

Globular grains, which deflect the adjacent foliation (e.g. BOUCHEZ 1977, GARCIA CELMA 1983, LAW et al. 1984, LAW 1986) are rare but not entirely absent in the deformed quartz veins. Their orientation is also presented in Figure 41. The preservation of such apparently hard, low strain orientations is not well understood. They have been used by TULLIS et al. (1973), BOUCHEZ (1977), LAW (1986) and MANCKTELOW (1981*a*) as indicators of essentially coaxial deformation, but this does not seem appropriate for a major fault zone such as the SFZ.

5.6 Effects of Recrystallization

In the previous work of LAW et al. (1984) and SCHMID et al. (1981) from zones with an established sense of shear, there is a clear fabric transition towards straight single girdle patterns with increasing recrystallization. Recrystallization appears to preferentially eliminate orientations on the arms of the second crossed girdle component of the patterns (e.g. Fig. 14 in LAW et al. 1984).

Dynamic recrystallization in quartz, as in many other materials, may occur by two differing mechanisms: subgrain rotation (POIRIER & NICOLAS 1975, POIRIER & GUILLOPÉ 1979) or grain boundary migration (POIRIER & GUILLOPÉ 1979). Which mechanism dominates will depend on the deformation conditions, grain boundary migration usually becoming more important at higher temperatures (e.g. SCHMID et al. 1987*a* for Carrara marble). However, the optical microstructure in deformed quartzites often indicates a component of grain boundary migration even under lowermost greenschist metamorphic conditions (e.g. Fig. 5*b* in LAW 1986, where peak temperatures are considered to be 280°C). The two dynamic recrystallization mechanisms can have markedly differing effects on the deformation texture developed. Rotation recrystallization produces new orientations which may differ markedly from the original host (e.g. BELL & ETHERIDGE 1976, LAW 1986 Figs. 15–17). This can accelerate the development of a strong texture conducive to easy slip. Not only would unfavoured "hard" orientations, with higher dislocation density and internal strain energy (SCHMID & CASEY 1986), be preferentially consumed but this material would be transformed into new grains whose crystallographic orientation may be more favourable for easy slip. By comparison, grain boundary migration recrystallization does not, in itself, produce new orientations; it can only consume less favourably oriented grains with higher defect energies. In the case of bulge nucleation (e.g. Fig. 36), the two mechanisms can act together: a bulging grain boundary may develop a dislocation wall across the narrow "neck" of material connecting it to its original host, and by continued rotation develop into a small new grain.

The quartz veins and quartzites from the SFZ have recrystallized both by subgrain rotation and by grain boundary migration, but as noted above, the grain boundary migration mechanism dominates towards the southeast. This affords an opportunity to study the modification of microstructure and texture with increasing recrystallization by grain boundary migration, to complement the earlier published studies on the effects of increasing dynamic recrystallization by subgrain rotation (BOUCHEZ 1977, BURG & LAURENT 1978, LAW 1986).

The most striking microstructural changes involve:

1. An increase in average grainsize, in contrast to subgrain rotation recrystallization which involves a grainsize reduction. It follows that highly strained rocks which have dynamically recrystallized by grain boundary migration may actually be coarser grained than less strained material. The association of "mylonites", involving a grainsize reduction, with high strain shear zones is only valid within the generally lower homologous temperature field in which dynamic recrystallization is dominated by subgrain rotation (see Appendix A). Grain boundary migration is hampered by the presence of other phases, such that the average grainsize of quartz is coarser in monomineralic quartz veins than in quartzites with minor additional phases (often phyllosilicates) or in the gneisses or schists. The reverse is commonly the case within the field of subgrain rotation recrystallization: the strongly dynamically recrystallized quartz veins have the finest average grainsize.
2. Lobate boundaries indicative of grain boundary migration are commonly observed. Studies in metallurgy, ceramics and with analogue materials indicate that boundaries with high crystallographic misorientation will be more mobile than low-angle boundaries (e.g. URAI et al. 1986). Although the specification of the full misorientation is complex, it is immediately clear in thin section that grains with high *c*-axis misorientations overwhelmingly show lobate, mobile boundaries

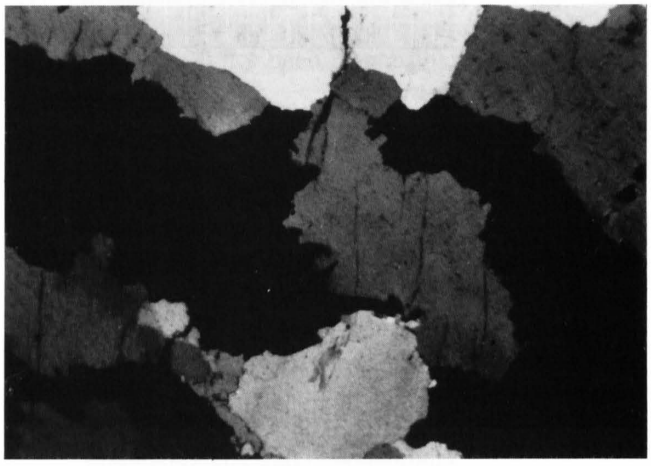

Fig. 42: Photomicrograph of Specimen 51 from the Isorno Domain, showing very irregular, lobate boundaries between grains with high angular misorientations of the *c*-axis (large difference in interference colours-black/white), and much straighter boundaries where misorientations are lower (similar grey/white interference colours). See also Specimens 50–52, Appendix C.

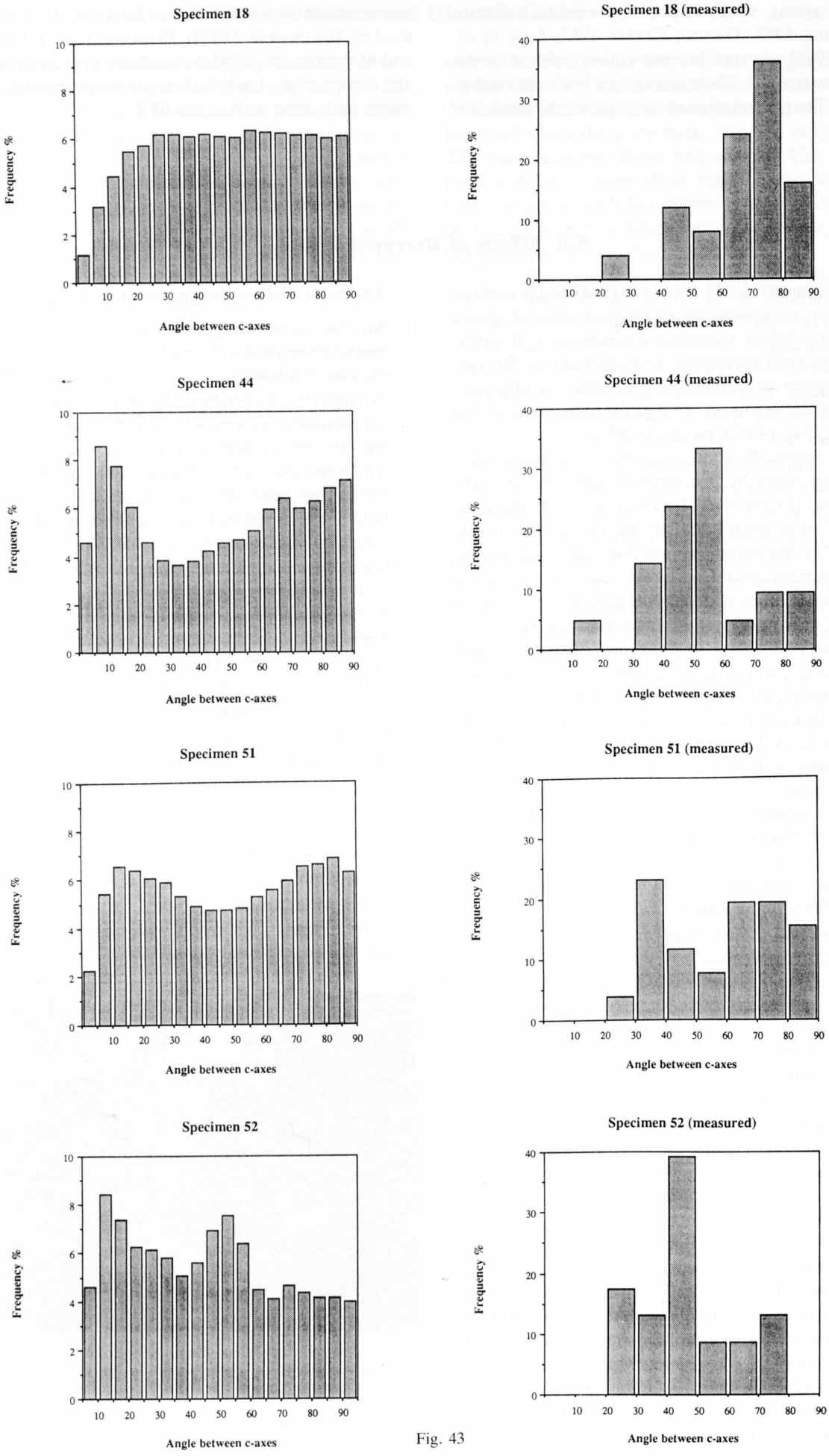
Specimen 18
Specimen 18 (measured)
Specimen 44
Specimen 44 (measured)
Specimen 51
Specimen 51 (measured)
Specimen 52
Specimen 52 (measured)
Frequency %
Angle between c-axes

Fig. 43

(Fig. 42), whereas grains with low *c*-axis misorientations often have low energy, nearly straight boundaries. Where three low-angle grains abut, they may develop ca. 120° triple points. This qualitative observation is confirmed by plots of the difference in *c*-axis orientation for adjacent grains showing strongly lobate-cuspate boundaries (Fig. 43). In comparison with histograms for the distribution of this angular difference for a random selection of possible neighbours, there is a marked preference towards higher angles, even though angular differences as low as 7–10° are detectable optically.

3. The analogue and metallurgical studies have also indicated that during dynamic grain boundary migration, grain boundaries tend to migrate away from their centres of curvature (URAI et al. 1986). An attempt was therefore made to measure the orientation of grains to either side of clear cuspate-lobate boundaries, with the aim of determining which orientations were preferentially consumed during grain boundary migration recrystallization. The results, as presented in Figure 44, although dependent on a subjective analysis of grain boundary curvature, are remarkably consistent. It appears that orientations with the *c*-axis nearly parallel to the intermediate *Y* axis are preferentially consumed. This microstructural observation is consistent with the clear reduction in the number of grains with this orientation as grain boundary migration becomes more advanced towards the Isorno Domain in the southeast (see Appendix C). Increasing grain boundary migration is usually associated with increasing temperature (e.g. SCHMID et al. 1987*a*), as is observed along the SFZ (see above and Fig. 46). Experimental studies (TULLIS et al. 1973, LINKER et al. 1984) and measured textures (WILSON 1975, BOUCHEZ 1977, SCHMID et al. 1981) have consistently suggested that prism slip, associated with a strong *c*-axis parallel to *Y* texture, becomes increasingly important at higher temperatures. It is suggested that in the Simplon Alps, the increase in temperature was sufficient to promote grain boundary migration recrystallization over rotation recrystallization, but insufficient for prism slip to be favoured over rhomb and basal slip. However, it should be noted that the "atypical textures" (Appendix C, Specs. 30, 31, 48) described in detail by MANCKTELOW (1987*b*), in which subgrain rotation recrystallization has produced a marked "core-mantle" microstructure, have strong *c*-axis maxima textures oriented near parallel to *Y*. An alternative interpretation would be that grain boundary migration preferentially consumes grains deforming by prism slip, whereas rotation recrystallization favours this orientation.

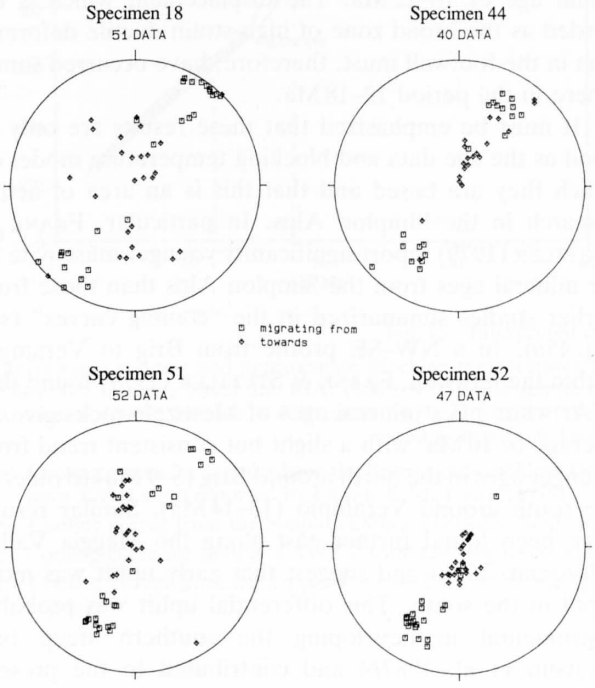

Fig. 44: Stereograms indicating the interpreted migration direction of lobate grain boundaries. Grain boundaries migrate away from the side with a *c*-axis orientation indicated by □ towards the side with an orientation indicated by ◇.

In the coarse-grained samples showing dominant grain boundary migration, there are still fairly common large grains with *c*-axes nearly parallel to *Y*; otherwise the observations of Figure 44 would not have been possible. This implies that there has either been only a single wave of recrystallization, and that the *c*-axis nearly parallel to *Y* grains are simply relicts or, more likely, that there have been multiple waves of recrystallization and that some other mechanism (subgrain rotation recrystallization, bulge nucleation?) has been responsible for regenerating these orientations.

Fig. 43: Misorientation angles across grain boundaries. The left column indicates the frequency distribution of all possible angles for each specimen considered, calculated between every pair of measured *c*-axes in the optic textures of Appendix C. A wide range of angles are possible, generally approximating a random distribution. In the right column, the frequency distribution is given for angles between the *c*-axes of adjacent grains which are separated by highly lobate grain boundaries. The clear preference for moderate to large angles confirms the observation in Figure 42 that lobate boundaries are preferentially observed between adjacent grains with a marked *c*-axis misorientation.

6. The Age of the Simplon Fault Zone

Workers from the radiometric age group at Berne University have argued over many years that mineral ages in the Pennine Alps can be best interpreted in terms of a "blocking temperature" specific to each particular mineral (e.g. ARMSTRONG et al. 1966, CLARK & JÄGER 1969, HUNZIKER & BEARTH 1969, WAGNER et al. 1977, HURFORD 1986). Minerals which crystallized below their blocking temperature retain a "formation age", whereas those which crystallized above their blocking temperature retain the age at which they eventually cooled through this temperature; i.e. they give a "cooling age". In the Simplon Alps, the white mica Rb/Sr, K/Ar, biotite Rb/Sr and K/Ar, zircon and apatite fission track ages do not cluster around a single value (as would be expected for formation ages), but give a remarkably consistent sequence of ages, which may be interpreted in terms of a cooling path. If a particular segment of a cooling path is due to simple uplift with a constant geothermal gradient then, as noted by WAGNER et al. (1977), the uplift rate can be calculated by simply dividing the cooling rate by the geothermal gradient.

Several features of the SFZ geometry and microfabric established above are critical in evaluating the absolute age of deformation and the possible amount of relative displacement. It is clear that temperatures within the footwall were, at least initially, sufficient for extensive ductile deformation of quartz during movement on the SFZ, leading to the observed microstructure and strong crystallographic preferred orientations. Dislocation glide in quartz is thermally activated and there will be a low temperature transition below which this deformation mechanism is incapable of producing significant strain. This is considered to occur around 300°C by SIBSON et al. (1979) and in the range 300–400°C by ATKINSON (1982). The lower limit of this range is suggested by the observations of LAW (1986) on plastically deformed quartzites from Brittany, where the maximum metamorphic temperature apparently did not exceed 300°C. It follows that ductile mylonite formation in the footwall occurred at temperatures above ca. 300°C. The maximum possible temperature during these movements can also be established for both the footwall and the hangingwall. Feldspar (both plagioclase and K-feldspar) did not deform plastically during SFZ movements, indicating the temperature of deformation was below ca. 500–550°C (WHITE 1975, TULLIS 1983). Metamorphism during the Simplon Phase was retrograde (to greenschist facies) within the footwall block, with the development of syntectonic chlorite within the northern Gebidum and Berisal Domains and a transition to syntectonic chlorite + biotite in the Simplon and Isorno Domains (MANCKTELOW 1985, MERLE et al. 1986, STECK 1987). Such chlorite-muscovite-quartz assemblages are stable below ca. 550°C, with only limited dependence on pressure and composition (WINKLER 1979, p. 77). In the hangingwall, there is no evidence of a pervasive ductile deformation associated with the SFZ and this block must have already cooled through the ductile/brittle transition temperature for quartz-rich rocks (i.e. ca. 300°C) prior to development of the SFZ.

These observations can be related directly to the cooling curves for samples from the footwall and hangingwall. If temperatures in the footwall during this phase initially exceeded 300°C, the initiation of these movements cannot by younger than ca. 12 Ma (Fig. 45). For temperatures within the hangingwall during the same period to have been less than this transition temperature, the deformation must not have begun before 20–22 Ma. As discussed above, temperatures in the footwall mylonites did not exceed 550°C during deformation; this also implies a maximum age of 18–22 Ma. The displacement which is recorded as the broad zone of high-strain ductile deformation in the footwall must, therefore, have occurred somewhere in the period 12–18 Ma.

It must be emphasized that these results are only as good as the age data and blocking temperature model on which they are based and that this is an area of active research in the Simplon Alps. In particular, FRANK & STETTLER (1979) report significantly younger muscovite K/Ar mineral ages from the Simplon Alps than those from earlier studies summarized in the "cooling curves" (see Fig. 45*a*). In a NW–SE profile from Brig to Verampio within the footwall, FRANK & STETTLER (1979) found that K/Ar white mica mineral ages of Mesozoic rocks give an average of 10 Ma, with a slight but consistent trend from younger ages in the north around Brig (8–9 Ma) to older in the south around Verampio (13–14 Ma). Similar results have been found further east along the Maggia Valley (HURFORD 1986) and suggest that early uplift was more rapid in the south. This differential uplift was probably instrumental in developing the southern steep belt (SCHMID et al. 1987*b*) and contributed to the present elongate domal shape of the Toce Culmination.

In the northern Berisal Domain adjacent to the Rhone Valley, the retrograde mylonite foliation of the footwall is folded about the south-vergent Berisal–Glishorn backfolds. The limbs of these backfolds still preserve the microstructure and texture of the earlier mylonitic foliation, rotated such that shear senses are reversed on opposing limbs (Fig. 30). Small scale folds are intermediate between Type 1 (parallel) and Type 2 (similar, RAMSAY 1967), with clear thickening of the hinge region (Fig. 31). The backfolding was therefore also associated with ductile deformation of quartzo-feldspathic units, although of much weaker magnitude than that associated with the mylonite foliation, and must also have begun prior to cooling through the ca. 300°C transition temperature at around 12 Ma.

Late fissure veins, commonly containing quartz, adularia and muscovite crystals of high quality, are found scattered throughout the region (STALDER et al. 1973) and clearly postdate all pervasive ductile deformation. As discussed by PURDY & STALDER (1973), the K/Ar muscovite

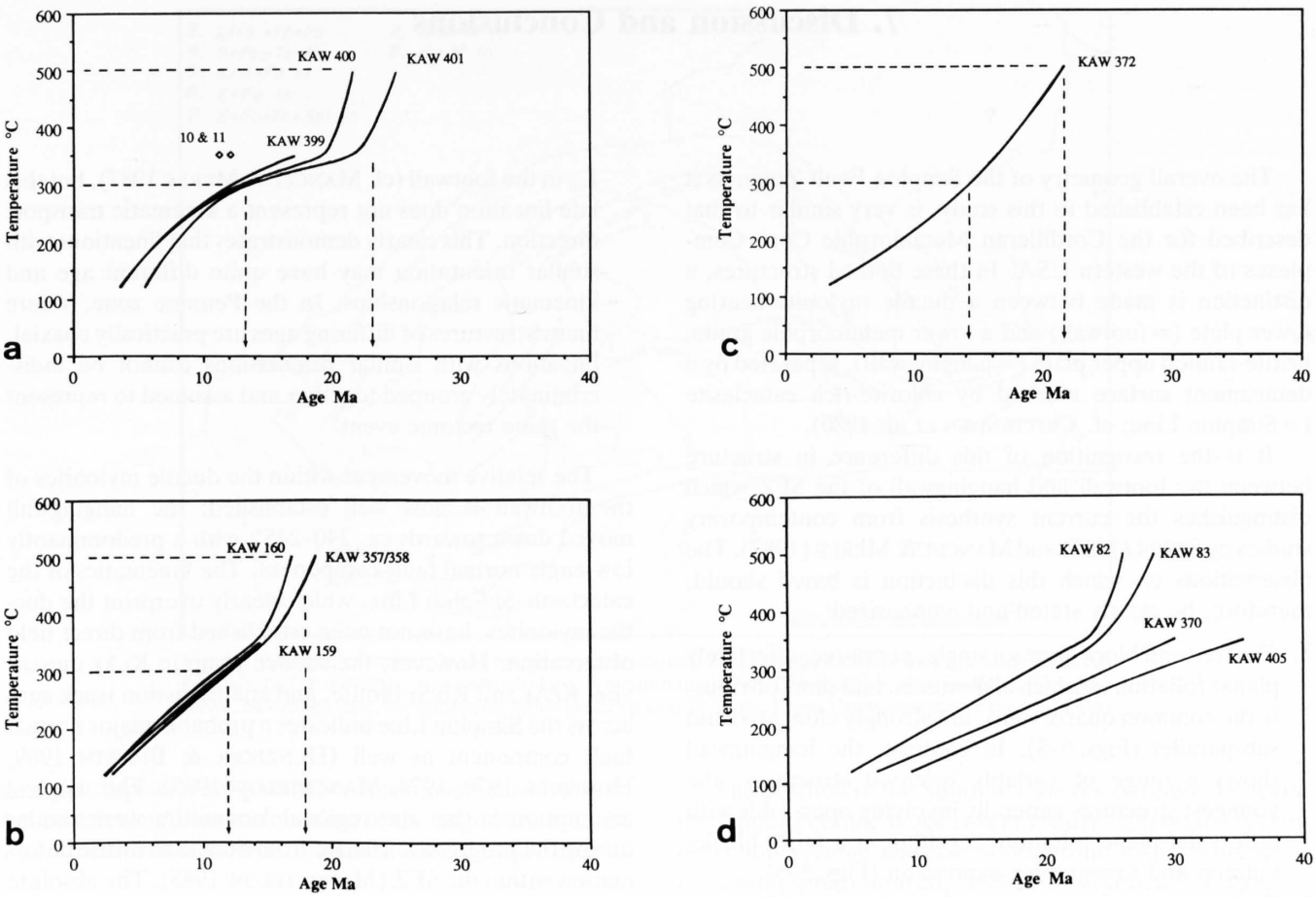

Fig. 45: Interpreted cooling curves for the Simplon Alps.

The isotopic systems and approximate blocking temperatures are (e.g. HURFORD 1986): white mica Rb/Sr (500 ± 50 °C), white mica K/Ar (350 ± 50 °C), biotite Rb/Sr and K/Ar (300 ± 50 °C), and apatite fission-track (120 ± 25 °C). Data for the construction of the curves derives from JÄGER et al. (1967), HUNZIKER & BEARTH (1969), HUNZIKER (1969) and PURDY & JÄGER (1976). Detailed locations for each of the samples can be found in PURDY & JÄGER (1976) and WAGNER et al. (1977).

(a) Cooling curves for samples from the Berisal and Gebidum Domains (cf. Fig. 23). The considerably younger ages for samples 10 and 11 (white mica K/Ar) were reported by FRANK & STETTLER (1979).

(b) Cooling curves from the Simplon Domain between Simplon village and Zwischbergen.

(c) Cooling curve for sample KAW372 from the Bognanco Valley, Isorno Domain.

(d) Cooling curves from the Upper Pennine Domain (hangingwall). Note the considerably slower cooling rates since 20 Ma compared with (a)–(c).

and adularia ages from these veins, when not obscured by problems of excess argon, may represent either cooling or formation ages, dependent upon the temperature of the host rock at the time of vein introduction. Vein mineral ages significantly younger than the host rock are interpreted as formation ages, while concordant ages suggest that both host rock and vein cooled together through the blocking temperature. In the Simplon Rail Tunnel, vein mineral ages are similar to those of the host rock, at around 9 Ma (cf. the results of FRANK & STETTLER 1979 discussed above). In the Robiei area, within the continuation of the Berisal Domain of younger backfolding, fissure vein muscovite yields a K/Ar age of 13.7 Ma and adularia 13.6 Ma. The extensive backfolding in this region must clearly be older than these veins. Whether backfolding in the Robiei area is strictly synchronous with that of the Simplon Pass is still open for debate. However, when the observations from the fissure veins are combined with those on microstructure and retrograde metamorphism discussed above, it is at least clear that the ductile movements in the footwall of the SFZ, leading to the development of the mylonitic foliation, must have occurred in the Early to Middle Miocene. Unfortunately, Rb/Sr studies of the fissure vein minerals from these critical regions are still lacking; the higher blocking temperature of the Rb/Sr muscovite system would provide either older cooling ages or formation ages which would more tightly constrain the timing of the Simplon Phase.

The brittle, cataclastic component of the SFZ, most spectacularly seen as the Simplon Line discontinuity, is clearly younger than the ductile mylonites and the minimum age of these movements is not constrained by the above arguments. The Simplon Line is itself broadly folded, coaxial with the higher amplitude Berisal–Glishorn backfolds, which may indicate that most movement was still at relatively elevated temperatures, not long after attainment of the brittle/ductile transition in the footwall at ca. 12 Ma. The SFZ is not currently seismically active.

7. Discussion and Conclusions

The overall geometry of the Simplon Fault Zone, as it has been established in this study, is very similar to that described for the Cordilleran Metamorphic Core Complexes of the western USA. In these domed structures, a distinction is made between a ductile mylonite-bearing lower plate (= footwall) and a lower metamorphic grade, brittle-faulted upper plate (= hangingwall), separated by a detachment surface marked by chlorite-rich cataclasite (= Simplon Line; cf. CRITTENDEN et al. 1980).

It is the recognition of this difference in structure between the footwall and hangingwall of the SFZ which distinguishes the current synthesis from contemporary studies by STECK (1987) and MANCEL & MERLE (1987). The observations on which this distinction is based should, therefore, be clearly stated and emphasized:

1. The footwall block shows a single, pervasive, effectively planar foliation in which all features, and most obviously the common quartz veins, are strongly elongated and sub-parallel (Figs. 6–8). In contrast, the hangingwall shows a range of variably oriented structures, the youngest structures generally involving open folds with little axial plane foliation, resulting in a fairly blocky outcrop and topographic expression (Figs. 3–5).
2. With the exception of the northern domain of Berisal–Glishorn backfolding (the Berisal Domain), the mylonitic foliation in the immediately adjacent footwall block is nearly concordant with the Simplon Line (Plate). Structures in the hangingwall are often markedly discordant. This is particularly clear from the trend of the dominant foliation (e.g. Plate; Fig. 2 in MANCKTELOW 1985; Fig. 4 in MANCEL & MERLE 1987), where it can be seen that the foliation in the hangingwall is often abruptly truncated by the Simplon Line at a high angle.
3. The mineral cooling ages indicate that the hanging wall had already cooled through the critical temperature for thermally activated ductile flow in quartz-rich rocks (ca. 300°C, SIBSON et al. 1979, ATKINSON 1982) around 25–30 Ma. Cooling through this transition in the footwall block did not occur until around 12–16 Ma. The exposed level of the hangingwall block was not capable of pervasive ductile deformation during movement on the Simplon Fault Zone.
4. The Simplon Line represents a very marked fabric boundary, as is seen, for example, in the microstructures and textures from mono-mineralic quartz veins within the footwall and hangingwall blocks (Figs. 13, 14). The textures from the footwall are clearly related to the lineation L_m (Fig. 14, Appendices C, D). Textures from the hangingwall, however, have no affinity with this direction (Fig. 14*b*, *c*). They apparently maintain a memory of NW–SE directed movements (Fig. 14*a*, *b*), approximately perpendicular to the movement direction of the SFZ. A late lineation (generally a crenulation or fold axis lineation) within the hangingwall is directed towards the WSW, approximately parallel to L_m in the footwall (cf. MANCEL & MERLE 1987), but this late lineation does not represent a kinematic transport direction. This clearly demonstrates that lineations with similar orientation may have quite different age and kinematic relationships. In the Pennine zone, where many structures of differing ages are practically coaxial, lineations with similar orientations cannot be indiscriminately grouped together and assumed to represent the same tectonic event.

The relative movement within the ductile mylonites of the footwall is now well established: the hangingwall moved down towards ca. 240–245°, with a predominantly low-angle normal fault component. The kinematics of the cataclastic Simplon Line, which clearly overprint the ductile mylonites, have not been established from direct field observation. However, the sudden jump in K/Ar muscovite, K/Ar and Rb/Sr biotite, and apatite fission track ages across the Simplon Line indicates a probable major normal fault component as well (HUNZIKER & BEARTH 1969, HUNZIKER 1970, 1974, MANCKTELOW 1985). The simplest assumption is that the regional kinematics were similar during the progressive change from ductile to brittle deformation within the SFZ (MANCKTELOW 1985). The absolute displacement across the SFZ is difficult to estimate with any accuracy. The discrepancy in metamorphic temperatures of ca. 200–210°C which existed in the now adjacent footwall and hangingwall prior to displacement suggests a vertical component of ca. 7 km (MANCKTELOW 1985), within the range 5–8 km suggested by HUNZIKER (1970). For the average plunge of L_m around 25°, this translates into relative displacement parallel to L_m of ca. 16 km. However, as is obvious from the long-section of the Plate, the plunge of L_m decreases towards the northeast onto the Toce Culmination, and probably also decreases towards the southwest below the Upper Pennine Domain. The updoming of the Toce Culmination has probably outlasted the movement on the SFZ, as indicated by the occurrence of the youngest biotite and muscovite ages in the core of the culmination (e.g. HUNZIKER 1974). The original plunge of the movement vector may, therefore, have been less than 25°, and the absolute displacement correspondingly larger.

MANCEL & MERLE (1987) have suggested that displacement of the metamorphic boundary marking the transition from albite to oligoclase (An >17, BEARTH 1958, WENK & KELLER 1969, Fig. 46 from TROMMSDORFF & EVANS 1974) indicates a significant sinistral, hangingwall to the southeast, displacement across the Simplon Line. Such a relative displacement in map view is also possible by continued normal displacement of the hangingwall. If the horizontal offset of the oligoclase boundary across the Simplon Line is taken at ca. 18 km from the regional compilation of TROMMSDORFF & EVANS (1974, cf. Fig. 46) and the average orientations of the Simplon Line (27°→220°) and movement direction (25°→243°) are taken from Figure 24*a*,

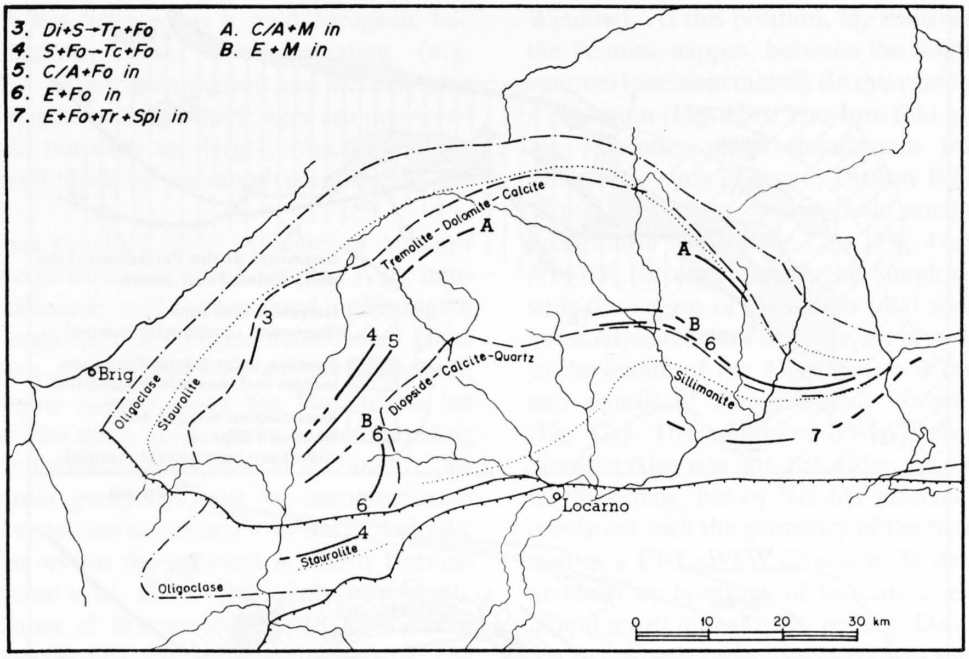

Fig. 46: Summary of mineral zone boundaries and isograds in ultramafic schists in the Lepontine Alps. Abbreviations for minerals: A = anthophyllite, B = cummingtonite, Di = diopside, E = enstatite, Fo = forsterite, M = magnesite, S = antigorite, Spi = green spinel, Tc = talc. From TROMMSDORFF & EVANS (1974).

then the displacement parallel to this movement direction can be calculated for various dips of the oligoclase boundary to the northwest (→315°). These are listed in Table 1.

Table 1: *Calculated Displacement versus Initial Dip of the Oligoclase Boundary*

Dip of boundary to NW	*Displacement in km*
10°	9
20°	22
30°	46
40°	101
50°	317

It is obvious that realistic estimates are only obtained if the oligoclase boundary was initially dipping quite shallowly towards the northwest when it intersected the Simplon Line. This is not unreasonable. The mylonitic S_m foliation is clearly retrograde, postdating the development of oligoclase, and the oligoclase boundary would have been passively rotated into near parallelism with S_m in the highly foliated zone of the footwall, adjacent to the Simplon Line. The orientation of this boundary should, therefore, not differ greatly from that of the S_m foliation in the immediate vicinity of the Simplon Line (cf. cross-section of the Plate); this foliation is generally asymptotic to the Simplon Line and only steepens at depth within the northern steep belt (cf. STRECKEISEN et al. 1974, MILNES 1975). Rotation of the oligoclase boundary into an orientation asymptotic to the Simplon Line may mean that the actual horizontal displacement across the Simplon Line discontinuity is considerably less than the 18 km obtained by continuing it directly southwestwards until it intersects the Simplon Line (cf. Fig. 1 in FREY 1974). The displacement on the Simplon Line cataclasites would be proportionally reduced, part of the displacement being accommodated instead within the mylonitic zone of the footwall as expected from the overall geometry of the SFZ.

The position of the Simplon Line discontinuity beneath the Upper Pennine block is very clearly seen on the recent reflection seismic traverse south from Visp (Nationales Forschungsprogramm 20, 1989). In character it exactly mimics what is seen in the Simplon Pass region: an Upper Pennine Zone of blocky outcrop character in which flat-lying, planar reflectors are largely lacking separated by a sharp discontinuity from the strongly foliated, mylonitic footwall (the Lower Pennine Zone), in which the parallelism of lithologic boundaries provide a multitude of strong reflectors. In an approximately N–S profile, these reflectors pitch around 15–20° south, directly comparable to the pitch of the S_m foliation in the profile of the Plate. The large amplitude backfolding of the Berisal Domain, which is responsible for the "northern steep belt" of MILNES 1974*a*, only occurs below the Simplon Line discontinuity. This zone should also be visible in the seismic profiles to the southwest as a transparent zone lacking horizontal reflectors.

The location of the SFZ, and the Simplon Line in particular, is now well established between the Isorno Valley in northern Italy and the Saas Valley near Visp. The occurrence of a late stretching component towards ca. 240°, strongly developed adjacent to the Rhone Valley itself (e.g. Fig. 27), but also discernible throughout much of the western Helvetic Alps and Aar Massif (DURNEY & RAMSAY 1973, STECK 1984) is consistent with a further continuation to the west along the Rhone Valley (e.g. STECK 1987). A sense of shear related to this lineation can sometimes be determined (e.g. Fig. 19, STECK 1984), and is consistent with that of the SFZ (i.e. upper block down towards the southwest, with a dextral horizontal component). This continuation further to the west, along the Rhone Valley, has not been directly addressed in this study and any extension towards the Western Alps is purely conjectural. However, it is unlikely that the SFZ continues

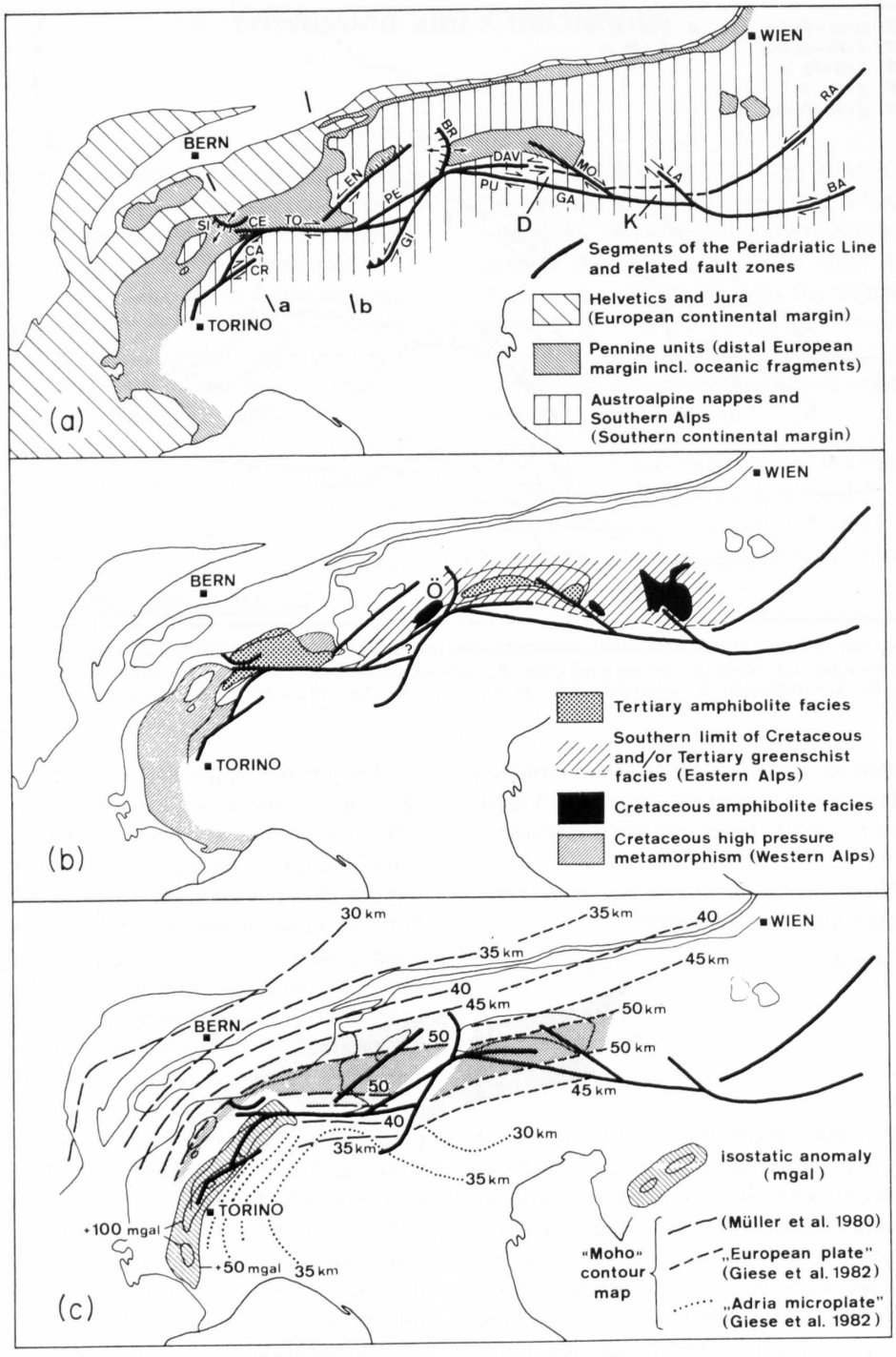

Fig. 47: Summary figure from SCHMID et al. (1989), showing the various segments of the Periadriatic Line in relation to the main subdivision of the Alps (a), the metamorphism (b), and the geophysical data (c). The Simplon Line is indicated in (a) by SI. Crustal thickness is shown in (c) as contours on the crust/mantle boundary (the "Moho").

below the Western Alps and the European foreland of the Massif Central. It seems much more likely that the overall shape is that of a broad spoon, related to the regional Wildstrubel–Bernard Depression. The extensional normal fault displacement observed in the Simplon Alps may be directly related to approximately coeval (mid-Miocene or younger), southwest-directed thrusting in the Western Alps (e.g. see references in the recent review of PLATT et al. 1989).

Such a spoon shaped displacement zone, with normal fault movements in the internal region transforming to reverse movements in the external part is suggestive of gravity driven allocthonous sheets. Models for such gravitational tectonic denudation associated with rapid unroofing of thickened, metamorphic fold belts have been discussed recently by PLATT (1986) and DAVY & GILLET (1987). The Upper Pennine Zone would represent the uppermost block, at temperatures below the brittle/ductile

transition, which has behaved as a rigid "orogenic lid" during this Simplon Phase of deformation (e.g. LAUBSCHER 1983). Earlier deformation and metamorphic events of Meso-Alpine and Eo-Alpine ages are preserved within this block, but they are largely obscured in the underlying footwall block by the more recent ductile deformation.

This study has provided clear evidence of a major WSW–ENE directed extension of the Simplon Alps, initiated during the Miocene, and concentrated in this region within the low-angle normal Simplon Fault Zone. Units from the Southern Alps, which were already juxtaposed against the Pennine nappes along the Periadriatic (or Insubric) Line at this time, do not show a corresponding pervasive Alpine deformation (SCHMID et al. 1987*b*). This difference in strain geometry must be accommodated either along the mylonites associated with the Periadriatic Line itself and/or within the adjacent northern Pennine nappe units (SCHMID et al. 1989). These units (the Monte Rosa and Sesia zones, cf. SCHMID et al. 1987*b*) form part of the hangingwall to the SFZ within the Simplon Alps. The observation from this more northern region that the hangingwall is not pervasively deformed during movements on the SFZ may not be extended further south to the region adjacent to the Periadriatic Line, although it may be that here again the strain is concentrated within a relatively narrow mylonite zone.

As noted by SELVERSTONE (1988) and SCHMID et al. (1989), the SFZ occurs adjacent to a major bend in the Periadriatic Line (as does the possibly kinematically comparable Brenner Line at the western end of the Tauern Window). At this position, the transverse distance across the Pennine nappes, between the Southern Alps and the external basement massifs (in this case the Aar Massif) is at a minimum (Fig. 47*a*). The Jura fold arc (initiated during the Miocene, major detachment folding during late Miocene to early Pliocene, TRÜMPY 1980) is also restricted to that part of the Alpine chain northwest of this major bend in the Periadriatic Line (Fig. 47*a*). It follows that a NW–SE traverse through the Simplon Alps corresponds with the region of maximum total shortening across the Swiss Alpine chain. However, the crustal thickness parallel to the length of the Alpine chain is remarkably constant and significant variation only occurs across the chain (Fig. 47*c*). The additional NW–SE shortening within the Simplon Alps was not, therefore, accommodated by crustal thickening, but by NE–SW directed extension. This is consistent with the geometry of the SFZ, involving extension in a ENE–WSW direction. In detail, this may have involved an interplay of tectonic crustal thickening and lateral gravitational collapse (e.g. DAVY & GILLET 1987), but the overall geometric effect was shortening transverse to the Alpine chain matched by extension approximately parallel to the chain. That NNW–SSE shortening was still occurring during ENE–WSW extension is shown by the relationship between the SFZ and the northern backfolds (Glishorn–Berisal folds) discussed previously. It is also indicated by the concurrent detachment and folding of the Jura in the Alpine foreland. The SFZ is not, then, a result of continental extension, but rather of lateral escape during continental compression in a region of overthickened continental crust.

Acknowledgments

Thanks are due to all my colleagues in Zürich. Particular thanks are extended to John Ramsay, Stephan Schmid, Geoff Milnes, Eva Klaper, Johannes Hunziker, Tony Hurford, Michael Soom, Volkmar Trommsdorff, Olivier Merle and Albrecht Steck for discussion of the many problems in the Pennine Alps, and to Mark Handy for his perceptive comments on an earlier version of the manuscript. My interest in the Simplon Fault was first aroused during an excursion to the Simplon Alps led by Geoff Milnes. Stephan Schmid and Martin Casey introduced me to fabric studies and encouraged me throughout; the FORTRAN computer program package developed by Martin Casey was crucial for the X-ray texture measurements presented in Appendix D. The Swiss National Hydrological and Geological Survey and Pascal Jeanbourquin (compiler) are also thanked for access to the still unpublished 1:25 000 geological map sheet Brig, which represents a synthesis of work from many authors.

Summary

The Simplon Fault Zone (SFZ), which has been mapped from near Visp in the Rhone Valley (Switzerland) to the Isorno Valley, northeast of Domodossola (Italy), consists of two distinct components: a broad, several-kilometre wide zone of ductile mylonites in the footwall, which is separated from the hangingwall (without a pervasive ductile SFZ overprint) by a narrow zone of cataclasites. The cataclasites brecciate the mylonites of the footwall and are clearly younger. It is this narrow cataclasite zone which forms the structural discontinuity (seen in the mineral ages, rock fabrics, and metamorphic mineral assemblages) and has been mapped previously as the Simplon Fault ("Simplon Störung") or Simplon Line. The Simplon Line becomes less clear to the southeast in the Isorno Valley where a change in microstructure (grain boundary migration and exaggerated grain growth) suggests increased temperature during SFZ movement; here the SFZ is a broad ductile shear zone containing strongly foliated rocks. Kinematic indicators within the mylonites of the footwall show a relative movement of the hangingwall down towards ca. 240–245°. The SFZ is predominantly a low-angle normal fault, reflecting extension of the Simplon Alps in a WSW–ENE direction. The total relative displacement is probably in the order of 15 km, but is not well constrained and depends on the original fault orientation. Kinematic indicators have not been observed in the poorly exposed cataclasites of the Simplon Line.

Quartz veins and occasional quartzites from the footwall of the SFZ provide excellent material for the study of texture development in a major fault zone. The *c*-axis patterns are very consistent, and represent variably kinked single or unequally-populated crossed girdles associated with a strong <*a*> maximum, rotated ≦30° away from the lineation and foliation with the sense of shear. Study of the most favoured orientations suggests that deformation was by multiple slip on prism, rhomb and basal planes, all with the Burgers vector <*a*>. In particular, the *c*-axis orientations of highly elongate ribbon grains seldom correspond with ones suitable for single slip, but require mixed slip on two or more systems. In the southeast of the study area, increased grain boundary migration recrystallization is associated with a contraction of orientations in the *c*-axis pole figures towards those favourable for rhomb slip. This is also seen in the optical microstructure as a tendency for grains oriented for easy prism slip to be preferentially consumed by their neighbours during grain boundary migration.

The age of the SFZ relative to the northern backfolding of the Penninic nappes can be established in the Simplon Pass region: large amplitude backfolds (Berisal–Glishorn) fold the retrograde mylonite foliation, but are restricted to the footwall. Corresponding folds in the Simplon Line and overlying hangingwall are of similar orientation but of much lower amplitude and broader wavelength. The difference in mineral ages and constructed cooling curves to either side of the Simplon Line suggest that initiation of the SFZ occurred in the Early to Middle Miocene. The intimate relationship between the SFZ and the northern backfolds, together with the approximately coeval or slightly later development of the Jura detachment and fold belt, indicates that ca. NNW–SSE shortening was still occurring across the Alpine chain during extensional SFZ movement. The SFZ occurs in the region of maximum total shortening across the Central Alps, and the extension in a WSW–ENE direction associated with the SFZ may be due to gravitational collapse and lateral escape in this direction during continued NNW–SSE shortening.

Zusammenfassung

Die Simplon-Störungszone (SFZ), die von Visp im Rhonetal (Schweiz) bis zum Isornotal nordöstlich von Domodossola (Italien) kartiert worden ist, kann in zwei Strukturelemente unterteilt werden: eine kilometerbreite Zone von duktilen Myloniten im Liegenden, die vom Hangenden (ohne durchgehende duktile Simplon-Überprägung) durch eine enge Kataklasitzone getrennt ist. Die Kataklasite haben die Mylonite im Liegenden eindeutig überprägt und sind sicher jünger. Diese schmale Zone entspricht einer strukturellen Diskontinuität, wie dies aus den unterschiedlichen Mineralaltern, Metamorphosegraden und Gesteinsgefügen im Hangenden und Liegenden deutlich hervorgeht. Diese Diskontinuität wurde bisher als «Simplon-Störung» oder «Simplon-Linie» kartiert; sie wird in südöstlicher Richtung, wo die veränderten Mikrostrukturen (zunehmende Korngrenzen-Wanderung, Kornwachstum) auf erhöhte Temperaturen während der SFZ-Bewegungen hindeuten, immer weniger ausgeprägt. Hier dürfte die SFZ als eine breite, stark verschieferte Zone vorliegen. Zahlreiche kinematische Indikatoren in den Myloniten des Liegenden bestätigen eine relative Abschiebung des Hangenden in Richtung ca. 240–245°. Die SFZ ist also hauptsächlich eine schwach einfallende Abschiebung, die auf WSW–ENE gerichtete Extension hinweist. Der totale Verschiebungsbetrag lässt sich nicht genau bestimmen; er ist stark von der ursprünglichen Lage der Verwerfung abhängig und dürfte in der Grössenordnung von ca. 15 km liegen. Kinematische Indikatoren sind in den schlecht aufgeschlossenen Kataklasiten der Simplon-Linie unbekannt.

Nahezu monomineralische Quarzgänge und gelegentliche Quarzite im Simplon-Gebiet liefern häufig ausgezeichnetes Material, um die Gefügeentwicklung in einer grossregionalen Störungszone zu erforschen. Die gemessenen *c*-Achsenverteilungen sind sehr konstant. Sie bilden leicht verbogene einfache oder asymmetrisch angeordnete gekreuzte Gürtel, die mit einem starken <*a*>-Maximum (≦30° von der Lineation wegrotiert) verknüpft sind. Ein Studium der bevorzugten Orientierungen zeigt, dass die Verformung auf Prismen-, Rhomben- und Basal-Gleitebenen verteilt ist, alle mit dem Burgers-Vektor <*a*>. Bemerkenswert ist, dass die *c*-Achsen der stark gelängten «ribbon grains» selten mit Orientierungen übereinstimmen, die für einfaches Gleiten geeignet sind; sie benützen offensichtlich gleichzeitig mehrere Gleitsysteme. Zunehmende Korngrenzen-Wanderung im Südosten ist mit einer Verengung der *c*-Achsenverteilung auf für Rhomben-Gleiten geeignete Orientierungen verbunden. Dies wurde auch durch die optische Mikrostruktur bestätigt: Sie zeigt die Tendenz, dass Körner, die eine für Prismen-Gleiten geeignete Orientierung besitzen, bei der Korngrenzen-Wanderung von ihren Nachbarn bevorzugt vertilgt wurden.

Das Alter der SFZ bezüglich der Rückfaltung der penninischen Decken im Norden konnte im Simplonpass-Gebiet bestimmt werden: die retrograde mylonitische Schieferung wurde durch die grossen Rückfalten (Berisal–Glishorn) verformt. Diese grossen Rückfalten beim Simplonpass sind nur im Liegenden zu sehen. Junge Falten in der Simplon-Linie selbst und in deren Hangendem sind von ähnlicher Orientierung, aber von viel kleinerer Amplitude und haben eine grössere Wellenlänge. Anhand der Unterschiede bezüglich der Mineralalter und der konstruierten Abkühlungskurven beidseits der Simplon-Linie kann für die Entstehung der SFZ auf ein früh- bis mittelmiozänes Alter geschlossen werden. Die enge Beziehung der SFZ mit den Rückfalten im Norden — zusammen mit der gleichzeitigen oder vielleicht etwas jüngeren Bildung der Jura-Faltengebirge — zeigt, dass ungefähr NNW–SSE gerichtete Verkürzungen der Alpenkette noch während der Entwicklung der SFZ stattgefunden haben. Die SFZ liegt im Bereich der maximalen Verkürzung der Zentralalpen, und die Streckung in WSW–ENE-Richtung, die mit der SFZ verknüpft ist, könnte durch gravitativen Kollaps und seitliches Ausweichen von Material in dieser Richtung während der NNW–SSE-Verkürzung verursacht sein.

References

AMSTUTZ, A. (1954): Pennides dans l'Ossola et problème des racines. – Arch. Sci. (Genève) *7*, 411.

ARGAND, E. (1911): Les nappes de recouvrement des Alpes Pennines et leurs prolongements structuraux. – Matér. Carte géol. Suisse [N.F.] *31*, 1–26.

– (1916): Sur l'arc des Alpes occidentales. – Eclogae geol. Helv. *14*, 145–191.

ARMSTRONG, R.L., JÄGER, E. & EBERHARDT, P. (1966): A comparison of K-Ar and Rb-Sr ages on Alpine biotites. – Earth and planet. Sci. Lett. *1*, 13–19.

ATKINSON, B.K. (1982): Subcritical crack propagation in rocks: theory, experimental results and applications. – J. struct. Geol. *4*, 41–56.

BATES, R.L. & JACKSON, J.A (1980): Glossary of Geology. – Amer. geol. Inst., Washington.

BAUMANN, W. (1979): Die Goldvererzungen der Antiform von Vanzone (Prov. Novara, Italien). – Diplomarb. Univ. Zürich (unpubl.).

BEARTH, P. (1956a): Zur Geologie der Wurzelzone östlich des Ossolatales. – Eclogae geol. Helv. *49*, 267–278.

– (1956b): Geologische Beobachtungen im Grenzgebiet der lepontinischen und penninischen Alpen. – Eclogae geol. Helv. *49*, 279–290.

– (1957): Die Umbiegung von Vanzone (Valle Anzasca). – Eclogae geol. Helv. *50*, 161–170.

– (1958): Über einen Wechsel der Mineralfazies in der Wurzelzone des Penninikums. – Schweiz. mineral. petrogr. Mitt. *38*, 363–373.

– (1972): Geologischer Atlas der Schweiz 1:25000, Blatt 61: Simplon. – Schweiz. geol. Komm.

– (1973): Erläuterungen zu Blatt Simplon (Atlasblatt 61). Geologischer Atlas der Schweiz 1:25000. – Schweiz. geol. Komm.

BEHRMANN, J.H. (1987): Large-scale subhorizontal extension in a convergent orogen: the Sterzing–Steinach mylonite zone in the Eastern Alps (abstract). – Terra cognita *7*, 89.

BELL, T.H. & ETHERIDGE, M.A. (1973): Microstructures of mylonites and their descriptive terminology. – Lithos *6*, 337–348.

– (1976): The deformation and recrystallization of quartz in a mylonite zone. – Tectonophysics *32*, 235–267.

BOUCHEZ, J.-L. (1977): Plastic deformation of quartzites at low temperatures in an area of natural strain gradient (Angers, France). – Tectonophysics *39*, 25–80.

– (1978): Preferred orientations of quartz *a* axes in some tectonites: kinematic inferences. – Tectonophysics *49* T25–T30.

BOUCHEZ, J.-L., LISTER, G.S. & NICOLAS, A. (1983): Fabric asymmetry and shear sense in movement zones. – Geol. Rdsch. *72*, 401–419.

BOYER, S.E. & ELLIOT, D. (1982): Thrust systems. – Bull. amer. Assoc. Petroleum Geol. *66*, 1196–1230.

BUNGE, H.J. (1969): Mathematische Methoden der Texturanalyse. – Akademie-Verl., Berlin.

BUNGE, H.J. & WENK, H.-R. (1977): Three-dimensional texture analysis of three quartzites (trigonal crystal and triclinic specimen symmetry). – Tectonophysics *40*, 257–285.

BURCHFIEL, B.C. & ROYDEN, L. (1985): North–south extension within the convergent Himalayan region. – Geology *13*, 679–682.

BURG, J.P. & LAURENT, P. (1978): Strain analysis of a shear zone in a granodiorite. – Tectonophysics *47*, 15–42.

BURRI, M. (1979): Les formations valaisannes dans la région de Visp. – Eclogae geol. Helv. *72*, 789–802.

BUTLER, R.W.H (1986): Thrust tectonics, deep structure and crustal subduction in the Alps and Himalayas. – J. geol. Soc. (London) *143*, 857–873.

CARRERAS, J. & GARCIA CELMA, A. (1982): Quartz *C*-axis fabric variation at the margins of a shear zone developed in schists from Cap de Creus (Spain). – Acta geol. hisp. *17*, 137–149.

CARTER, N.L. (1976): Steady state flow of rocks. – Rev. Geophys. (Space Phys.) *14*, 301–360.

CASEY, M. (1981): Numerical analysis of X-ray texture data: an implementation in FORTRAN allowing triclinic or axial specimen symmetry and most crystal symmetries. – Tectonophysics *78*, 51–64.

CLARK, S.P., Jr. & JÄGER, E. (1969): Denudation rates in the Alps from geochronological and heat flow data. – Amer. J.Sci. *267*, 1143–1160.

COBBOLD, P.R. (1977a): Description and origin of banded deformation structures. I. Regional strain, local perturbations, and deformation bands. – Canad. J. Earth Sci. *14*, 1721–1731.

– (1977b): Description and origin of banded deformation structures. II. Rheology and the growth of banded perturbations. – Canad. J. Earth Sci. *14*, 2510–2523.

COBBOLD, P.R., COSGROVE, J.W. & SUMMERS, J.M. (1971): Development of internal structures in deformed anisotropic rocks. – Tectonophysics *12*, 23–53.

CRITTENDEN, M.D., Jr., CONEY, P.J. & DAVIS, G.H. (Eds.), (1980): Cordilleran Metamorphic Core Complexes. – Mem. geol. Soc. Amer. *153*.

CURTI, E. (1987): Isotope geochemistry and fluid inclusion studies on the late metamorphic gold-quartz veins of the Monte Rosa area, northwestern Alps, Italy: the origin of metals and fluids. – Diss. ETH Zürich *8263*.

DAVY, PH. & GILLET, PH. (1987): Evidence for gravitational readjustments at crustal scale in a thickened crust: examples from the Central Alps. – Terra cognita *7*, 85.

DIAMOND, L.W. & WIEDENBECK, M. (1986): K-Ar radiometric ages of the gold-quartz veins at Brusson, Val d'Ayas, NW Italy: evidence of mid-Oligocene hydrothermal activity in the northwestern Alps. – Schweiz. mineral. petrogr. Mitt. *66*, 385–393.

DURNEY, D.W. & RAMSAY, J.G. (1973): Incremental strains measured by syntectonic crystal growth. In: DE JONG, K.A. & SCHOLTEN, R. (Eds.): Gravity and Tectonics (pp. 67–96). – Wiley, New York.

EISBACHER, G.H. (1970): Deformation mechanics of mylonitic rocks and fractured granites in Cobequid Mountains, Nova Scotia, Canada. – Bull. geol. Soc. Amer. *81*, 2009–2020.

ETCHECOPAR, A. (1977): A plane kinematic model of progressive deformation in a polycrystalline aggregate. – Tectonophysics *39*, 121–139.

ETHERIDGE, M.A., HOBBS, B.E. & PATERSON, M.S. (1973): Experimental deformation of single crystals of biotite. – Contr. Mineral. Petrol. *38*, 21–36.

ETHERIDGE, M.A. & HOBBS, B.E. (1974): Chemical and deformational controls on recrystallization of mica. – Contr. Mineral. Petrol. *43*, 111–124.

FRANK, E. (1979): Metamorphose mesozoischer Gesteine im Querprofil Brig–Verampio. – Diss. Univ. Bern.

– (1983): Alpine metamorphism of calcareous rocks along a cross-section in the Central Alps: occurrence and breakdown of muscovite, margarite, and paragonite. – Schweiz. mineral. petrogr. Mitt. *63*, 37–93.

FRANK, E. & STETTLER, A. (1979): K-Ar and ^{39}Ar-^{40}Ar systematics of white K-mica from an Alpine metamorphic profile in the Swiss Alps. – Schweiz. mineral. petrogr. Mitt. *59*, 375–394.

FREY, M. (1974): Alpine metamorphism of pelitic and marly rocks of the Central Alps. – Schweiz. mineral. petrogr. Mitt. *54*, 489–508.

FROST, H.S. & ASHBY, M.F. (1982): Deformation-mechanism Maps. – Pergamon Press, Oxford.

GAPAIS, D. & WHITE, S.H. (1982): Ductile shear bands in a naturally deformed quartzite. – Textures and Microstructures *5*, 1–17.

GARCIA CELMA, A. (1983): *C*-axis- and shape-fabrics in quartz-mylonites of Cap de Creus (Spain); their properties and development. – Ph. D. thesis, Univ. Utrecht.

GERLACH, H. (1869): Die penninischen Alpen. – N. Denkschr. schweiz. Ges. Natw. *23*.

– (1871): Das Südwestliche Wallis. – Beitr. geol. Karte Schweiz *9*.

– (1883): Die penninischen Alpen. – Beitr. geol. Karte Schweiz *27*.

GIESE, P., RUETTER, K.-J., JACOBSHAGEN, V. & NICOLICH, R. (1982): Explosion seismic crustal studies in the Alpine Mediterranean region and their implications to tectonic processes. In: BERCKHEMER, H. & HSÜ, K.J. (Eds.): Alpine-Mediterranean Geodynamics (pp. 39–73). – Amer. geophys. Union (geodyn. Ser.) *7*.

GREEN, H.W., GRIGGS, D.T. & CHRISTIE, J.M. (1970): Syntectonic and annealing recrystallization of fine grained quartz aggregates. In: PAULITSCH, W. (Ed.): Experimental and Natural Rock Deformation (pp. 272–335). – Springer, Heidelberg.

GRIGGS, D.T. & BLACIC, J.D. (1965): Quartz: anomalous weakness of synthetic crystals. – Science (London) *147*, 292–295.

HERREN, E. (1987): Zanskar shear zone: northeast–southwest extension within the Higher Himalayas (Ladakh, India). – Geology *15*, 409–413.

HUNZIKER, J.-C. (1969): Rb–Sr-Altersbestimmungen aus den Walliser Alpen. Hellglimmer- und Gesamtgesteinsalterswerte. – Eclogae geol. Helv. *62*, 527–542.

– (1970): Polymetamorphism in the Monte Rosa, Western Alps. – Eclogae geol. Helv. *63*, 151–161.

– (1974): Rb-Sr and K-Ar age determinations and the Alpine tectonic history of the Western Alps. – Mem. Ist. Geol. Mineral. Univ. Padova *31*.

HUNZIKER, J.-C. & BEARTH, P. (1969) Rb–Sr-Altersbestimmungen aus den Walliser Alpen. Biotitalterswerte und ihre Bedeutung für die Abkühlungsgeschichte der alpinen Metamorphose. – Eclogae geol. Helv. *62*, 205–222.

HURFORD, A.J. (1986): Cooling and uplift patterns in the Lepontine Alps South Central Switzerland and an age of vertical movement on the Insubric fault line. – Contr. Mineral. Petrol. *92*, 413–427.

JÄGER, E., NIGGLI, E. & WENK, E. (1967): Rb–Sr-Altersbestimmungen an Glimmern der Zentralalpen. – Beitr. geol. Karte Schweiz [N.F.] *134*.

KAMB, W.B. (1959): Theory of preferred orientation developed by recrystallization under stress. – J. Geol. *67*, 153–170.

KLAPER, E.M. (1988): Quartz *c*-axis fabric development and large-scale post-nappe folding (Wandfluhhorn Fold, Penninic nappes). – J. struct. Geol. *10*, 795–802.

KLEIN, J.A. (1978): Post-nappe folding southeast of the Mischabelrückfalte (Pennine Alps) and some aspects of the associated metamorphism. – Leidse geol. Meded. *51*, 233–312.

KLEINSCHRODT, R. (1987): Quarzgefügeanalyse im Altkristallin südlich des westlichen Tauernfensters (Südtirol/Italien). – Diss. Univ. Erlangen-Nürnberg.

KVALE, A. (1957): Gefügestudien im Gotthardmassiv und den angrenzenden Gebieten. – Schweiz. mineral. petrogr. Mitt. *37*, 398–434.

– (1966): Gefügestudien im Gotthardmassiv und den angrenzenden Gebieten. – Sonderveröff. Schweiz. geotech. Komm. und Schweiz. geol. Komm.

LADURON, D. & MERLYN, M. (1974): Evolution structurale et métamorphique de l'antiforme de Vanzone (Valle Anzasca et Valle Antrona, Province de Novara, Italie). – Bull. Soc. géol. France (7) *16*, 264–265.

LAPWORTH, C. (1885): The highland controversy in British geology; its causes, course and consequences. – Nature (London) *32*, 558–559.

LAUBSCHER, H.P. (1971): The large-scale kinematics of the Western Alps and the Northern Apennines and its palinspastic implications. – Amer. J. Sci. *271*, 193–226.

– (1983): Detachment, shear, and compression in the central Alps. – Mem. geol. Soc. Amer. *158*, 191–211.

LAW, R.D. (1986): Relationships between strain and quartz crystallographic fabrics in the Roche Maurice quartzites of Plougastel, western Brittany. – J. struct. Geol. *8*, 493–515.

LAW, R.D., CASEY, M. & KNIPE R.J. (1986): The kinematic and tectonic significance of microstructure and crystallographic fabrics within quartz mylonites from the Assynt and Eriboll regions of the Moine Thrust Zone, north-west Scotland. – Trans. r. Soc. Edinburgh (Earth Sci.) *77*, 99–125.

LAW, R.D., KNIPE, R.J. & DAYAN, H. (1984): Strain path partitioning within thrust sheets: microstructural and petrofabric evidence from the Moine Thrust Zone at Loch Eriboll, Northwest Scotland. – J. struct. Geol. *6*, 477–497.

LEU, W. (1986): Lithostratigraphie und Tektonik der nordpenninischen Sedimente in der Region Bedretto–Baceno–Visp. – Eclogae geol. Helv. *79*, 769–824.

LINKER, M.F., KIRBY, S.H., ORD, A. & CHRISTIE, J.M. (1984): Effects of compression direction on the plasticity and rheology of hydrolytically weakened synthetic quartz crystals at atmospheric presssure. – J. geophys. Res. *89*/B6, 4241–4255.

LISTER, G.S. (1977): Discussion: Crossed girdle *c*-axis fabrics in quartzites plastically deformed by plane strain and progressive simple shear. – Tectonophysics *39*, 51–54.

LISTER, G.S., PATERSON, M.S. & HOBBS, B.E. (1978): The simulation of fabric development in plastic deformation and its application to quartzite: the model. – Tectonophysics *45*, 107–158.

LISTER, G.S. & SNOKE, A.W. (1984): S-C mylonites. – J. struct. Geol. *6*, 617–638.

LISTER, G.S. & WILLIAMS, P.F. (1979): Fabric development in shear zones: theoretical controls and observed phenomena. – J. struct. Geol. *1*, 283–297.

LUGEON, M. (1903): Les grandes dislocations et la naissance des Alpes Suisses. – Eclogae geol. Helv. *7*, 335–346.

LUGEON, M. & ARGAND, E. (1905): Sur les grandes nappes de recouvrement de la zone du Piémont. – C.R. Acad. Sci. (Paris), 15 mai 1905, 1364.

MAINPRICE, D., BOUCHEZ J.-L., BLUMENFELD, P. & TUBIÀ, J.M. (1986): Dominant *c* slip in naturally deformed quartz: implications for dramatic plastic softening at high temperature. – Geology *14*, 819–822.

MANCEL, P. & MERLE, O. (1987): Kinematics of the northern part of the Simplon Line. – Tectonophysics *135*, 265–275.

MANCKTELOW, N.S. (1979): The development of slaty cleavage, Fleurieu Peninsula, South Australia. – Tectonophysics *58*, 1–20.

– (1981a): Strain variation between quartz grains of different crystallographic orientation in a naturally deformed metasiltstone. – Tectonophysics *78*, 73–84.

– (1981b): A least-squares method for determining the best-fit point maximum, great circle, and small circle to nondirectional orientation data. – Math. Geol. *13*, 507–521.

– (1985): The Simplon Line: a major displacement zone in the western Lepontine Alps. – Eclogae geol. Helv. *78*, 73–96.

– (1987a): Quartz textures from the Simplon Fault Zone, southwest Switzerland and north Italy. – Tectonophysics *135*, 133–153.

– (1987b): Atypical textures in quartz veins from the Simplon Fault Zone. – J. struct. Geol. *9*, 995–1005.

MERLE, O. (1987): Histoire de la déformation dans les Alpes lepontines occidentales (Alpes centrales). – Bull. Soc. géol. France (8) *3*, 183–190.

MERLE, O., COBBOLD, P.R. & SCHMID, S. (1989): Tertiary kinematics in the Lepontine dome. In: COWARD, M.P., DIETRICH, D. & PARK, R.G. (Eds.): Alpine Tectonics (pp. 113–134). – Spec. Publ. geol. Soc. London *45*.

MERLE, O. & LE GAL, PH. (1988): Post-amphibolitic westward thrusting and fold vergence in the Ticino domaine. – Eclogae geol. Helv. *81*, 215–226.

MERLE, O., LE GAL, PH. & MANCEL, P. (1986): Déformation et métamorphisme dans la région du Simplon (Alpes centrales). – Eclogae geol. Helv. *79*, 705–718.

MILNES, A.G. (1968): Strain analysis of the basement nappes in the Simplon region, northern Italy. – Rep. 23rd int. geol. Congr. Prague *3*, 61–76.

– (1971): Regional variations in quartz *c*-axis preferred orientations in the Central Alps. – Nature phys. Sci. *231*, 117–122.

– (1972): Petrofabric analysis of quartz in the Central Alps – a progress report. – Habilitationsschrift, ETH Zürich (unpubl.).

– (1973): A structural reinterpretation of the classic Simplon tunnel section of the Central Alps. – Bull. geol. Soc. Amer. *84*, 269–274.

– (1974a): Structure of the Pennine zone (Central Alps): a new working hypothesis. – Bull. geol. Soc. Amer. *85*, 1727–1732 (also: Mitt. geol. Inst. ETH u. Univ. Zürich, N.F. *203*).

– (1974b): Post-nappe folding in the western Lepontine Alps. – Eclogae geol. Helv. *67*, 333–348.

– (1975): On steep isogradic surfaces in the Simplon area: a discussion. – Contr. Mineral. Petrol. *53*, 65–68.

– (1979): Excursion along Val Antigorio and upper Val d'Ossola with a diversion along the Simplon pass road. In: STECK, A., RAMSAY, J.G., MILNES, A.G. & BURRI, M.: Compte rendu de l'excursion de la Société Géologique suisse et la Société Suisse de Minéralogie et Pétrographie en Valais et en Italie nord du 2 au 5 octobre 1978 (pp. 304–308). – Eclogae geol. Helv. *72*, 287–311.

MILNES, A.G., GRELLER, M. & MÜLLER, R. (1981): Sequence and style of major post-nappe structures, Simplon–Pennine Alps. – J. struct. Geol. *3*, 411–420.

MISES, R. VON (1928): Mechanik der plastischen Formänderung von Kristallen. – Z. angew. Math. Mech. *8*, 161–184.

MÜLLER, R. (1982): Die tektonische Erforschung der Penninischen Alpen. – Eclogae geol. Helv. *75*, 447–479.

– (1983): Die Struktur der Mischabelfalte (Penninische Alpen). – Eclogae geol. Helv. *76*, 391–416.

MÜLLER, S., ANSORGE, J., EGLOFF, R. & KISSLING, E. (1980): A crustal cross section along the Swiss Geotraverse from Rhinegraben to the Po Plain. – Eclogae geol. Helv. *73*, 463–483.

Nationales Forschungsprogramm 20 (1989): NFP20: Geologische Tiefenstruktur der Schweiz. – NFP20 Bull. *8*.

NIGGLI, P., PREISWERK, H., GRÜTTER, O., BOSSHARD, L. & KÜNDIG, E. (1936): Geologische Beschreibung der Tessiner Alpen zwischen Maggia- und Bleniotal. – Beitr. geol. Karte Schweiz [N.F.] *71*.

PATERSON, M.S. (1969): The ductility of rocks. In: ARGON, A.S. (Ed.): Physics of Strength and Plasticity (pp. 377–392). – M.I.T. Press, Cambridge, Mass.

PLATT, J.P. (1986): Dynamics of orogenic wedges and the uplift of high-pressure metamorphic rocks. – Bull. geol. Soc. Amer. *97*, 1037–1053.

PLATT, J.P., BEHRMANN, J.H., CUNNINGHAM P.C., DEWEY, J.F., HELMAN, M., PARISH, M., SHEPLEY, M.G., WALLIS, S. & WESTON, P.J. (1989): Kinematics of the Alpine arc and the motion of Adria. – Nature (London) *337*, 158–161.

PLATT, J.P. & VISSERS, R.L.M. (1980): Extensional structures in anisotropic rocks. – J. Struct. Geol. *2*, 397–410.

POIRIER, J.-P. & GUILLOPÉ, M. (1979): Deformation induced recrystallization of minerals. – Bull. Minéral. *102*, 67–74.

POIRIER, J.-P. & NICOLAS, A. (1975): Deformation-induced recrystallization due to progressive misorientation of subgrains, with special reference to mantle peridotites. – J. Geol. *83*, 707–720.

PURDY, J.W. & JÄGER, E. (1976): K-Ar ages on rock-forming minerals from the Central Alps. – Mem. Ist. Geol. Mineral. Univ. Padova *30*.

PURDY, J.W. & STALDER, H.A. (1973): K-Ar ages of fissure minerals from the Swiss Alps. – Schweiz. mineral. petrogr. Mitt. *53*, 79–98.

RAMSAY, J.G. (1967): Folding and Fracturing of Rocks. – McGraw-Hill, New York.

RAMSAY, J.G. & GRAHAM, R.H. (1970): Strain variation in shear belts. – Canad. J. Earth Sci. *7*, 786–813.

RAMSAY, J.G. & HUBER, M.I. (1983): The Techniques of Modern Structural Geology. Volume 1: Strain Analysis. – Academic Press, London.

RENEVIER, E. & GOLLIEZ, H. (1894): Voyage géologique au travers des Alpes Centrales et Occidentales de la Suisse de Zurich à Lugano. In: Livret-guide géologique dans le Jura et les Alpes de la Suisse. Congrès géologique international (pp. 197–233). – Payot, Lausanne.

SCHARDT, H. (1894): Excursion géologique au travers des Alpes Occidentales Suisses. In: Livret-guide géologique dans le Jura et les Alpes de la Suisse. Congrès géologique international (pp. 171–195). – Payot, Lausanne.

SCHMID, S.M. (1982): Laboratory experiments on rheology and deformation mechanisms in calcite rocks and their application to studies in the field. – Mitt. geol. Inst. ETH u. Univ. Zürich, N.F. *241*, 1–105.

SCHMID, S.M., AEBLI, H.R., HELLER, F. & ZINGG, A. (1989): The role of the Periadriatic Line in the tectonic evolution of the Alps. In: COWARD, M.P., DIETRICH, D. & PARK, R.G. (Eds.): Alpine Tectonics (pp. 153–171). – Spec. Publ. geol. Soc. London *45*.

SCHMID, S.M. & CASEY, M. (1986): Complete fabric analysis of some commonly observed quartz *c*-axis patterns. In: HOBBS, B.E. & HEARD, H.C. (Eds.): Mineral and Rock Deformation: Laboratory Studies. The Paterson Volume (pp. 263–286). – Monogr. Amer. geophys. Union *36*.

SCHMID, S.M., CASEY, M. & STARKEY, J. (1981): An illustration of the advantages of a complete texture analysis described by the orientation distribution function (ODF) using quartz pole figure data. – Tectonophysics *78*, 101–117.

SCHMID, S.M. & HAAS, R. (1987): The transition from near surface thrusting to intrabasement decollement along the Schlinig thrust. – Terra cognita *7*, 68.

SCHMID, S.M., PANOZZO, R. & BAUER, S. (1987a): Simple shear experiments on calcite rocks: rheology and microfabric. – J. struct. Geol. *9*, 747–778.

SCHMID, S.M., ZINGG, A. & HANDY, M. (1987b): The kinematics of movements along the Insubric line and the emplacement of the Ivrea Zone. – Tectonophysics *135*, 47–66.

SCHMIDT, C. (1894): Geologische Excursion durch die Centralen Schweizer-Alpen von Rothkreuz bis Lugano. In: Livret-guide géologique dans le Jura et les Alpes de la Suisse. Congrès géologique international (pp. 111–158). – Payot, Lausanne.

– (1907): Über die Geologie des Simplongebietes und die Tektonik der Schweizeralpen. – Eclogae geol. Helv. *9*, 484–584.

– (1908): Die Geologie des Simplongebirges und des Simplontunnels. – Rektorats-Progr. Univ. Basel (Friedrich Reinhard, Basel).

SCHMIDT, C. & PREISWERK, H. (1908): Geologische Karte der Simplongruppe, 1:50000. Mit Verwertung der Aufnahmen von A. STELLA. Geol. Spez.-Karte 48. Mit Erläuterungen (Nr. 6). – Schweiz. geol. Komm.

SELVERSTONE, J. (1988): Evidence for east–west crustal extension in the Eastern Alps: implications for the unroofing history of the Tauern Window. – Tectonics *7*, 87–105.

SIBSON, R.H. (1977): Fault rocks and fault mechanisms. – J. geol. Soc. (London) *133*, 191–213.

SIBSON, R.H., WHITE, S. & ATKINSON, B.K. (1979): Fault rock distribution and structure within the Alpine Fault Zone: a preliminary account. In WALCOT, R.I. & CRESSWELL, M.M. (Eds.): The Origin of the Southern Alps (pp. 55–66). – Bull. r. Soc. New Zealand *18*.

SIMPSON, C. & SCHMID, S.M. (1983): An evaluation of criteria to deduce the sense of movement in sheared rocks. – Bull. geol. Soc. Amer. *94*, 1281–1288.

SPICHER†, A. (1980): Tektonische Karte der Schweiz, 1:500000. – Schweiz. geol. Komm.

STALDER, H.A., DE QUERVAIN, F., NIGGLI, E. & GRAESER, ST. (1973): Die Mineralfunde der Schweiz. Neubearb. von PARKER R.L.: Die Mineralfunde der Schweizer Alpen. – Wepf, Basel.

STARKEY, J. (1970): A computer programme to prepare orientation diagrams. In: PAULITSCH, P. (Ed.): Experimental and Natural Rock Deformation (pp. 51–74). – Springer, New York.

STECK, A. (1980): Deux directions principales de flux synmétamorphiques dans les Alpes centrales. – Bull. Soc. vaud. Sci. nat. *75*, 141–149.

– (1984): Structures de déformations tertiaires dans les Alpes centrales (transversale Aar–Simplon–Ossola). – Eclogae geol. Helv. *77*, 55–100.

– (1987): Le massif du Simplon – Réflexions sur la cinématique des nappes de gneiss. – Bull. suisse Minéral. Pétrogr. *67*, 27–45.

STRECKEISEN, A., KRAMERS, J., HUNZIKER, J.-C. & FRANK, E. (1978): Gantergneis und Eistengneis im Simplongebiet. – Schweiz. mineral. petrogr. Mitt. *58*, 396–400.

STRECKEISEN, A., WENK, E. & FREY, M (1974): On steep isogradic surfaces in the Simplon area. – Contr. Mineral. Petrol. *47*, 81–95.

TROMMSDORFF, V. (1964): Gefügestudien an Calcitmarmor aus Val Prato (Tessin). – Schweiz. mineral. petrogr. Mitt. *44*, 595–611.

TROMMSDORFF, V. & EVANS, B.W. (1974): Alpine metamorphism of peridotitic rocks. – Schweiz. mineral. petrogr. Mitt. *54*, 333–352.

TROMMSDORFF, V. & WENK, E. (1963): Diskussion eines Zwillingsgefüges durch Achsenverteilungsanalyse an Quarz eines Tessinergneiss. – Schweiz. mineral. petrogr. Mitt. *43*, 687–698.

TROMMSDORFF, V. & WENK, H.-R. (1965): Die Regelung des Dolomites von Crevola (Simplongruppe). Ergebnisse und Probleme. – Schweiz. mineral. petrogr. Mitt. *45*, 551–569.

TRÜMPY R. (1980): Geology of Switzerland, a guide-book. Part A: An Outline of the Geology of Switzerland. – Schweiz. geol. Komm. (Wepf, Basel/New York).

TULLIS, J. (1983): Deformation of feldspars. In RIBBE, P.H. (Ed.): Feldspar Mineralogy (pp. 297–323). – Reviews in Mineralogy, Min. Soc. Amer.

TULLIS, J.A., CHRISTIE, J.M. & GRIGGS, D.T. (1973): Microstructures and preferred orientations of experimentally deformed quartzites. – Bull. geol. Soc. Amer. *84*, 297–314.

TULLIS, T.E. & TULLIS, J. (1986): Experimental rock deformation techniques. In HOBBS, B.E. & HEARD, H.C. (Eds.): Mineral and Rock Deformation: Laboratory Studies. The Paterson Volume (pp. 297–324). – Monogr. Amer. geophys. Union *36*.

TURNER, F.J. & WEISS, L.E. (1963): Structural Analysis of Metamorphic Tectonites. – McGraw-Hill, New York.

URAI, J.L. (1983): Water assisted dynamic recrystallization and weakening in polycrystalline bischofite. – Tectonophysics *96*, 125–157.

URAI, J.L., MEANS, W.D. & LISTER, G.S. (1986): Dynamic recrystallization of minerals. In: HOBBS, B.E. & HEARD, H.C. (Eds.): Mineral and Rock Deformation: Laboratory Studies. The Paterson Volume (pp. 161–199). – Monogr. Amer. geophys. Union *36*.

WAGNER, G.A., REIMER, G.M. & JÄGER, E. (1977): Cooling ages derived by apatite fission-track, mica Rb-Sr and K-Ar dating: the uplift and cooling history of the Central Alps. – Mem. Ist. Geol. Min. Univ. Padova *30*.

WEISS, L.E. & WENK, H.-R. (1985): An Introduction. In WENK, H.-R. (Ed.): Preferred Orientation in Deformed Metals and Rocks; An Introduction to Modern Texture Analysis (pp. 1–10). – Academic Press, Orlando.

WENK, E. (1955): Eine Strukturkarte der Tessineralpen. – Schweiz. mineral. petrogr. Mitt. *35*, 311–319.

WENK, E. & KELLER, F. (1969): Isograde in Amphibolitserien der Zentralalpen. – Schweiz. mineral. petrogr. Mitt. *49*, 157–198.

WHITE, S.H. (1973a): The dislocation structures responsible for the optical effects in some naturally deformed quartzites. – J. Mater. Sci. *9*, 490–499.

– (1973b): Syntectonic recrystallization and texture development in quartz. – Nature (London) *245*, 26–28.

– (1975): Tectonic deformation and recrystallization of oligoclase. – Contr. Mineral. Petrol. *50*, 287–304.

– (1976): The effects of strain on the microstructures, fabrics and deformation mechanisms in quartzites. – Phil. Trans. r. soc. London (A) *283*, 69–86.

– (1977): Geological significance of recovery and recrystallization processes in quartz. – Tectonophysics *39*, 143–170.

– (1979): Large strain deformation: report on a Tectonic Studies Group discussion meeting held at Imperial College, London on 14 November 1979. – J. struct. Geol. *1*, 333–339.

– (1982): Fault rocks of the Moine Thrust Zone: a guide to their nomenclature. – Textures and Microstructures *4*, 211–221.

WHITE, S.H., BURROWS, S.E., CARRERAS, J., SHAW, N.D. & HUMPHREYS, F.J. (1980): On mylonites in ductile shear zones. – J. struct. Geol. *2*, 175–188.

WHITE, S.H. & KNIPE, R.J. (1978): Microstructure and cleavage development in selected slates. – Contr. Mineral. Petrol. *66*, 165–174.

WILSON, C.J.L. (1975): Preferred orientation in quartz ribbon mylonites. – Bull. geol. Soc. Amer. *86*, 968–974.

WINKLER, H.G.F. (1979): Petrogenesis of Metamorphic Rocks, Fifth Edition. – Springer, New York.

Appendix A: Glossary

Mylonite

Mylonite is an example of a descriptive geological term which has evolved with time (cf. WHITE 1982). The word was first used by LAPWORTH (1885) to describe fine-grained rocks from the Moine Thrust in northwest Scotland. He considered the grainsize reduction to be due to mechanical grinding of the component minerals to produce a fine-grained rock-flour. This usage, with the connotation of fracturing and loss of cohesion during deformation, was current during the pioneering studies of the Simplon Fault Zone. The rocks which were described as "mylonites" at that time correspond to what are in this study called "cataclasites", and this difference in terminology must be considered when referring to the published literature ca. pre-1975. It was through experiments in rock mechanics and the application of observations long established in metallurgy that geologists came to realize that the grainsize reduction observed in highly strained rocks could occur by dynamic recrystallization during "ductile" crystal-plastic deformation, and need not necessarily involve "brittle" fracturing (e.g. GREEN et al. 1970, BELL & ETHERIDGE 1973, 1976, WHITE 1973*a*, *b*, 1976).

Discussion of whether mylonites are "ductile" or "brittle" is fraught with problems. There is no universally accepted definition of ductile and brittle. In rock mechanics the ductility of a material is the amount of strain before failure, where failure is supposedly marked by a sudden stress drop (cf. TULLIS & TULLIS 1986). This is a phenomenological observation and places no restriction on the deformation mechanisms on a granular scale. This is important, because cataclastic flow, where cohesion across grain boundaries is not maintained, is under some conditions associated with high ductility. Many authors use ductile at least implicitly as synonymous for crystal-plastic grain scale deformation. However, this is again a matter of scale, for as is obvious in samples from the SFZ, the deformation mechanisms can vary from phase to phase (e.g. in this study, quartz deforming plastically, feldspar breaking along cleavage planes, and mica forming multiple kinks).

A definition is recommended which de-emphasizes the genetic connotations and which can be effectively used as a descriptive term in the field. For this reason, the definition of BELL & ETHERIDGE (1973) is used in this study: "a *mylonite* is a foliated rock, commonly lineated and containing megacrysts, which occurs in narrow, planar zones of intense deformation. It is often finer grained than the surrounding rocks, into which it grades."

The essential basis of this definition of "mylonite" is its restriction to zones of intense deformation; finer grainsize is seen as a common, but not essential, feature. Dynamic grainsize reduction may occur by subgrain rotation recrystallization, cataclasis and syntectonic reaction. In contrast, dynamic recrystallization by grain boundary migration (usually at higher temperatures, cf. SCHMID 1982) can lead to a coarsening of the average grainsize. This transition is clearly seen within the Simplon Alps, where there is an increase in the amount of grain boundary migration, and hence grainsize, towards the southeast into the Isorno Domain (see main text). The highly strained and foliated rocks of the SFZ in the Isorno Domain are still mylonites in the broad sense of BELL & ETHERIDGE (1973), even though they are no longer fine-grained.

Fabric

Fabric has been used in the English literature as a translation of the German word "Gefüge", and has a well established and broad meaning, namely: the complete spatial and geometric configuration of all those components that make up a deformed rock (BATES & JACKSON 1980). Thus we can describe shape fabrics, preferred grain boundary orientation fabrics, crystallographic preferred orientation fabrics, and so on. The terms *S*-fabric, *SL*-fabric, *LS*-fabric and *L*-fabric are sometimes used in this study with the following meanings:

- *S*-fabric: a planar preferred shape orientation or a foliation with a weak to non-existent lineation.
- *SL*-fabric: a predominantly planar preferred shape orientation with a linear component or a foliation with a discernible lineation.
- *LS*-fabric: a predominantly linear preferred shape orientation with a planar component or a lineated rock with a less strongly developed foliation.
- *L*-fabric: a linear preferred shape orientation or a lineated rock with weak to non-existent foliation.

Texture

The term texture is used in various geological and petrological fields with quite different meanings (cf. Glossary of Geology from BATES & JACKSON 1980). It is used here strictly in the metallurgical sense as a synonym for the *crystallographic preferred orientation fabric* (e.g. WEISS & WENK 1985). The texture can be represented as a series of pole figures (upper hemisphere, equal area stereographic projection) for specific crystallographic planes, which can be contoured in intervals of a uniform distribution density (Appendices C, D). It can be completely represented as an Orientation Distribution Function (ODF, cf. BUNGE 1969, BUNGE & WENK 1977, CASEY 1981).

Recrystallization

Recrystallization can be defined as the crystallographic reorientation of material domains, without significant displacement of the material itself, to angles of misorientation with the host grain such that a clearly defined new grain boundary is visible under the petrological microscope. The new grain boundary separates material points which were once of the same crystallographic orientation. From this it

follows that a grain itself is defined as a domain of similar crystallographic structure and orientation, separated from domains of different orientation and/or structure by a grain boundary. As this difference may be diffuse, rather than discrete, there can be a gradual transition, eventually resulting in the formation of a distinct new grain boundary. This is the case, for example, with recrystallization by subgrain rotation, in which within a single host grain a whole range of structures may be observed in TEM, with increasing misorientation across them: e.g. dislocation walls, polygonized dislocation arrays separating subgrains, and optically visible new grains with clear boundaries to the new orientation domain.

Recrystallization may be either *dynamic*, i.e. occurring during deformation under a deviatoric stress field, or may be *static*, i.e. under isostatic stress and not associated with deformation. An excellent review of the driving forces for dynamic and static recrystallization is given in URAI et al. (1986).

As displacement of material points is excluded, recrystallization cannot be a deformation mechanism. Compositional or phase changes, as well as the long range transfer of material to new sites of grain growth (diffusional mass transfer or "pressure solution") are also excluded and considered to be examples of *neocrystallization*. This distinction is usually clear, but can become rather artificial should minor compositional changes occur during "recrystallization" (e.g. ETHERIDGE & HOBBS 1974 for mica). Problems can arise where deformation is accommodated by combined diffusion (Coble or Naborro-Herring creep) and intracrystalline dislocation creep. Dynamic recrystallization may be driven by both the chemical potential and internal defect strain energy and a distinction between neo- and recrystallization is not possible.

Appendix B: Orientation and Location of Specimens

To fully orient specimens in three dimensions, a consistent convention must be established (Fig. B_1). This is particularly critical when the reference foliation, S_m, is folded (Plate, Fig. B_2). To this end, the lineation L_m has been defined as a vector always directed towards the southwestern quadrant (unless specifically noted, as is the case for samples from the hangingwall, where L_m is irrelevant). This lineation points towards the right in the stereograms and photomicrographs of Appendices C and D; an additional vector perpendicular to the foliation, **Z**, always points upwards in these stereograms and photomicrographs (Fig. B_1). The direction of this vector (when samples are consistently oriented to show dextral sense of shear, as is the convention followed in this section) is also given in the following Tables 2 and 3. This is indicated by U (up) and D (down) when S_m dips less than 50° and a horizontal direction (SE or NW) for steeper foliation dips.

The location of all samples for which the texture has been measured (see Appendices C, D), are given on the simplified tectonic map of Fig. B_3 and accurate coordinates from the Swiss national topographic map grid are listed in Tables 2 and 3.

All samples are from practically mono-mineralic quartz veins (with occasional minor feldspar and white mica) or quartzites (Specs. 15, 17, 55).

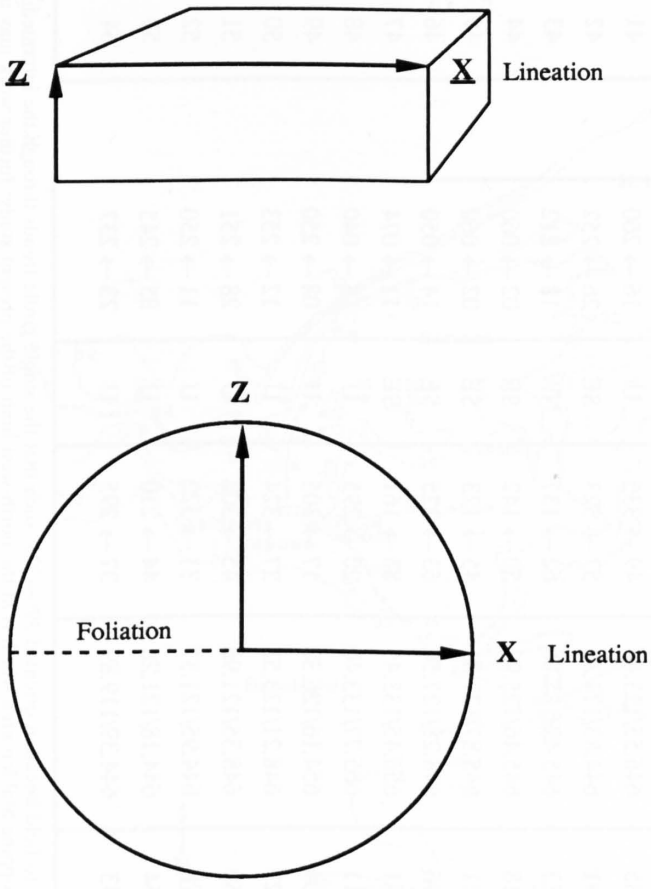

Fig. B_1: Key to the orientation of stereograms in Appendices C and D, as discussed in the text. The foliation is always E–W and vertical, the lineation horizontal and directed to the east, and the vector Z horizontal and pointing north. The approximate direction of Z in the field is listed in the location table and, taken together with the lineation and foliation orientation, fully determines the three dimensional orientation of specimens.

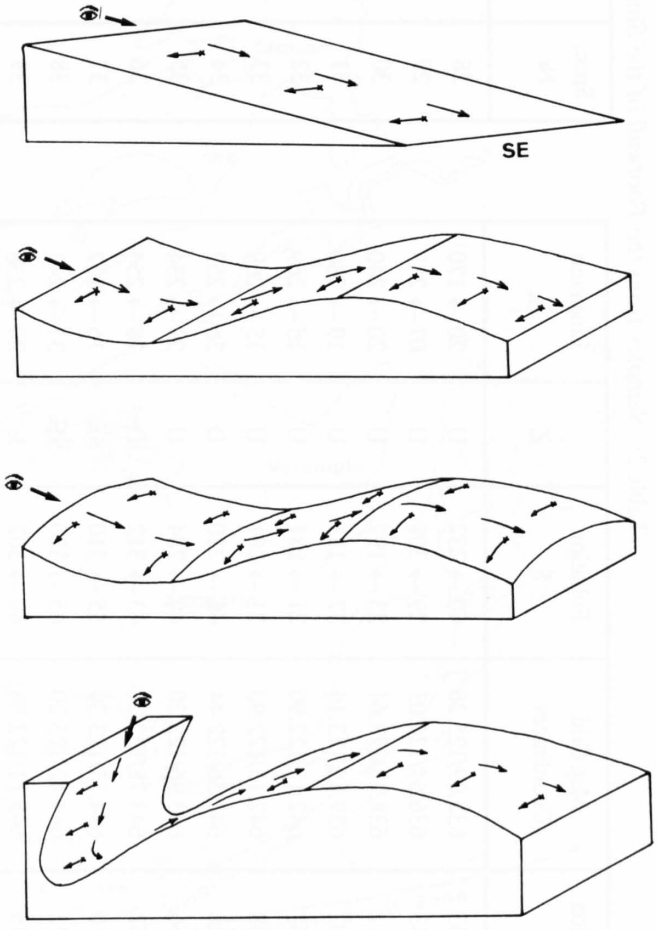

Fig. B_2: Sketch to show the effect on the shear sense of folding coaxial with the movement direction, which is indicated by the crossed arrow ⋇. The shear sense will remain the same if a consistent viewing direction is used, given by →, which takes account of the fold structure. This is the approach for all samples from the SFZ footwall in Appendices C and D. If the L_m lineation (⋇) points towards ca. 230–250°, the viewing direction indicated by → will always give a dextral shear sense.

Table 2: *Samples from the Footwall of the Simplon Fault Zone*

Spec. Nr	Collection Code	Map Grid Coordinates	Foliation S	Z	Lineation X
1	SP 333	635.09/125.26	40 → 232	U	20 → 170[1)]
2	SP 543	636.64/125.03	29 → 308	U	07 → 233
3	SP 411	638.73/123.64	23 → 197	U	20 → 240
4	SP 407	639.15/123.16	32 → 181	U	19 → 230
5	SP 157	642.13/122.90	21 → 281	U	15 → 269
6	SP 158	642.13/122.90	21 → 281	U	15 → 269
7	SP 428	643.36/122.44	46 → 210	D	36 → 252
8	SP 166	643.96/122.20	40 → 284	U	29 → 234
9	SP 352	643.78/123.28	43 → 312	D	28 → 254
10	SP 170	644.35/123.30	55 → 310	SE	16 → 232
11	SP 172	644.42/123.20	65 → 320	SE	31 → 247
12	SP 385	645.11/122.86	40 → 302	U	20 → 238
13	SP 79	645.27/122.34	25 → 291	U	18 → 249
14	SP 185	646.55/123.44	49 → 335	U	16 → 260
15	SP 491	644.83/124.12	57 → 323	SE	26 → 252
16	SP 323	645.47/125.86	62 → 137	NW	18 → 212
17	SP 518	645.46/125.92	50 → 142	SE	02 → 060
18	SP 321	645.87/127.01	45 → 123	SE	02 → 060
19	SP 496	648.28/127.56	63 → 325	SE	14 → 050
20	SP 281	656.45/133.45	83 → 161	SE	11 → 074
21	SP 311	665.77/133.40	20 → 295	U	18 → 040
22	SP 304	654.16/126.38	17 → 305	U	08 → 250
23	SP 327	648.21/123.58	27 → 324	U	12 → 253
24	SP 269	648.35/121.96	45 → 302	U	28 → 251
25	SP 178	644.95/121.37	31 → 322	U	11 → 250
26	SP 154	644.18/121.28	44 → 210	U	35 → 245
27	SP 143	644.39/119.89	37 → 295	U	23 → 237
28	SP 11A	644.70/119.35	23 → 202	U	18 → 248
29	SP 10A	644.77/119.34	23 → 202	U	18 → 248
30	SP 107	645.68/118.80	29 → 221	U	27 → 244
31	SP 108	645.68/118.80	29 → 215	U	27 → 238
32	SP 75B	646.88/117.65	31 → 272	U	30 → 248
33	SP 54B	647.70/116.34	33 → 244	U	32 → 236
34	SP 190	648.50/115.58	40 → 231	U	39 → 256
35	SP 13B	649.23/115.07	30 → 235	U	27 → 241
36	SP 15	649.24/114.40	32 → 190	U	27 → 238
37	SP 16	649.21/114.37	35 → 202	U	27 → 238
38	SP 113	652.50/112.98	35 → 193	U	28 → 229
39	SP 2B	652.56/112.64	37 → 175	U	22 → 237
40	SP 30	652.77/112.97	41 → 182	U	28 → 236
41	SP 207	654.75/113.08	43 → 192	U	21 → 231
42	SP 203	654.93/113.12	28 → 175	U	19 → 230
43	SP 217	657.45/111.95	32 → 199	U	30 → 223
44	SP 37	658.58/110.00	23 → 203	U	19 → 234
45	SP 38	658.58/110.00	23 → 203	U	19 → 234
46	SP 128	659.00/109.09	31 → 212	U	28 → 239
47	SP 129	659.00/109.09	31 → 212	U	28 → 239
48	SP 140	662.08/108.59	52 → 164	SE	14 → 086
49	SP 45	663.33/108.80	64 → 161	SE	11 → 246
50	SP 50	665.12/109.47	73 → 158	SE	16 → 244
51	SP 134	669.21/111.89	66 → 146	SE	23 → 068
52	SP 136	670.86/113.14	63 → 092	SE	56 → 053
53	SP 290A	659.75/124.22	34 → 306	U	03 → 219
54	SP 298	661.65/124.03	12 → 000	U	02 → 050

[1)] Rotated relative to field lineation oriented 39°→225° such that the single girdle trends through the intermediate *Y* axis. This sample is currently considered to lie in the footwall, but was collected from the poorly outcropping Stalden area which is at the north-west limit of the present study; further work may modify the current interpretation.

Table 3: *Samples from the Hangingwall of the Simplon Fault Zone*

Spec. Nr	Collection Code	Map Grid Coordinates	Foliation S	Z	Lineation X
55	SP 420[1)]	638.78/122.58	35 → 161	U	32 → 132
56	SP 163[2)]	642.04/122.28	13 → 257	U	09 → 311
57	SP 344[3)]	646.15/116.95	27 → 264	U	25 → 240

[1)] Quartzite from Staldener Lappen of hangingwall. The lineation is seen as a weak elongation of quartz grains. A second crenulation lineation is oriented 07°→230° similar to the L_m and later backfolding axes in the footwall.

[2)] Isoclinally folded quartz veins in Staldener Lappen of the hangingwall, with fold axes 12°→260°. The stereogram is oriented relative to a weak (stretching?) lineation at an angle of 50° to this intersection lineation. The lineation 09°→311° is pointing left in the stereograms of Appendix B, to maintain a consistent orientation with Specimen 55.

[3)] Deformed quartz vein from hangingwall with a single lineation similiar in orientation to L_m of the footwall.

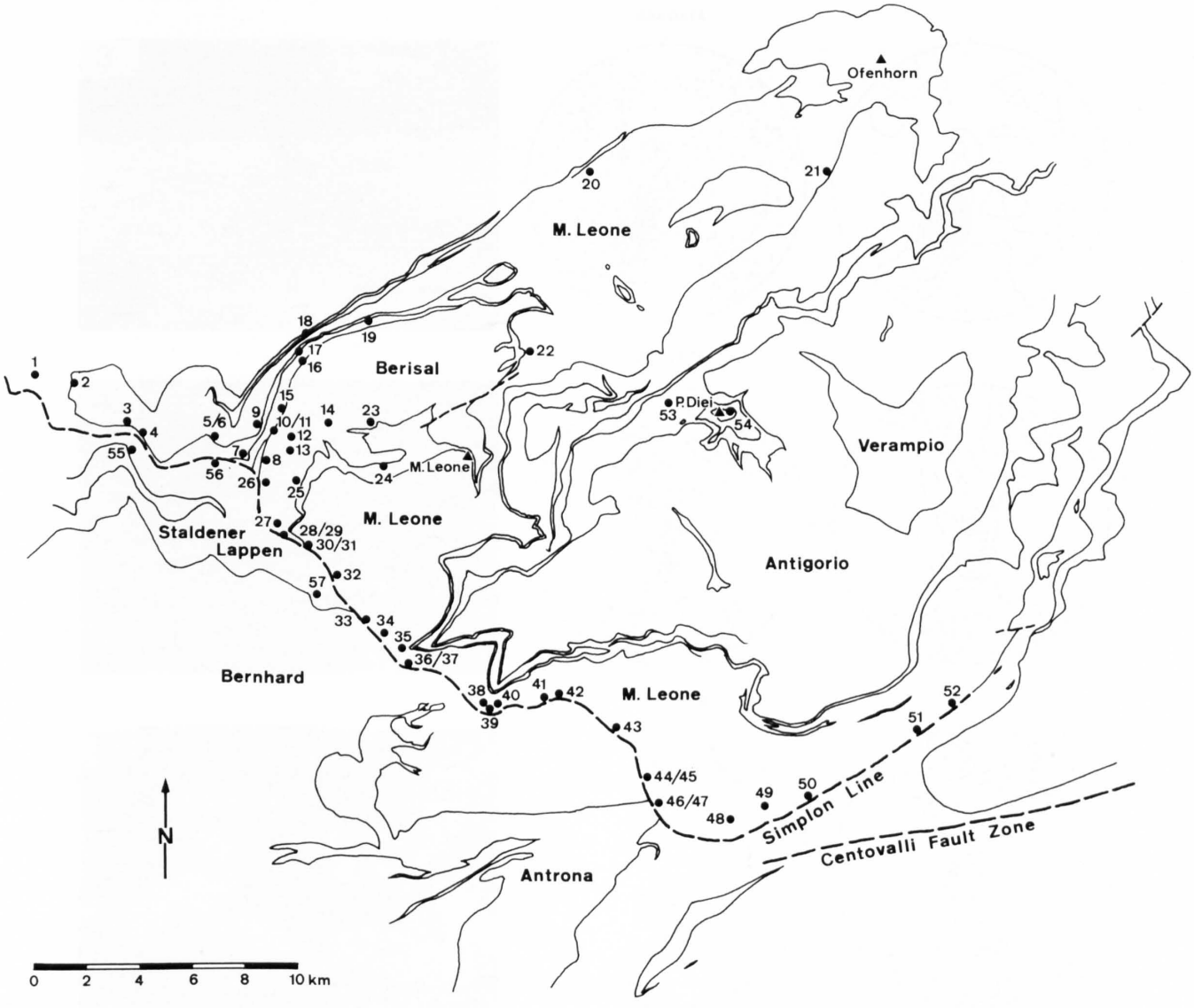

Fig. B3: Location of specimens.

Appendix C: Quartz *C*-Axis Textures

The quartz *c*-axis textures presented here were all measured optically on a universal stage, using the methods described in TURNER & WEISS (1963). The data are plotted on *upper hemisphere, equal area* stereographic projections, with the foliation S_m aligned vertically E–W and the lineation L_m horizontal, following the convention established in Appendix B. Sample locations are given in the same appendix. All samples have been oriented such that the shear sense is dextral; this aids the direct comparison between measured textures from the length of the SFZ.

The three samples from the hangingwall of the SFZ (Specs. 55–57), in which S_m and L_m are not developed, obviously cannot be related to this kinematic framework and are referred to individually in the footnotes.

The contoured stereograms are produced by a computer program originating from STARKEY (1970) and modified by M. Casey and the author. Contour intervals are 1, 2, 3, 4, 5, 6... for Specimens 1–7, 9, 11, 15–18, 20, 22, 42, 53–57; otherwise they are 1, 2, 3, 4, 6, 8, 10... times uniform. Width of field for photomicrographs is 3 mm.

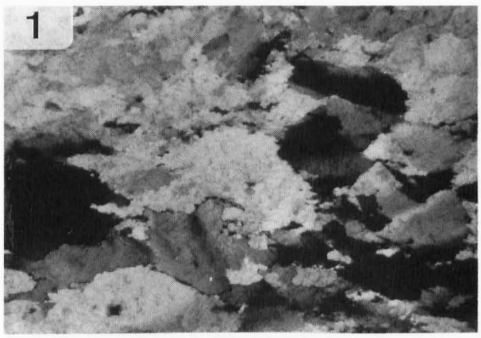

467 DATA

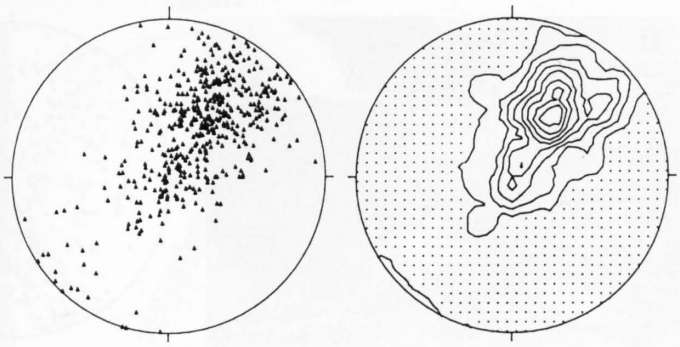

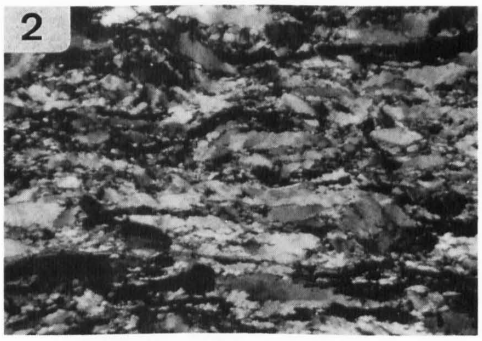

647 DATA

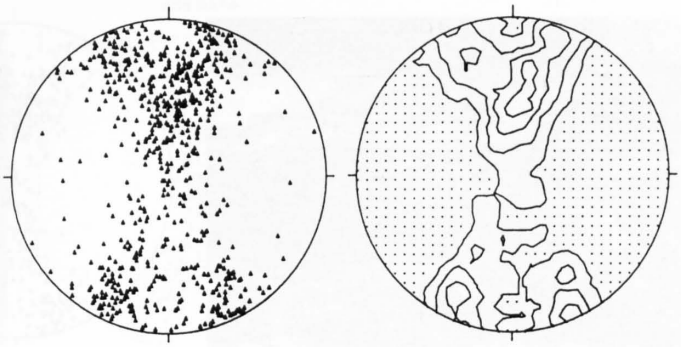

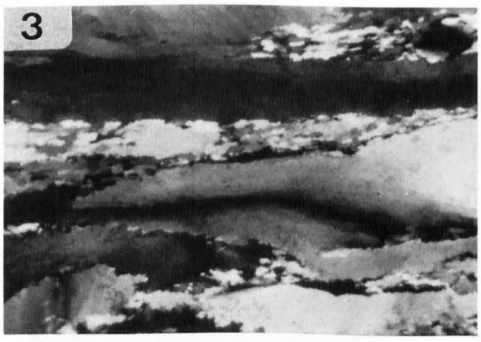

634 DATA

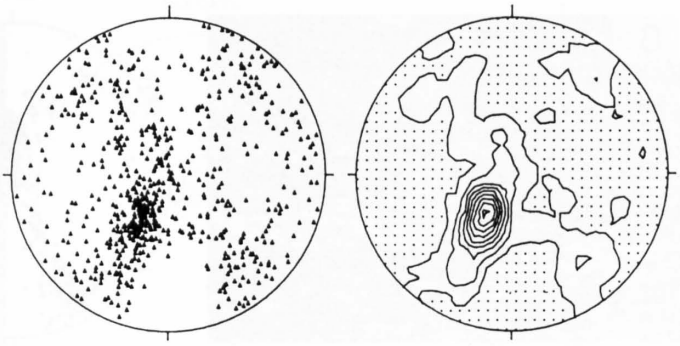

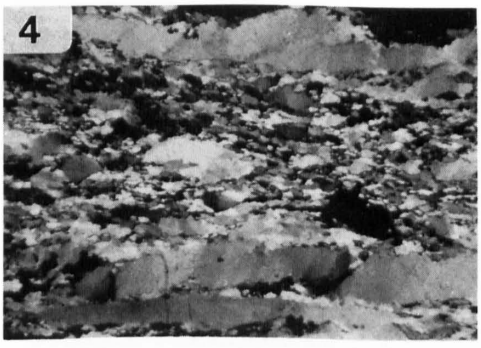

651 DATA

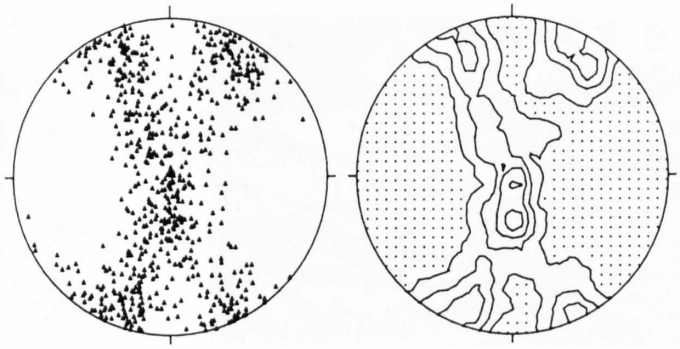

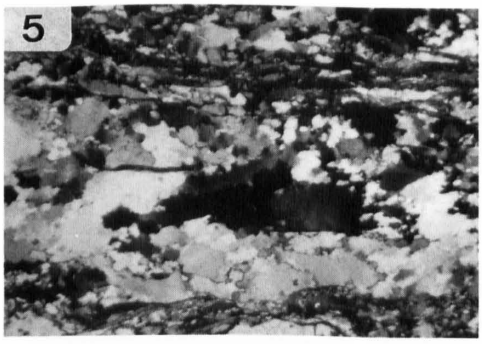

228 DATA

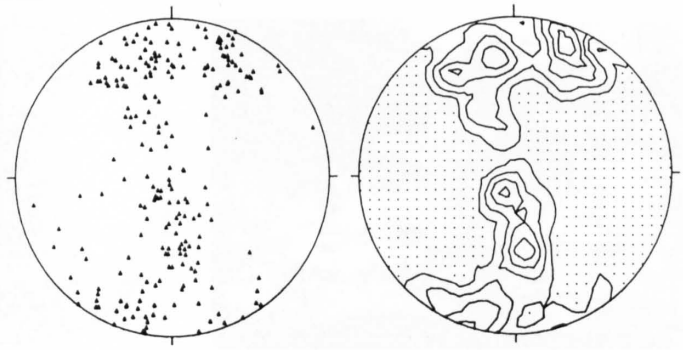

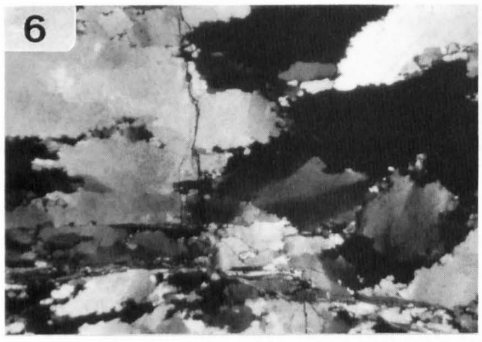
6

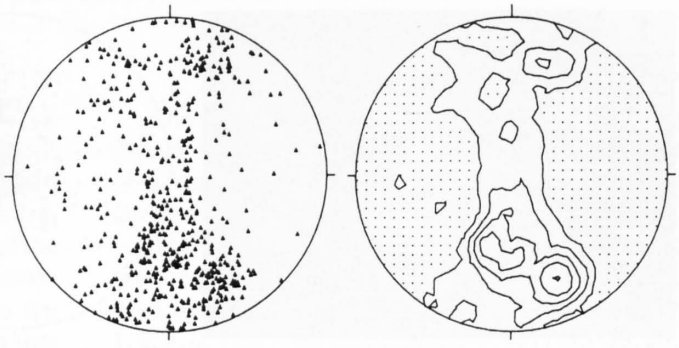
569 DATA

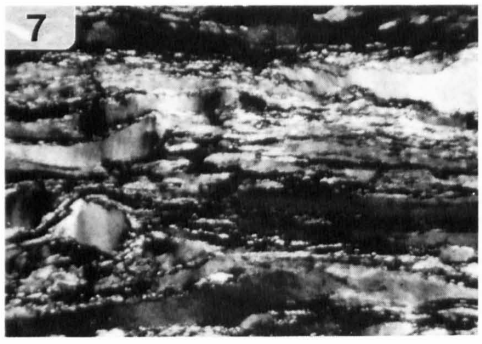
7

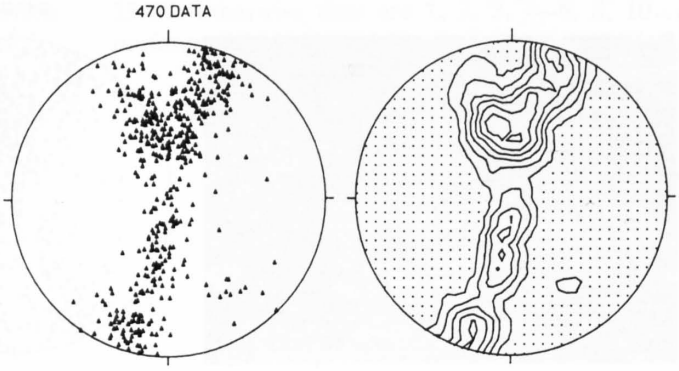
470 DATA

8

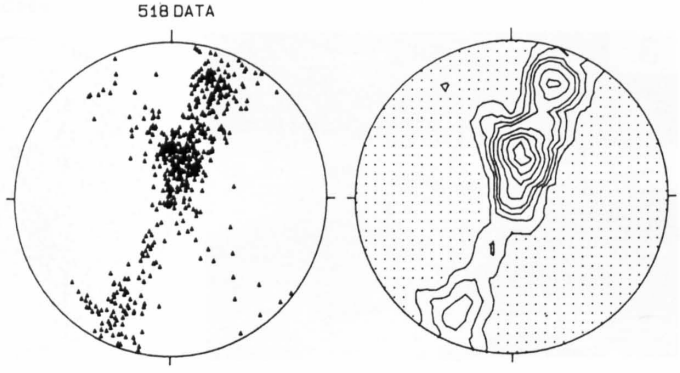
518 DATA

9

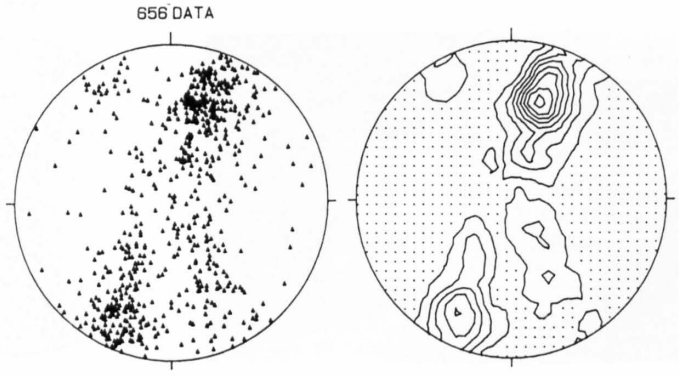
656 DATA

11

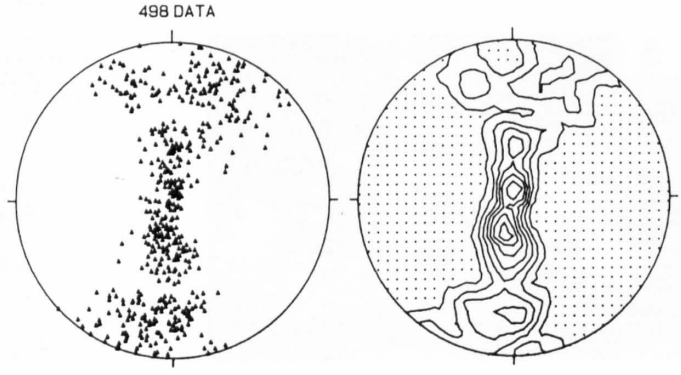
498 DATA

12

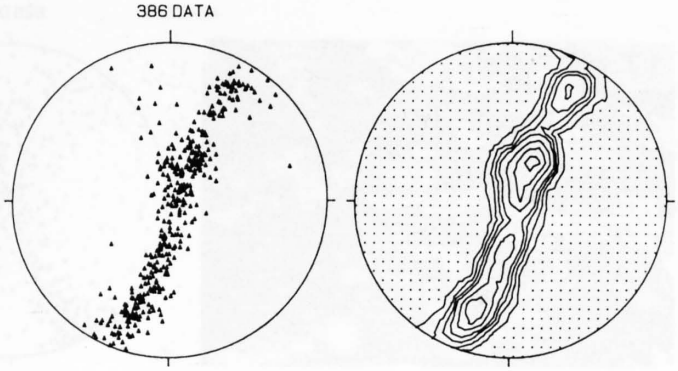
386 DATA

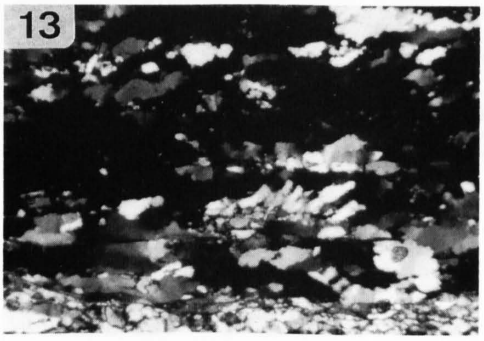
13

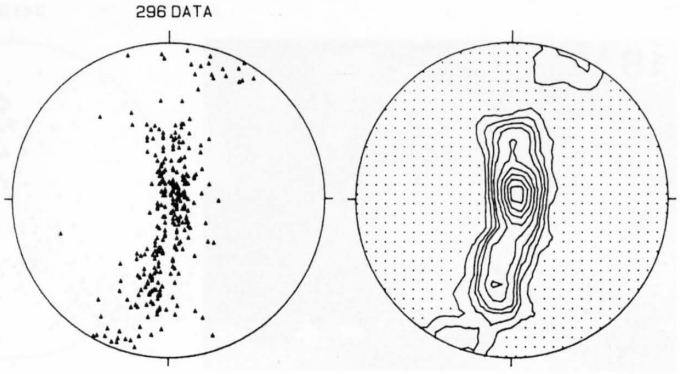
296 DATA

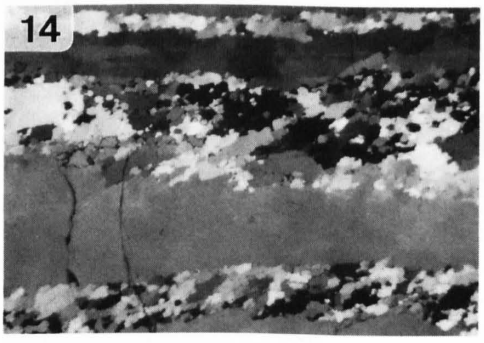
14

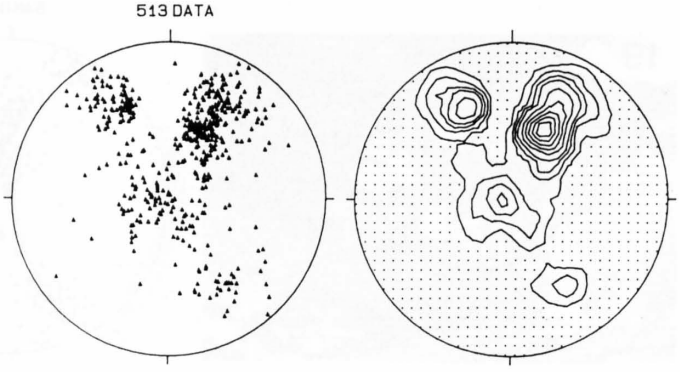
513 DATA

15

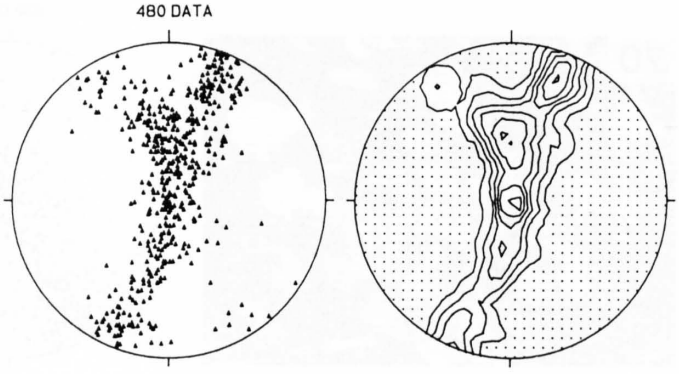
480 DATA

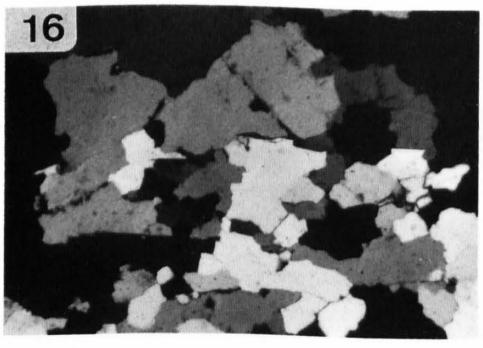
16

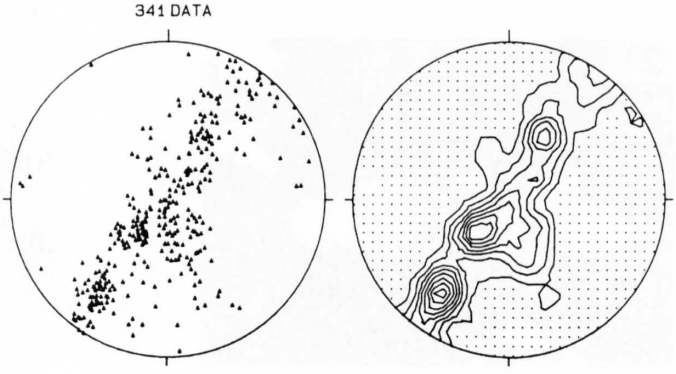
341 DATA

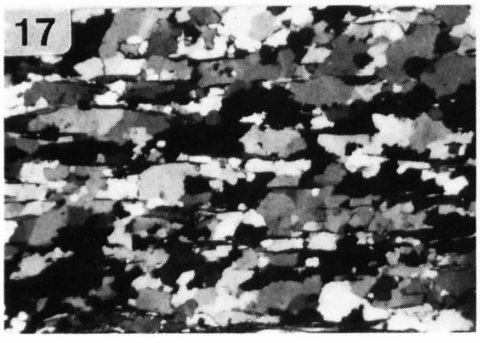

628 DATA

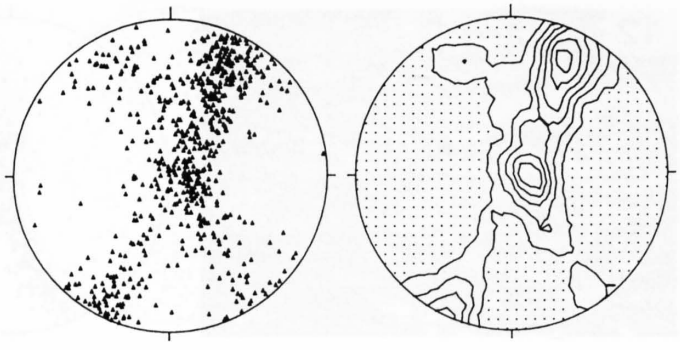

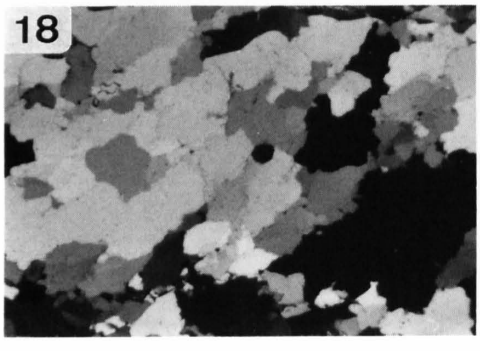

343 DATA

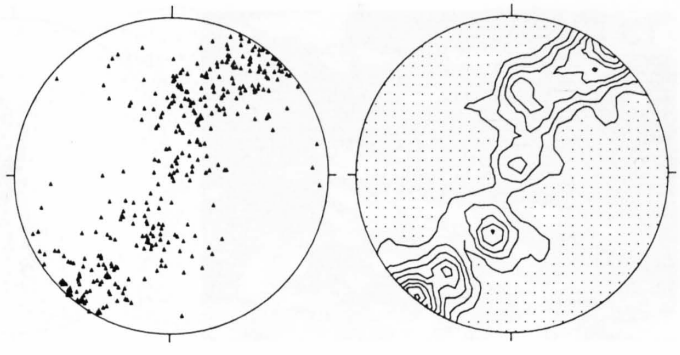

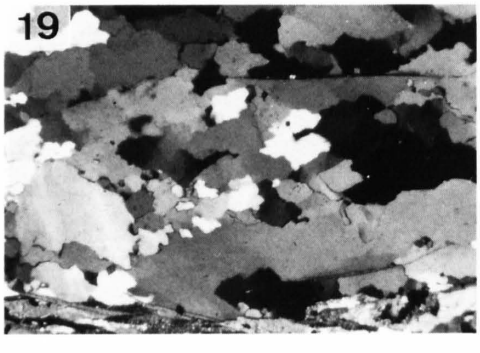

548 DATA

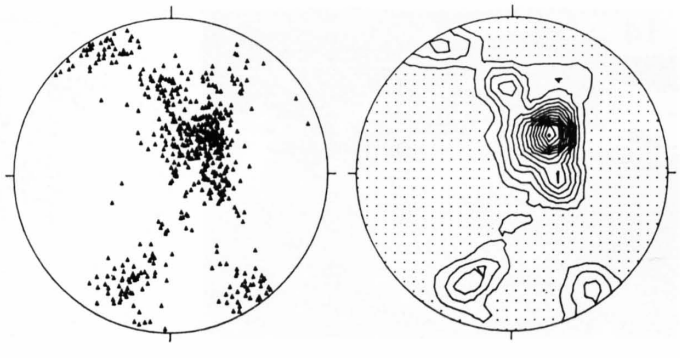

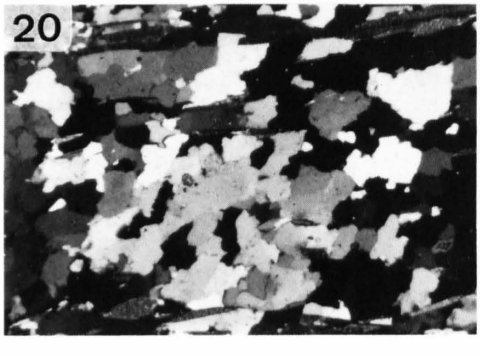

398 DATA

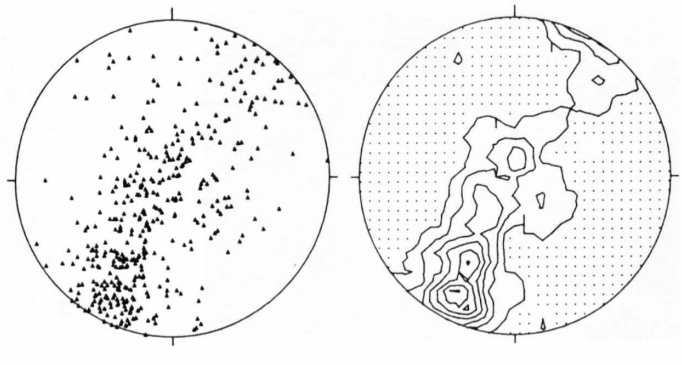

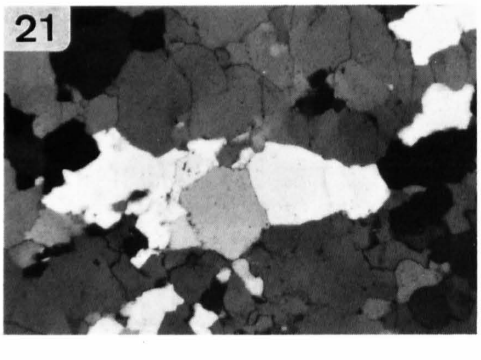

370 DATA

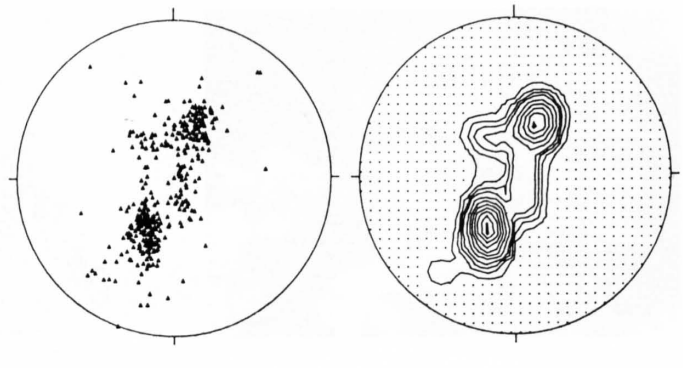

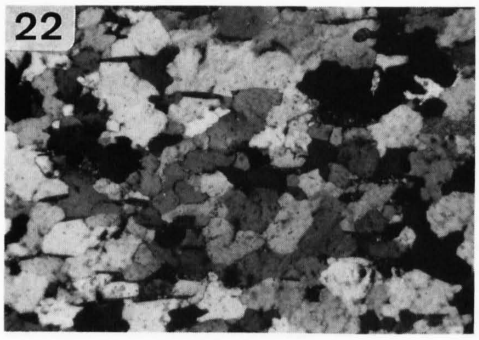

318 DATA

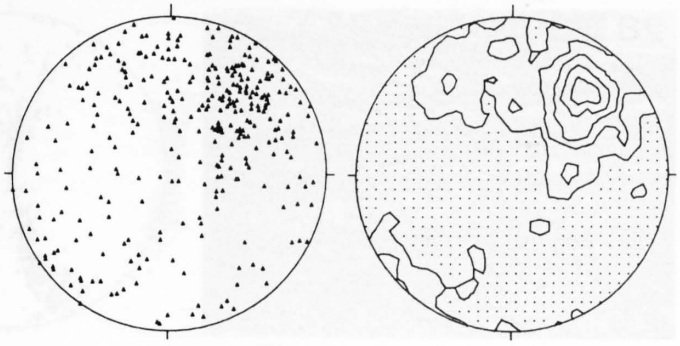

540 DATA

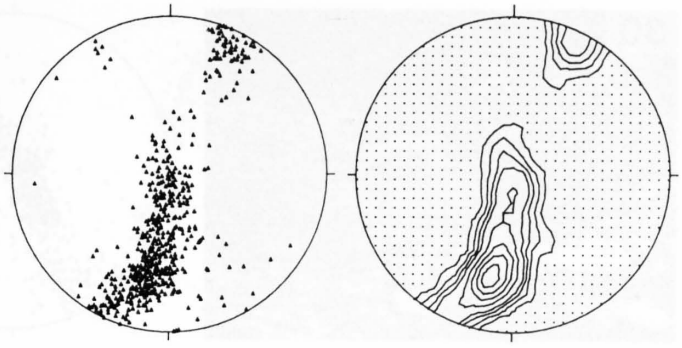

477 DATA

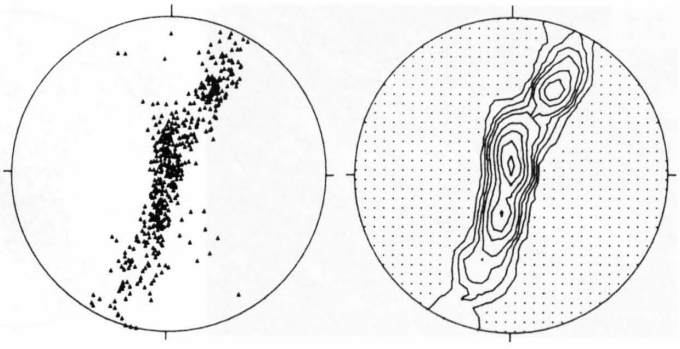

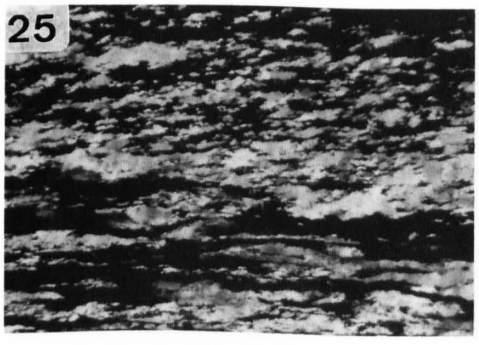

416 DATA

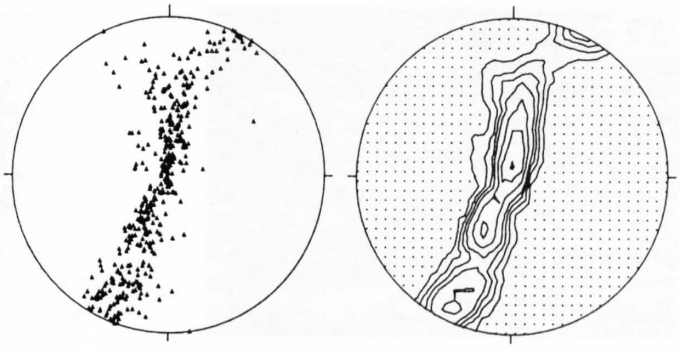

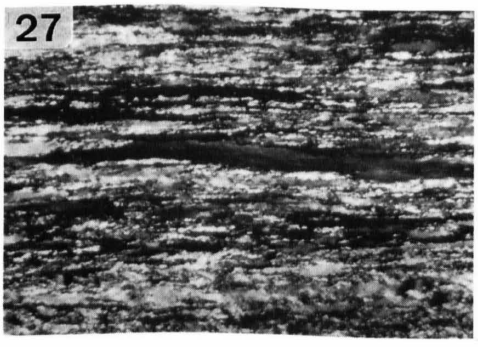

458 DATA

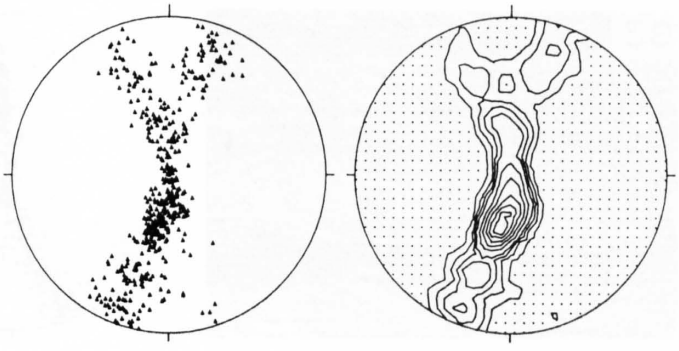

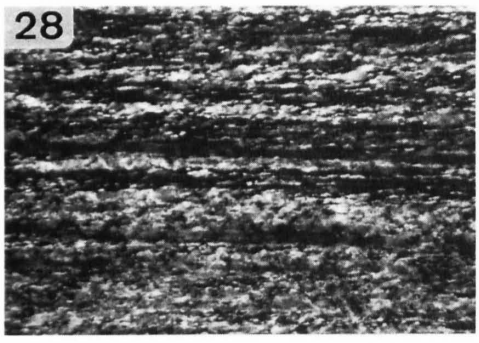

438 DATA

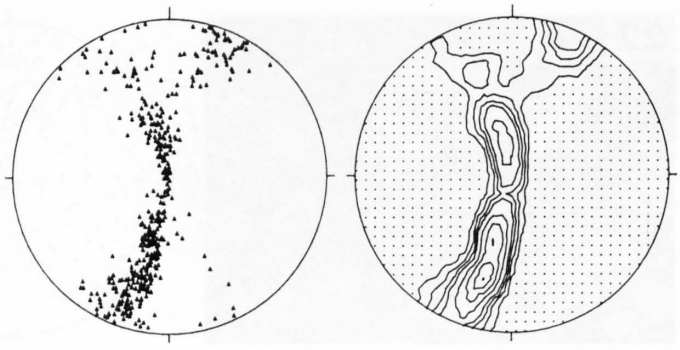

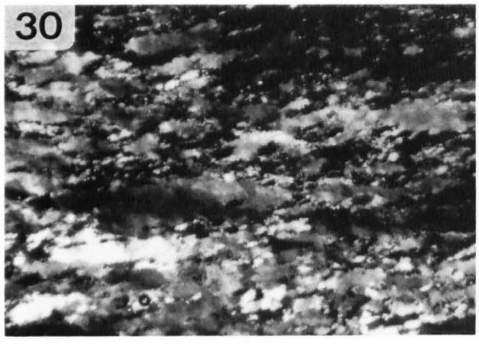

466 DATA

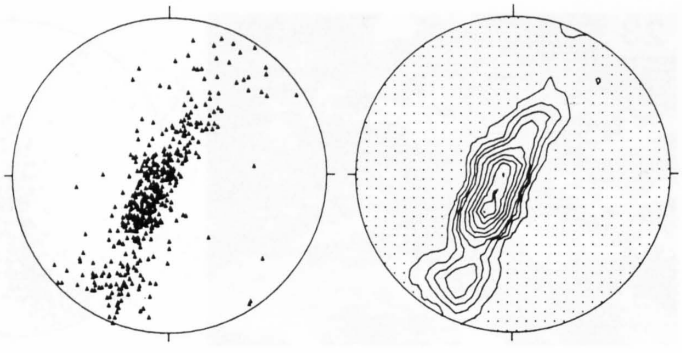

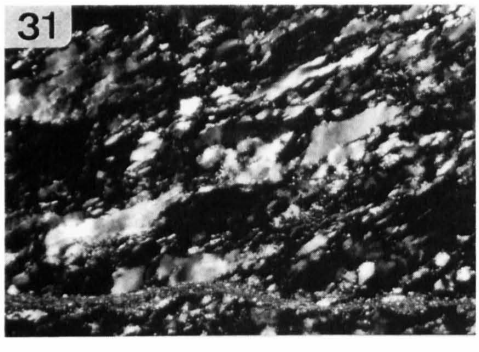

476 DATA

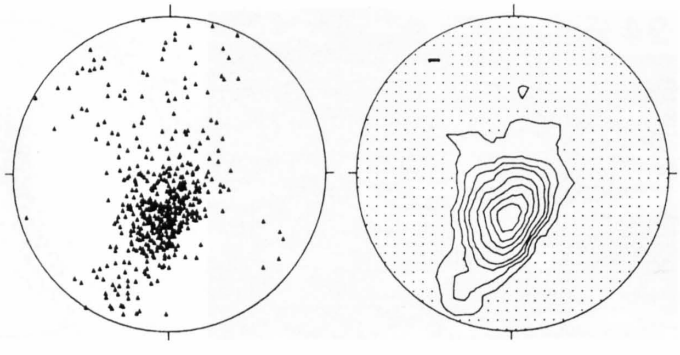

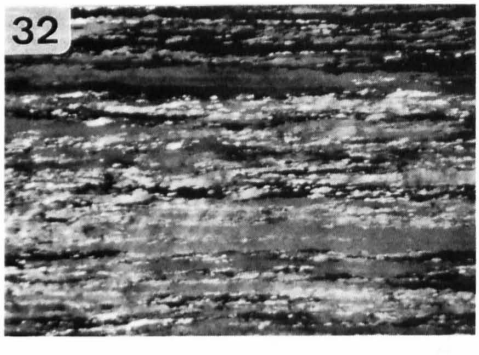

359 DATA

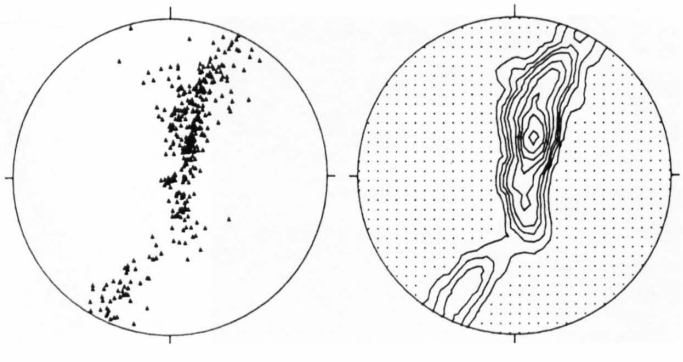

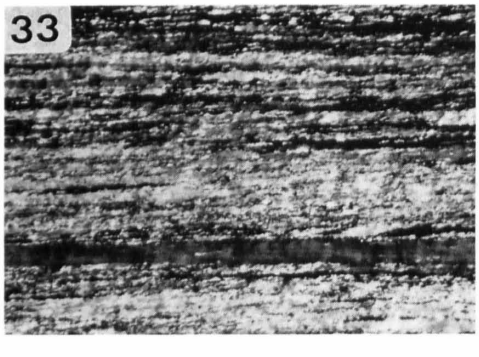

638 DATA

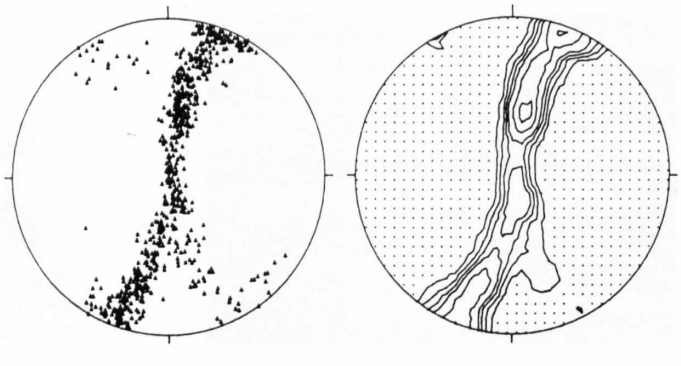

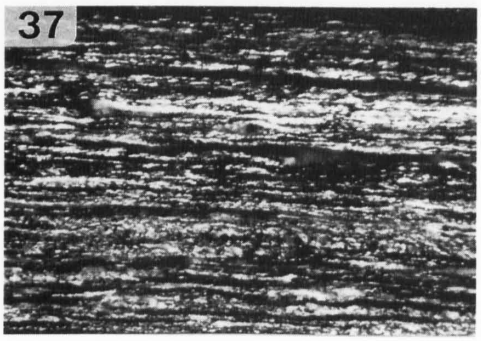
37

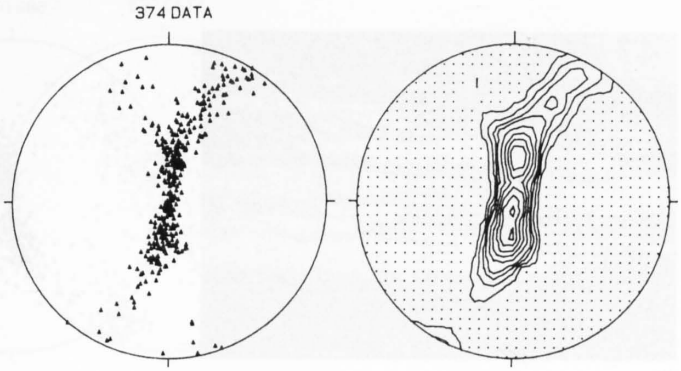
374 DATA

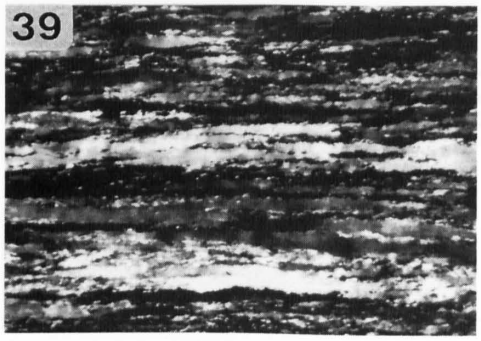
39

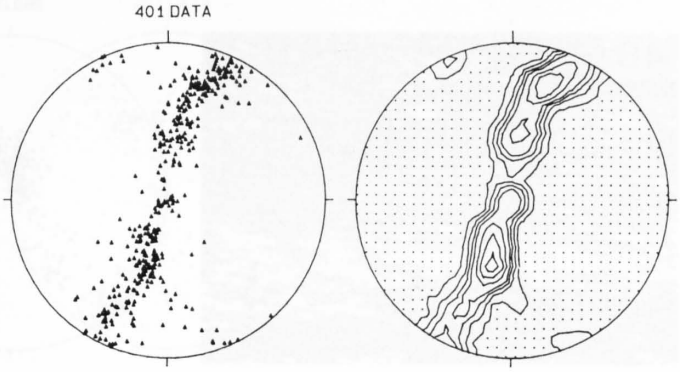
401 DATA

42

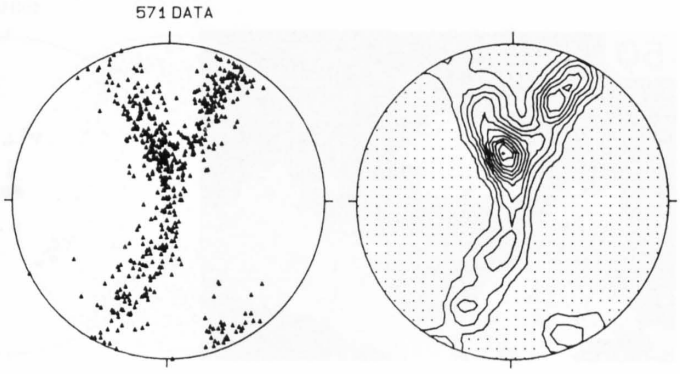
571 DATA

43

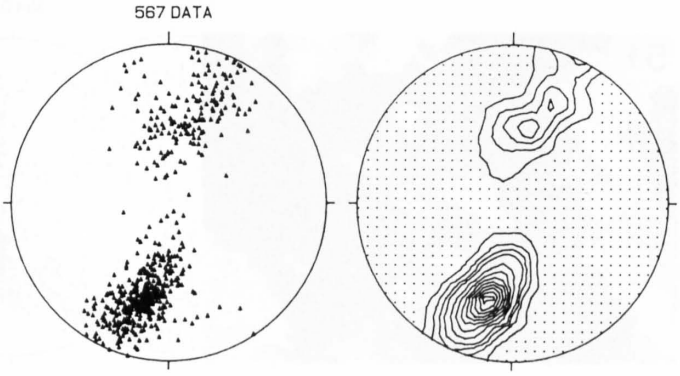
567 DATA

44

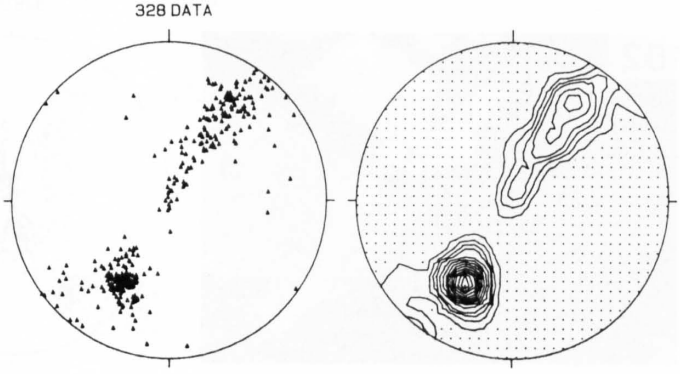
328 DATA

582 DATA

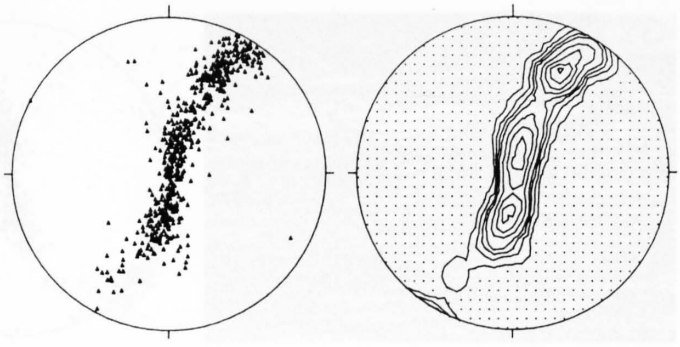

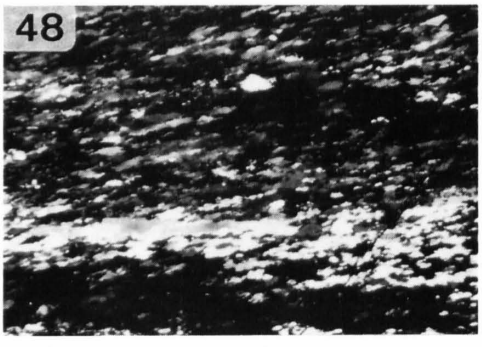

289 DATA

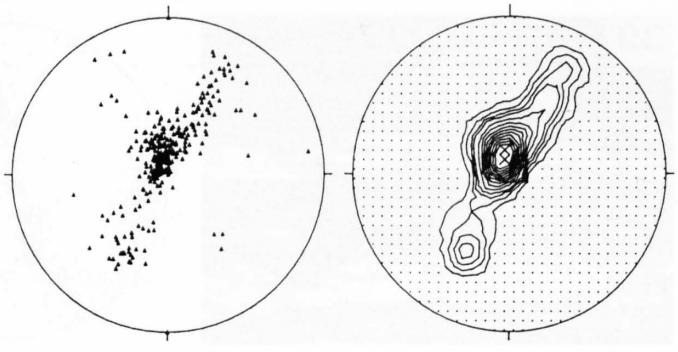

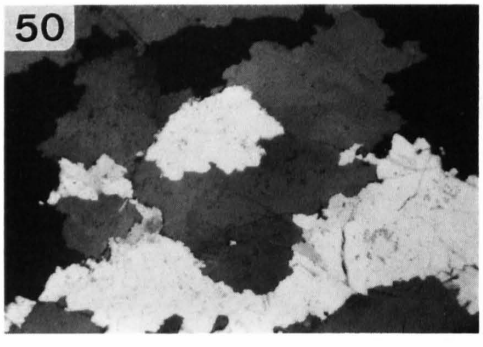

159 DATA

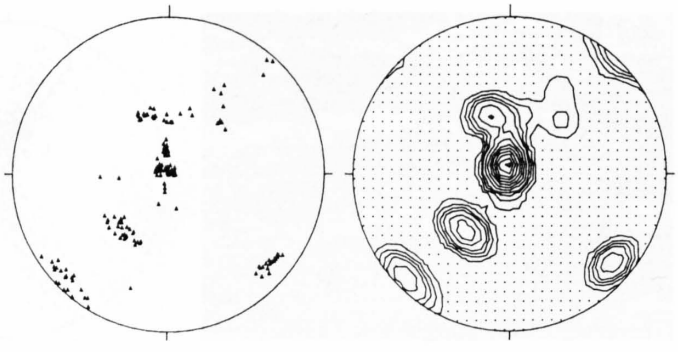

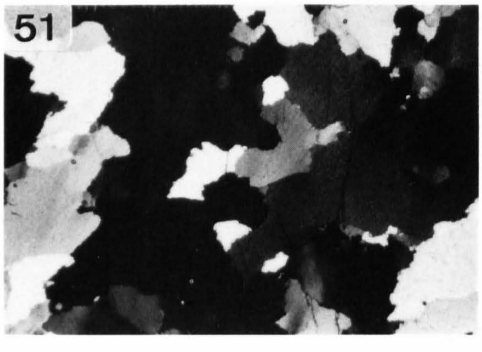

384 DATA

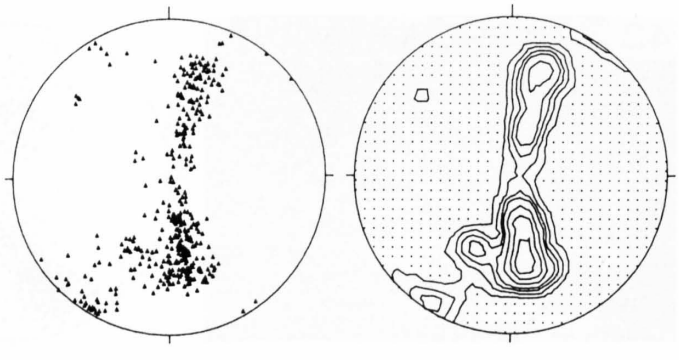

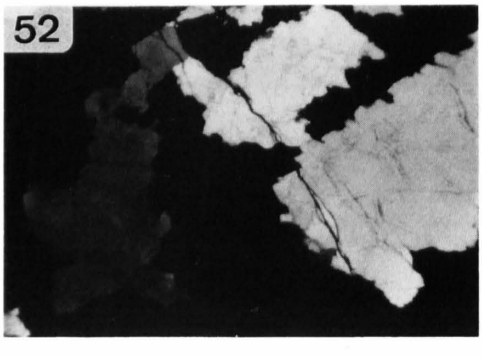

348 DATA

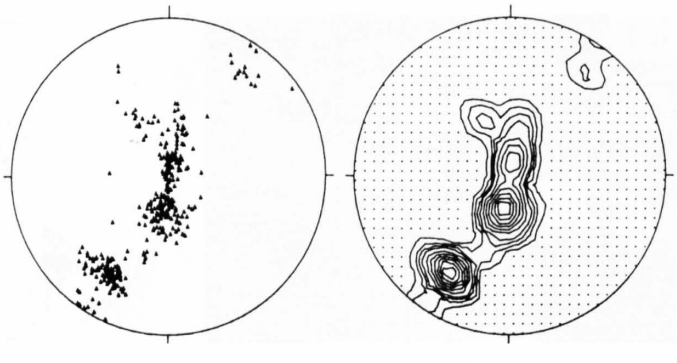

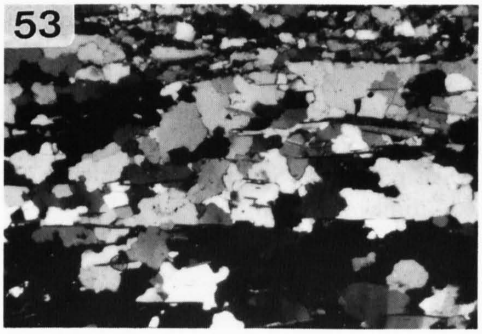

537 DATA

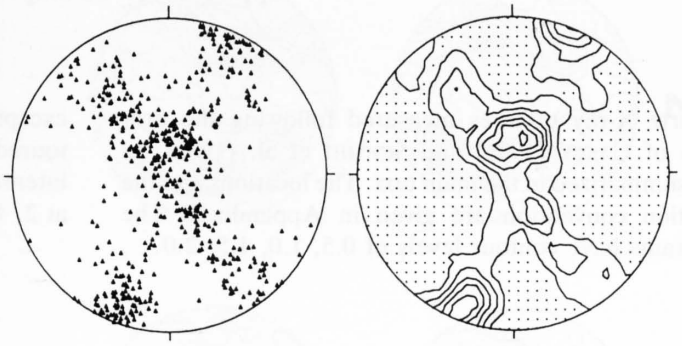

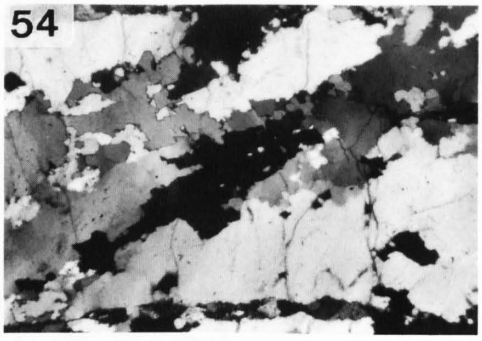

351 DATA

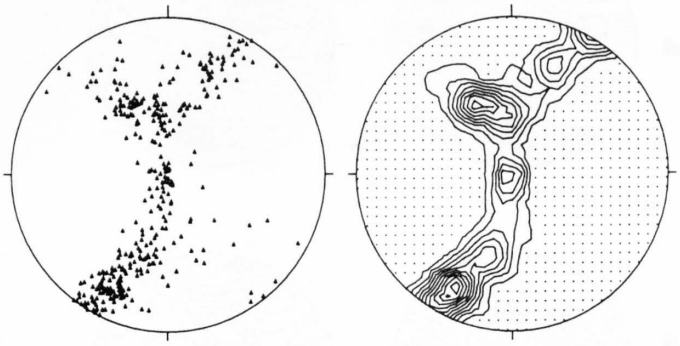

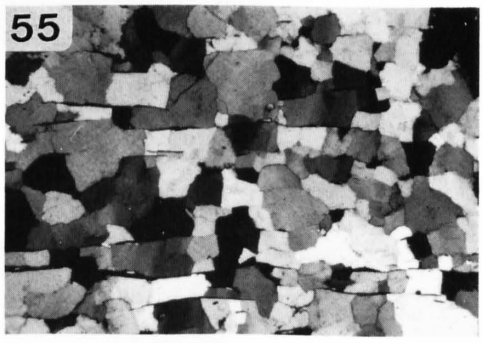

551 DATA

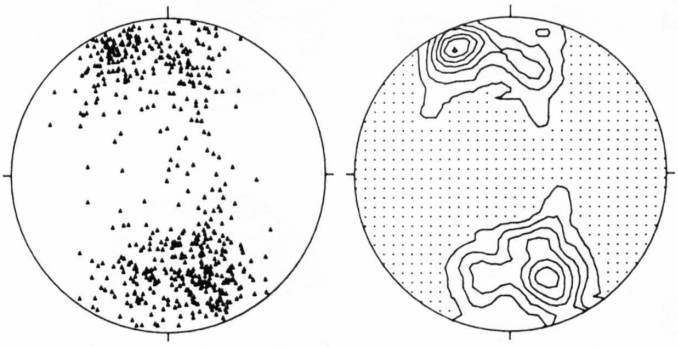

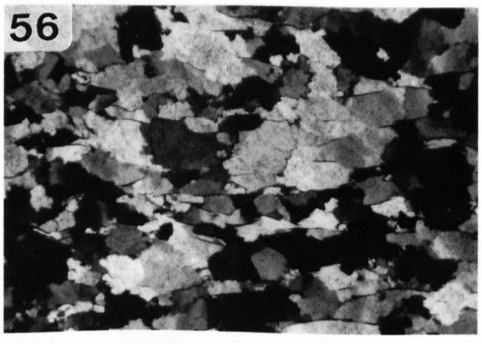

646 DATA

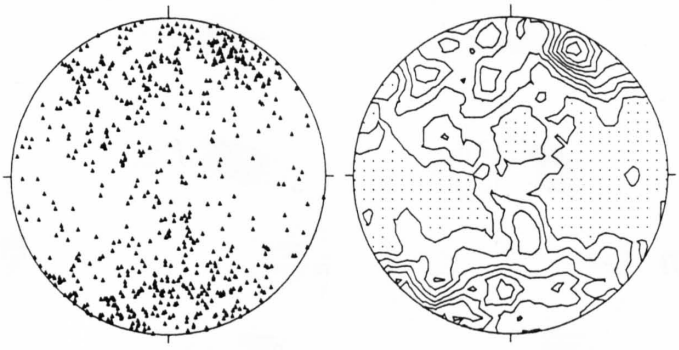

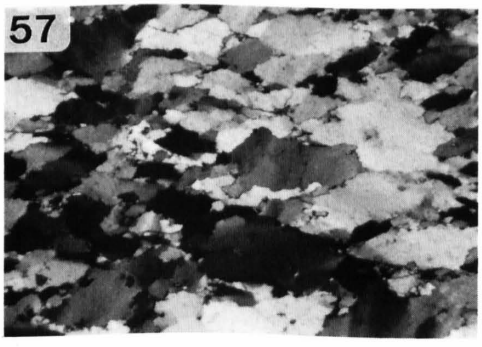

648 DATA

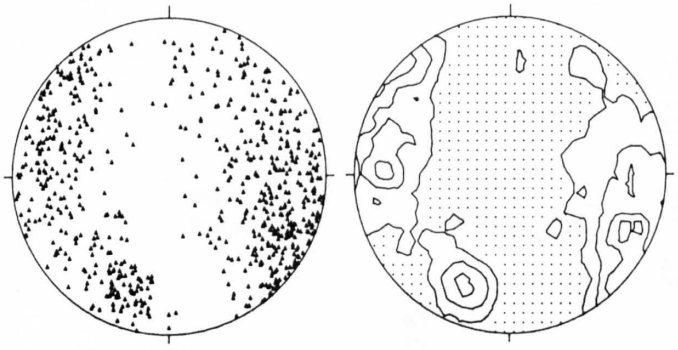

Appendix D: X-Ray Textures

Quartz X-ray textures measured following the procedures of CASEY (1981) and SCHMID et al. (1981), as briefly summarized in the main text. The locations and the orientation convention are given in Appendix B. The stereograms have contour levels of 0.5, 1.0, 1.5, 2.0..., except the regenerated *c*-axis pole figures, which are contoured at levels 1, 2, 3, 4... times uniform, and the very intense *c*-axis pattern of Specimen 44, which is contoured at 2, 4, 6... times uniform.

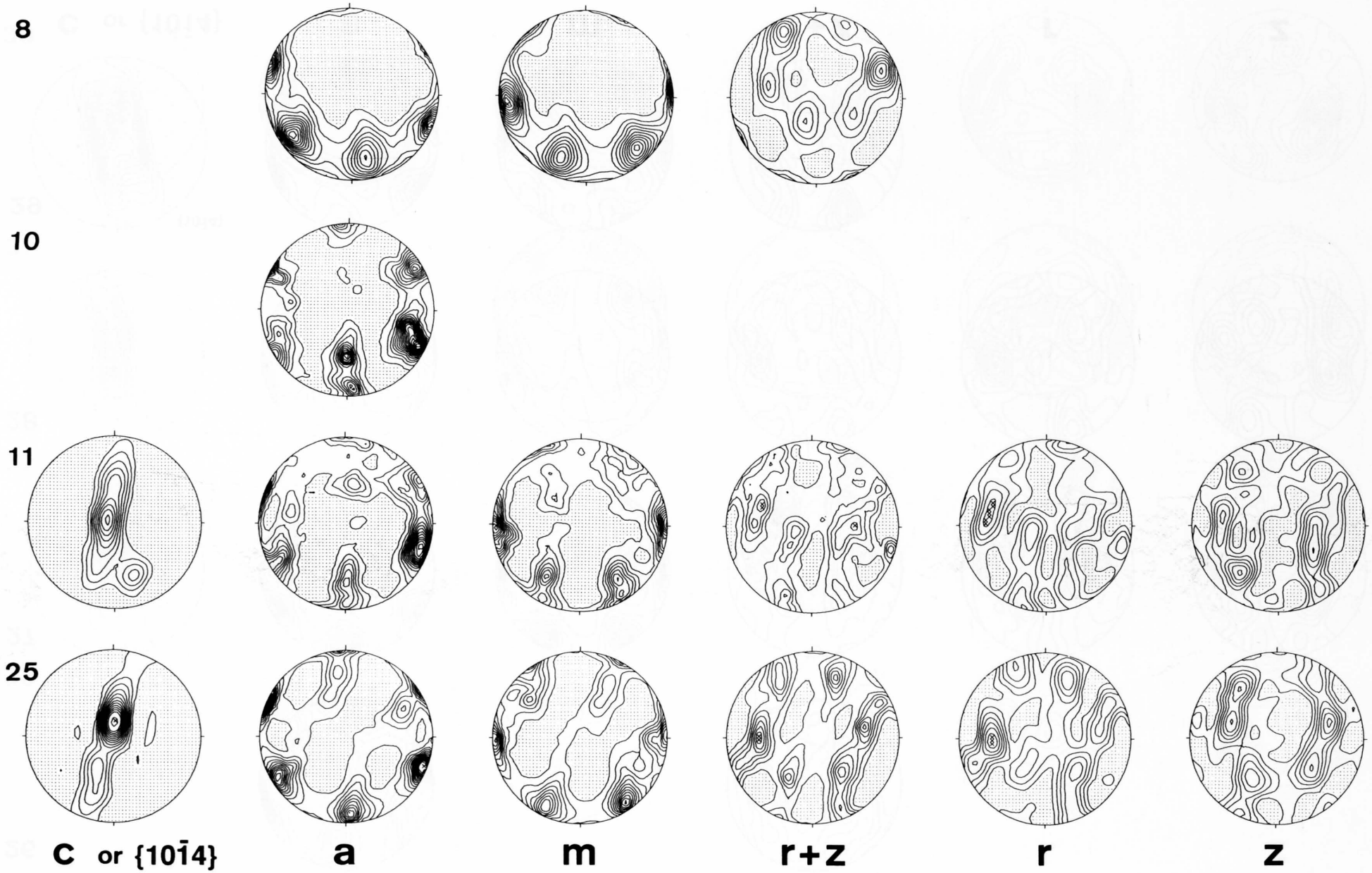
8
10
11
25
c or {10$\bar{1}$4}
a
m
r+z
r
z

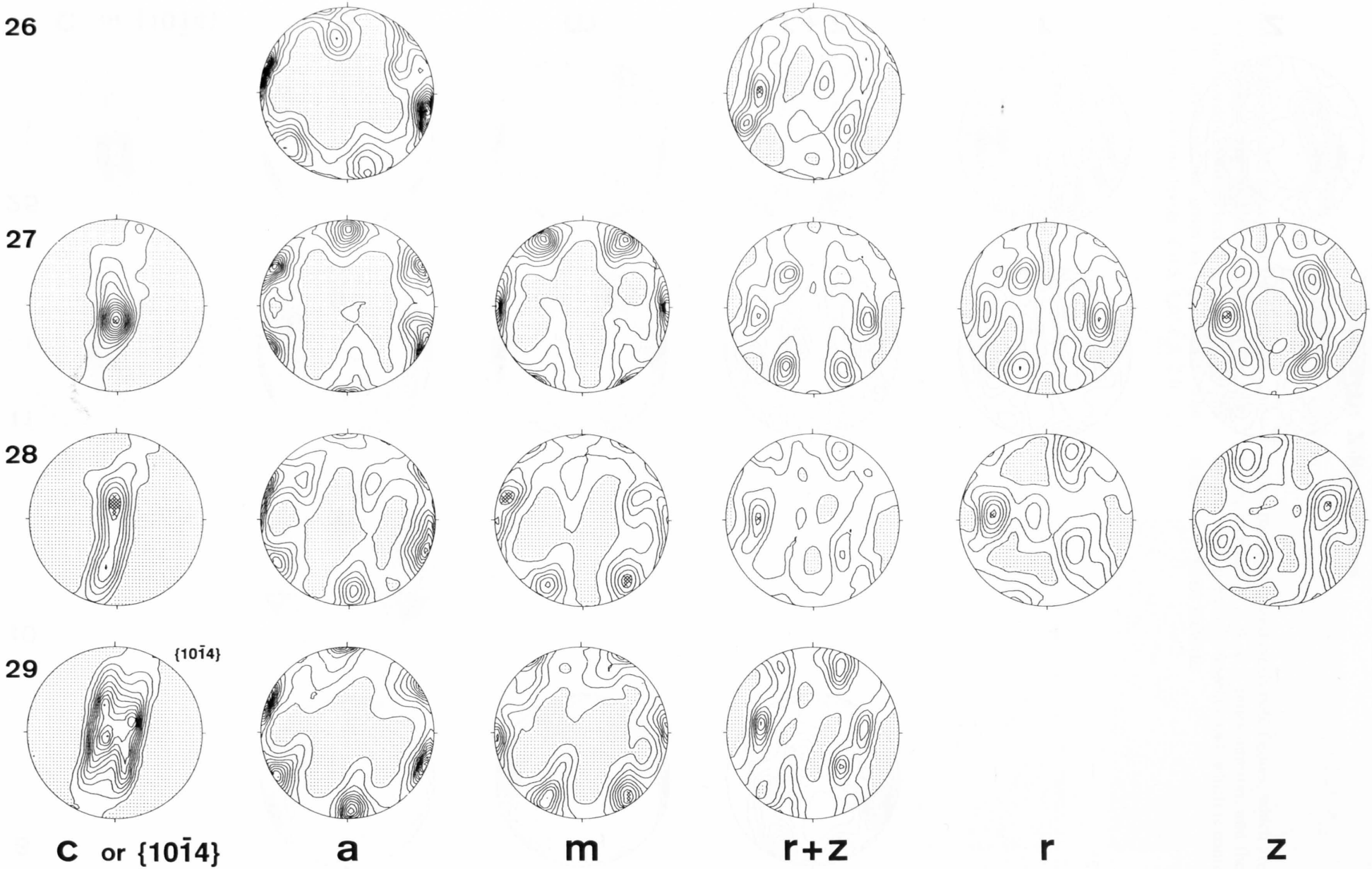
26
27
28
29
{10$\bar{1}$4}
c or {10$\bar{1}$4}
a
m
r+z
r
z

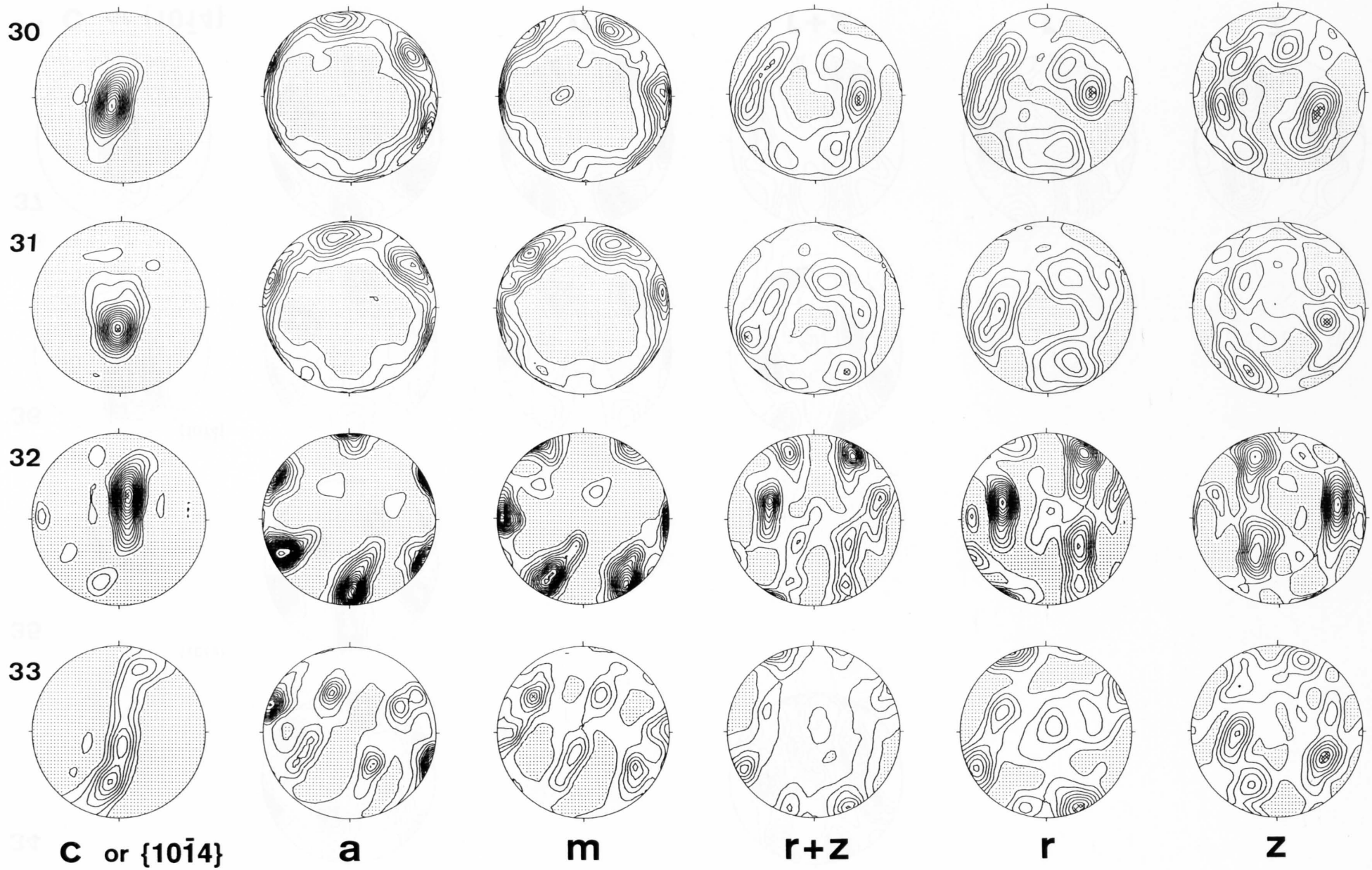
30
31
32
33
c or {10$\bar{1}$4}
a
m
r+z
r
z

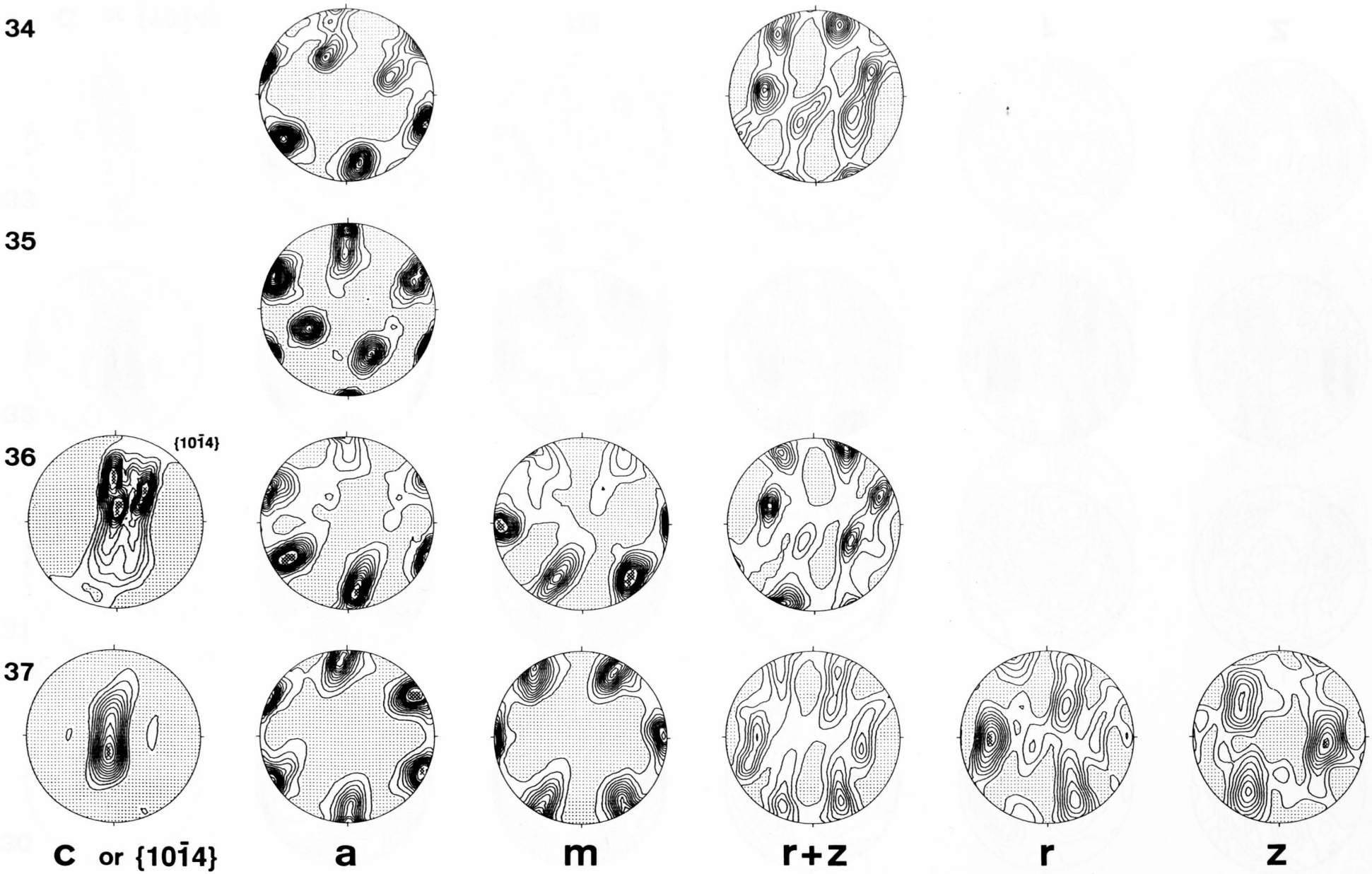
34
35
36
{10$\bar{1}$4}
37
c or {10$\bar{1}$4}
a
m
r+z
r
z

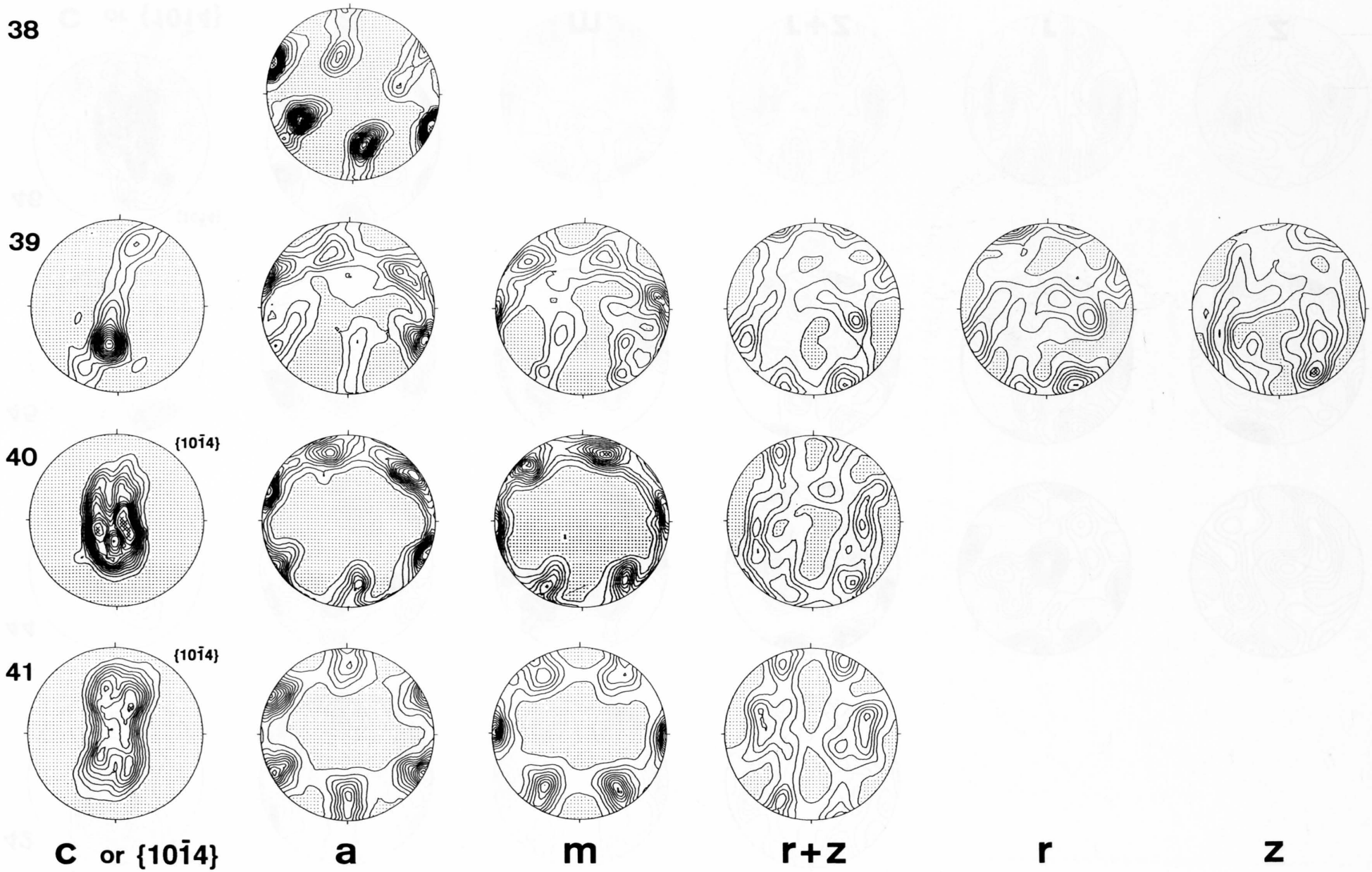
38
39
40
41
{10$\bar{1}$4}
{10$\bar{1}$4}
c or {10$\bar{1}$4}
a
m
r+z
r
z

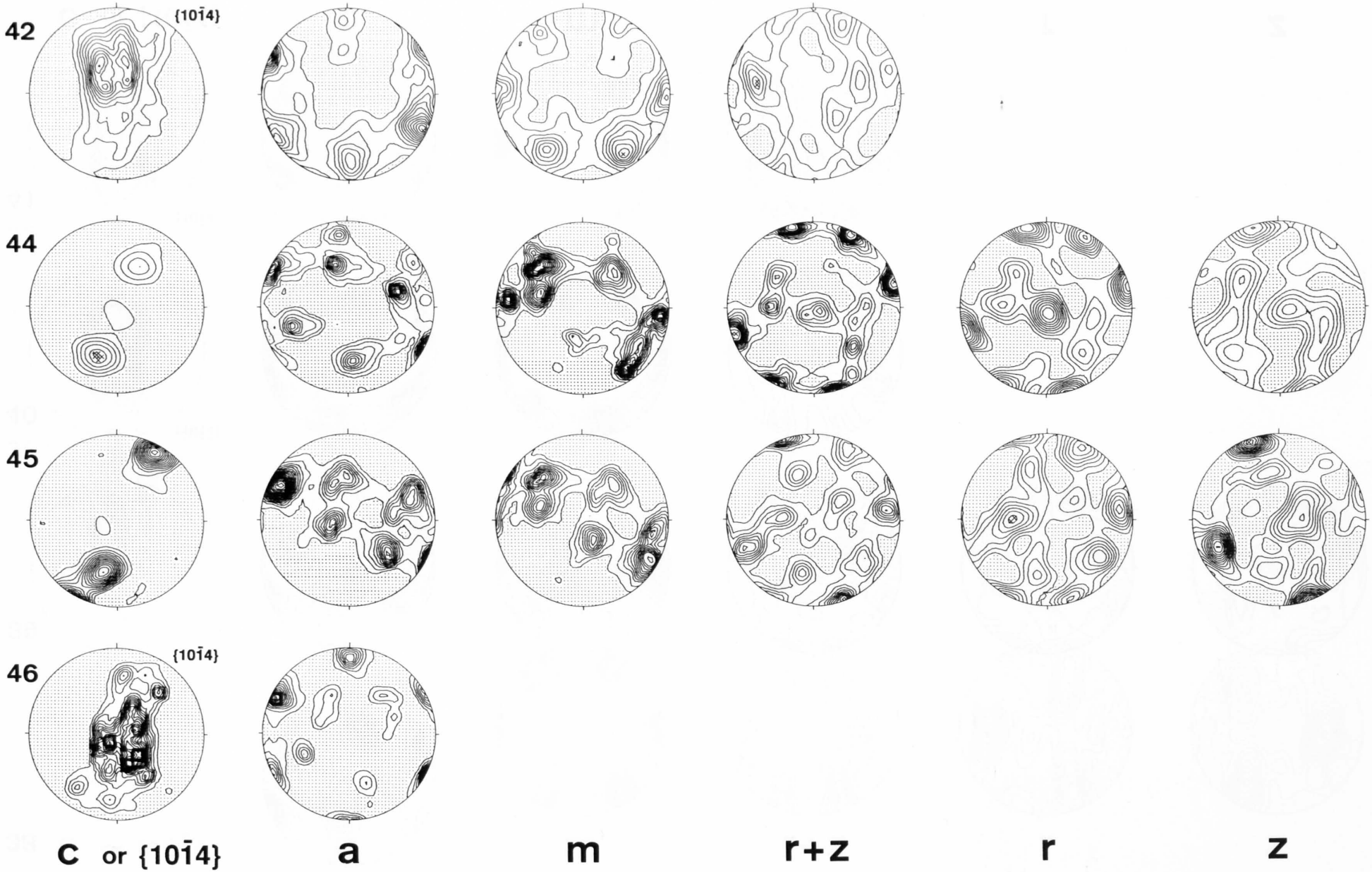
42
{10$\bar{1}$4}
44
45
46
{10$\bar{1}$4}
c or {10$\bar{1}$4}
a
m
r+z
r
z

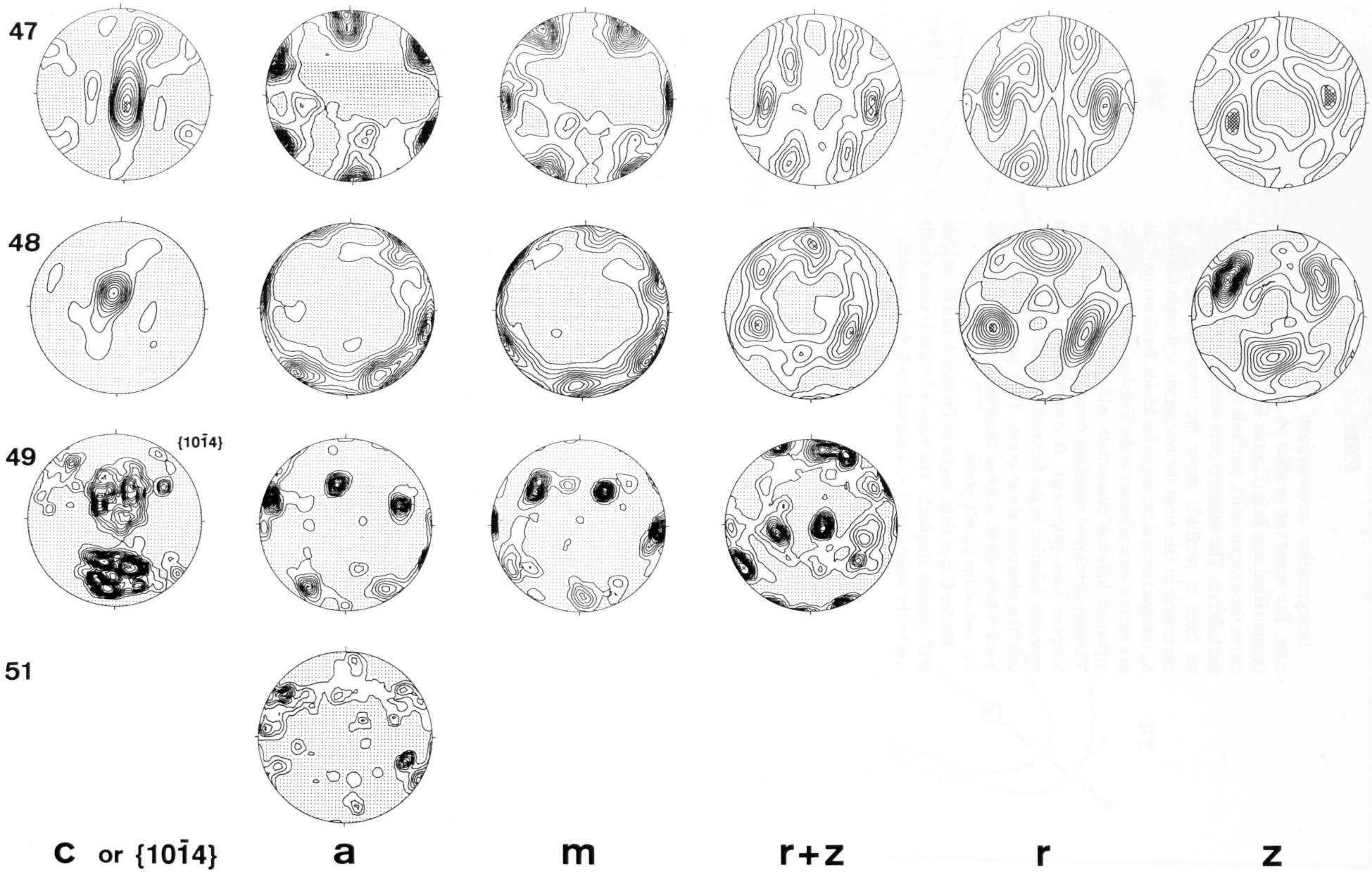
47
48
49
{10$\bar{1}$4}
51
C or {10$\bar{1}$4}
a
m
r+z
r
z

Plate

Interpretative cross-sections through the Simplon Alps. The upper two profiles (A, B) strike 150° and pass through Ried near Brig (Coords. 644.40/129.15). Profile A shows the tectonic units, profile B the trend of the dominant foliation. The enlarged inset across the Glishorn–Berisal folds in profile B shows the complicated geometry discernible in this area: the retrograde mylonitic foliation S_m is folded around the major backfolds, but is overprinted in a narrow zone adjacent to the Simplon Line by a similar, mylonitic foliation concordant with the Simplon Line. Variably developed cataclasis occurs to both sides of the Simplon Line (stippling). It overprints the concordant mylonitic foliation in the footwall. The small arrows indicate the observed shear sense. They point towards the block which shows relative movement to the southwest, i.e. out of the profile plane.

Profile C is at right angles to Profiles A and B, striking 060° through Engiloch. The sense of shear is consistently top to the southwest, i.e. a normal fault displacement.
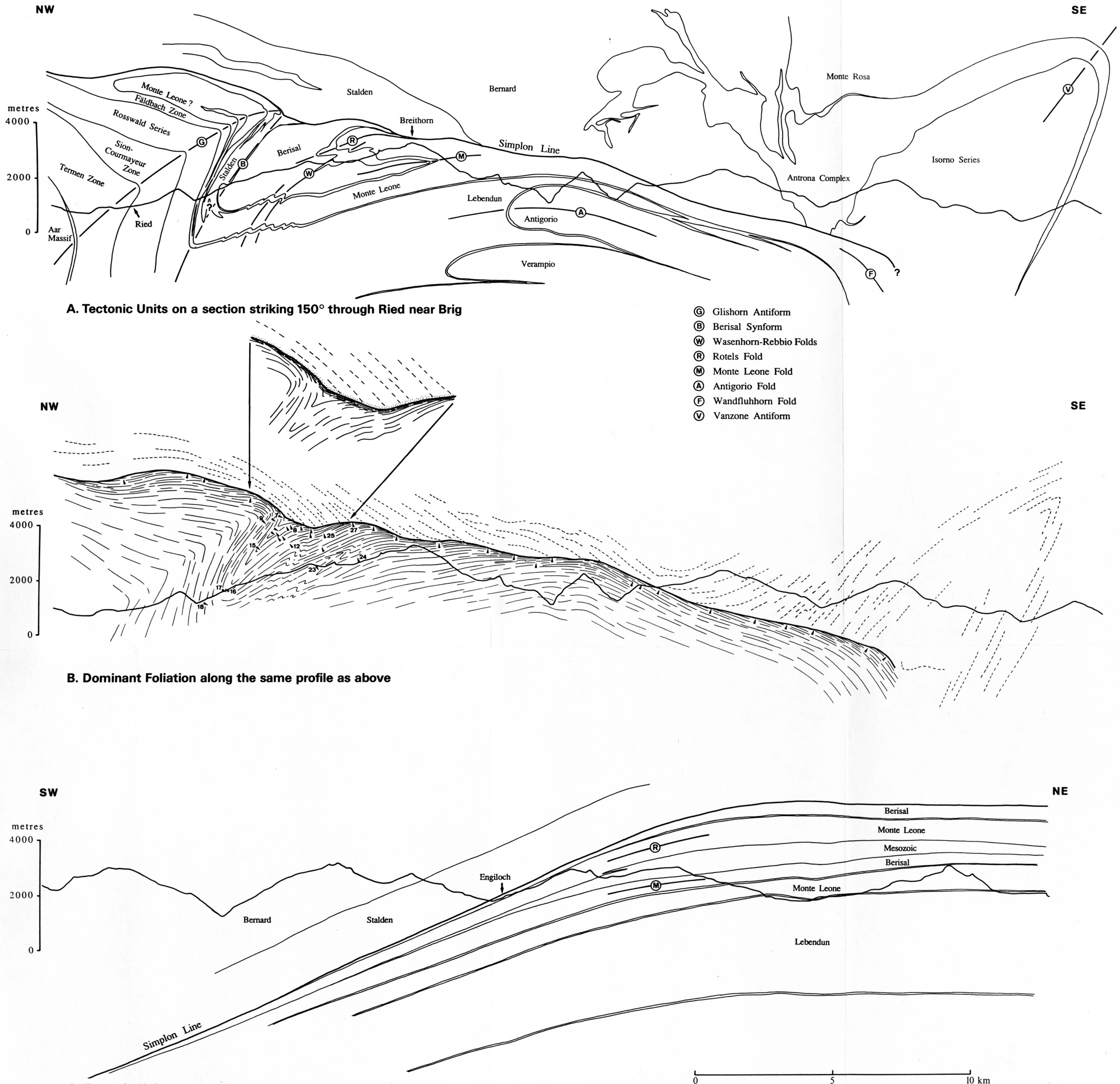
Interpretative Cross-Sections through the Simplon Alps